# Smart Antennas & Power Management in Wireless Networks

by

Vikash Srivastava

Thesis submitted to the Faculty of
Virginia Polytechnic Institute and State University
In partial fulfillment of the requirements for the degree of

MASTER OF SCIENCE
In
Electrical Engineering

Annamalai Annamalai Jr. Chair
Jeoffrey H. Reed
Luiz Da'Silva
January 28, 2002
Blacksburg, Virginia

Keywords:
Wireless Communications, Smart Antenna, Adaptive Beam-Forming, Ad-Hoc Network, Network Throughput, Indoor Propagation Environment, Wireless LAN802.11b.

**Smart Antennas & Power Management in Wireless Networks**

Vikash Srivastava

(Abstract)

The proliferation of wireless ad-hoc networks, especially wireless LAN (IEEE 802.11b Standard), in the commercial market in recent years has reached a critical mass. The adoption and strong support of wireless IEEE 802.11 standard, coupled with the consequent decline in costs, has made wireless LAN deployment as one of the fastest growth area in communication access technology. With the ever-increasing use of wireless LAN technology the various networks are reaching their full capacity in terms of network throughput and number of users and interference level in the wireless channel.

In this thesis work I propose to the use smart antenna technology and a power management scheme in the wireless ad-hoc networks to increase the network capacity in terms of throughput and number of simultaneous communication and to lower the average transmit power and consequently co-channel interference. Power management scheme can be used to maximize the power efficiency of the transmitter by choosing an optimum transmit power level. Smart antenna or adaptive antenna array technology has reached a level of sophistication that it is feasible to use it on small mobile terminals like handheld PDA, LAPTOP and other mobile devices with limited battery power.

The simulation results of various ad –hoc network scenario shows that there are significant gains to be had if these technologies can be integrated in the existing wireless LAN physical layer and/or in the standard them self. Smart antennas along with slight modification in channel access scheme reduce co-channel interference dramatically and increases the number of simultaneous transmissions hence improves network throughput. Power management algorithm is shown to improve average transmission of a node.

We present a mathematical framework to characterize the outage probability of cellular mobile radio system with selective co-channel interference receiver in overloaded array environments. The mathematical framework outlines a general numerical procedure for

computing the probability of outage of a cellular mobile radio system that is equipped with a smart antenna to suppress a few strongest co-channel interferers (CCI) out of a total of $N_I$ active interferers by null steering.

**ACKNOWLEDGMENTS**

First and foremost I thank my parents for their unwavering support and faith in me. They have guided and motivated me through the most onerous days of my life. They taught me the importance of education and always encouraged me to work harder and better to achieve what I want.

My sincere appreciation and gratitude goes to my academic advisor, Dr. Annamalai Annamalai Jr. for his guidance and advice throughout my tenure in Virginia Tech. He has vastly improved my engineering and technical writing skills. I am grateful to my committee members Dr. Jeffrey H. Reed and Dr. Luiz Da'Silva for their constant help and suggestions.

It is my pleasure to acknowledge and extend a special thanks to my colleagues Payal Jain Shakeela Marikar, Vikas Kukshya, and Ramesh Chembil Palat for their constant motivation and various informative discussions I had with them over the course of my tenure. I would also like to thank the wonderful staff members of MPRG Michael Hill, Shelby Smith, Kristen Funk and Hilda Reynolds, have also been extremely kind and helpful throughout my stay.

Table of figures:

# Chapter 1 Introduction

Wireless ad-hoc networks especially, IEEE 802.11 based networks, are being deployed to provide full-fledged intranet as well as internet connectivity to both mobile and stationary users. These wireless networks are no longer an add-on support for the fixed Ethernet based network but have grown in stature and have become the backbone network carrying the traffic and serving the mobiles nodes. With the increase in traffic and number of nodes, these networks are reaching their capacity constrains in terms of network throughput and number of simultaneous transmissions and facing increased co-channel interference. Another critical issue is the limited battery supply on the mobile nodes. With the exponential increase in their use, the wireless nodes need a way to reduce their total operating power so that they can have more *up time*.

The issue of reducing operating power is basically a battery conservation problem and is critical in commercial environment, where consumer can be very demanding. Longer up time with a given battery power can be an important criteria for the consumer in buying a specific device or technology. Even in tactical networks (for e.g. military, secret operations) the issue of battery power consumption can become critical in hostile environment.

The bottleneck in network throughput for the existing IEEE 802.11b based wireless networks comes partly due to inefficient channel access mechanism. The RTS-CTS (request to send – clear to send) protocol, though successful in preventing any hidden terminal problem, is very inefficient in spatial channel access if used with omidirectional antennas at the wireless nodes. The pros and cons of using smart antennas in the physical layer of the IEEE 802.11 based networks are explored in great details in this thesis.

In the next section, we will review some of the literature already available on smart antennas and ad-hoc networks. This section also identifies the area of our research work and provides the background material to understand the need for a modified RTS-CTS protocol that will enhance the network capacity. Section 1.2 describes the motivation for

our work. Section 1.3 discusses the specific contributions of the thesis. The organization of this thesis is provided in section 1.4.

## *1.1 Review*

Smart antennas or adaptive antenna arrays are a well-researched area. But the application of smart antenna technology for small battery powered terminals has not been being investigated in great detail. Adaptive antenna array has long been regarded as a physical layer issue, with the research concentrating on the convergence of the various adaptive antenna algorithms, antenna beam patterns and other hardware implementation issues The impact of adaptive beam forming on higher layer protocols and it's interaction with Media Access Control (MAC) layer has not been adequately explored in the literature. Part of the reason is that till recently, the adaptive array algorithms and smart antenna hardware were not suitable for implementation in small mobile terminals. But with the recent advances in efficient algorithms and low power hardware implementation it has become feasible to implement antenna array technology on low power mobile nodes.

An analog beam forming architecture has been proposed in Takashi *et al*. [1] as an adaptive antenna suitable for battery operated terminals. The author(s) propose an interesting beam forming technique called Microwave Beam forming (MBF). MBF is a technique that forms antenna beam pattern at the radio frequency RF stage, as opposed to Digital Beam Forming, which is implemented at the baseband portion of the transreceiver. The conflicting requirements of high functionality and low power consumption are satisfied by analog based beam forming technique. Analog beamforming can be controlled digitally.

The ability to implement smart antenna technology at the mobile node of an ad-hoc network opens up a lot of new research areas, which can improve network and node performances. Some research has been conducted on the adaptive Medium Access Control (MAC) protocol that can utilize the smart antenna technology for improving the performance of the wireless ad-hoc networks. An adaptive MAC protocol designed to exploit the smart antenna technology has been proposed in Bandyopadhyay *et al*. [2]. The proposed MAC layer assumes that the nodes have the positional information of other nodes of the ad-hoc network. Thus the packet transmissions are done using directional

beampattern, which reduced overall co-channel interference in the network. But assuming that every node has positional information of every other node may not be practical or cost effective (If using GPS or other dedicated hardware to obtain the positional information). The performance improvement in wireless LAN using antenna beam forming for the access node has been studied in Anderson *et al.* [3]. They investigated the performance of an Access Node (AN), which employs a five-element smart antenna array and an adaptive beamforming algorithm. They reported substantial improvement in the average received SNR with using smart antennas as compared to the omni directional antenna.

An interesting result, based on the transmission range, has been reported by Kaixin Xu *et al.* [4]. They investigated the effect of interference from transmitting nodes, which are far from the receiving node. They reported that the a simple RTS-CTS based virtual carrier sensing mechanism will suffer in performance as interference range could be greater than the transmission range of the transmitter. This because the signal power required for interrupting a packet reception is lower than the signal power required to deliver a packet successfully. This reinforces the fact that power management is essential even in ad-hoc wireless network, as it can have substantial effect on the overall co-channel interference of the network. The level of co-channel interference determines the noise floor at the receivers and affects their bit error rate (BER) performance.

A relative direction determination using switched beams and a modified MAC layer has been presented in Kalis et al. [5]. They proposed a method of relative direction determination for mobile network nodes. They reported a significantly better BER for both BPSK and QPSK DSSS modulation for IEEE 802.11 based network. The proposed MAC layer was novel idea. In this thesis we extend the work of the modified MAC as proposed by kalis et al. to include the adaptive antenna array at the mobile nodes of the ad-hoc networks based on IEEE 802.11b standard. We outline a general numerical procedure for computing the probability of outage of a cellular mobile radio system that is equipped with a smart antenna to suppress a few strongest co-channel interferers (CCI) out of a total of $N_I$ active interferers by adaptive null-steering. Aside from the interference-limited case, refined outage criterion that either treat receiver noise as CCI or consider a minimum detectable receiver signal threshold are studied. Exact closed-

form expressions for both the basic and refined outage criterion are also derived by assuming that all the CCI signals are subject to Nakagami-m fading with a positive integer fading severity index. Selected numerical examples are provided to illustrate the application of the theory which includes the investigation into the effects of fade distribution of the CCI signals and traffic loading on the outage probability, and also the study of spectrum utilization efficiency improvement using a selective co-channel interference nulling (cancellation) technique.

## *1.2 Motivation*

From the above discussion it is apparent that a detail investigation of the effect of smart antennas on the wireless ad-hoc networks is required to fully understand the impact on the network throughput, the number of simultaneous transmission and the power efficiency of the wireless networks. It is also apparent from the above discussion that every research work on the use of adaptive antennas in wireless LAN environment either assumes an ideal physical layer response or a fixed gain by the smart antenna section in any given physical condition and direction. The impact of imperfect beam forming, non-convergence of the adaptive algorithms and the effect of fading, log normal shadowing and other wireless channel impairments have not been investigated in detail. The convergences behaviors of different adaptive antenna algorithms are different and hence the beam pattern formed by them may not be similar. The hardware implementation issue also needs to be investigated in detail to determine the complexity and cost of the smart antenna subsystem. This thesis investigates and extends the MAC protocol based on [3]. We will investigate the performance of the wireless LAN system under more realistic conditions like channel fading, imperfect algorithm convergence and co-channel interference. We will show that by using adaptive antenna arrays at the physical layer, the network throughput can be increased. Smart antenna also helps in lowering the Bit Error Rate (BER) at the receiver hence allowing the receivers to operate in the higher SNR region and give better performance.

Power management in ad-hoc network is a relatively new research area. It has been investigated in detail for cellular environments, which has a centralized architecture. But for wireless ad-hoc networks, which by definition are scattered and decentralized, power

management of the network cane be completely different. For battery powered wireless mobile terminals, the transmitter consumes the bulk of the battery power. It would be beneficial if the transmitter power efficiency can be optimized or if the transmitter utilizes the minimum required power to reach a given destination node. Stated another way if a transmitter uses a varying power level, depending on the network scenario (distance between transmitter, receiver, and channel fading) to adjust the transmission power then the power efficiency of the mobile terminal can be improved considerably. We propose a distributed algorithm employing smart antennas to implement a simple power management in the wireless ad-hoc networks. The algorithm, which will be implemented on every node, will work on link-by-link basis. By improving the transmission efficiency of each node, we can improve the power efficiency of the wireless network considerably.

## *1.3 Contribution*

The thesis contribution is two folds:

- Smart antenna in ad-hoc networks
    - Proposal of the modified MAC layer to accommodate the smart antenna in the wireless ad-hoc network.
    - The evaluation of the modified MAC using a simulation model consisting of various wireless network scenarios.
    - Proposal of a distributed algorithm for power management in the ad-hoc networks.
    - The evaluation of the power management algorithm using a simulation model consisting of various wireless network scenarios.
- Cellular system design using smart antenna. General numerical procedure for computing the probability of outage of a cellular mobile radio system in following scenario has been presented:
    - Interference limited case
    - Minimum signal requirement case
    - Treating receiver noise as CCI

- Numerical results for spectral utilization efficiency and reuse distance showing the practical usage of the proposed numerical methods.

The performance of each of the algorithms is presented in terms of network throughput, number of simultaneous transmissions and the average power required by the transmitter to transmit one packet. We also present the performance comparison between the smart antenna and omni-directional antenna scenario.

## *1.4 Thesis Outline*

This thesis is organized as follows. In chapter 2, an overview of the smart antenna technology and requirements for it's integration to wireless ad-hoc networks are discussed. We present various network models and scenarios to characterize the benefits of the smart antenna system. The different types of smart antenna algorithm are defined and explained in this chapter. Channel modeling, co-channel interference and their effect on the performance of smart antenna algorithms are explained in this chapter. Chapter 3 describes in detail the proposed algorithm for power management in wireless ad-hoc networks. The parameters pertaining to the algorithm are explained in this chapter. The performance results for the power management algorithm also presented in chapter 3. Chapter 4 discusses the mathematical model for the outage probability of cellular mobile radio system with selective co-channel interference cancellation in overloaded array environment. Some results are also presented in this chapter. Finally we conclude the thesis with some closing remarks and directions of further research.

# Chapter 2 Smart Antenna in Ad-Hoc Network

## *2.1 Introduction*

The objective of this chapter is to introduce and explain the characteristics of various facets of a smart antenna system. We will discuss various ways in which they can be integrated in a wireless ad-hoc network. We also explain the network scenarios and the different modes in which smart antennas may be used by a wireless mobile terminal. We will present a modified MAC protocol for the IEEE 802.11b based wireless LAN system employing RTS-CTS protocol that will enable the integration of smart antennas in the existing systems. The discussions and analyzes of the wireless network performance under various conditions are also presented in this chapter.

## *2.2 Smart antenna Requirements & Constraints*

Smart antenna is a term used for an array of two or more antenna elements weighted by complex weights. An adaptive algorithm assigns complex weights to each element. These weights are iteratively updated; hence the name adaptive antenna arrays. The assigned weights decide the resulting beampattern of the antenna array. The individual beampattern of the elements can be omni-directional or directional. When individual gain pattern are combined with the complex weights, the combined antenna beam pattern points towards the desired direction (i.e. the antenna array has its maximum gain towards the desired angle of arrival). The elements of the antenna arrays can be arranged in any physical configuration. Each configuration has its advantages and disadvantages. For simplicity in analysis we will consider a Linear Equally Spaced array (LES). Figure 2-1 shows the conceptual baseband complex envelope representation of a two-element LES array. As shown in Figure 2-1 each antenna element or branch has a complex weight "w" attached to it. This weight has both magnitude as well as phase. The signal received at the antenna element "m" is given by the following expression:

$$u_m(t) = As(t)e^{-jbm\Delta d} = As(t)e^{-jbm\Delta x\cos(f)\sin(q)} \qquad \textbf{Equation 2-1}$$

In the above expression we have assumed that each antenna array element has an isotropic (omni directional) beampattern and "A" is an arbitrary gain constant. "$x_m$" is given below

$$x_m = m\Delta x \qquad \textbf{Equation 2-2}$$

Where "m" is the antenna element number. The plane wave is represented by its baseband complex envelop "s(t)".

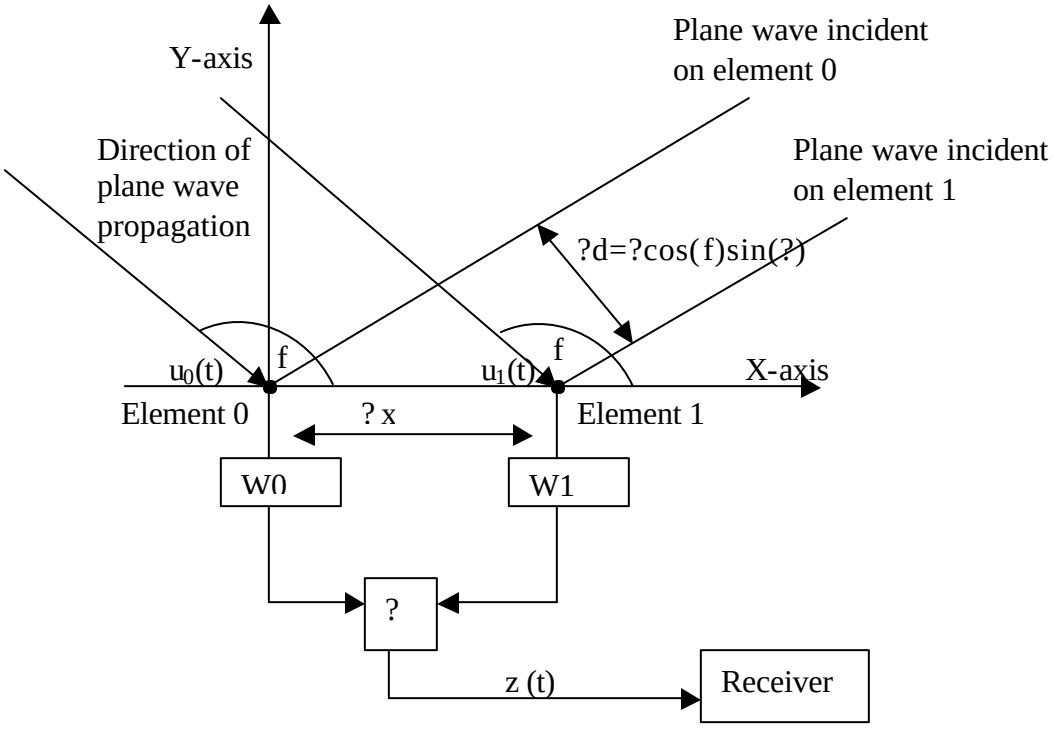


Figure 2-1. A baseband complex envelop model of a linear equally spaced array (M = 2) oriented along the x-axis, receiving a plane wave from direction (?,f) .

The signal at the output of receiver array "z(t)" is the summation of the signal received at each antenna element weighed by the weights of that element and can be represented as

$$z(t) = \sum_{m=0}^{M-1} w_m u_m(t) = As(t) \sum_{m=0}^{M-1} w_m e^{-jbm\Delta x \cos(f)\sin(q)} = As(t)\, f(q,f)$$

**Equation 2-3**

Where "f(?,f)" is known as the "Array Factor." Array factor determines the ratio of the received signal available at the array output, i.e "z(t)," to the signal "As(t)" measured at the reference element (Element 0) as a function of "(?,f)" or Direction-of-Arrival (DOA). It is apparent from equation 2.3 that by manipulating the weights "w" that are associated with each element branch we can steer the maximum of the beampattern in any desired direction of arrival. To illustrate this point let us consider the beampattern for a two element (M = 2, LES) antenna array with different complex weights presented in Figure 2-2 and Figure 2-3. As can be observed in Figure 2-2, with weights of (1,-1) the maximum of the beampattern is toward $0^0$ or the array is pointing towards $0^0$, while with a weight of (0.0422 -0.999i, 0.8206 + 0.5716 i) the array is pointing towards $45^0$ as shown in Figure 2-3

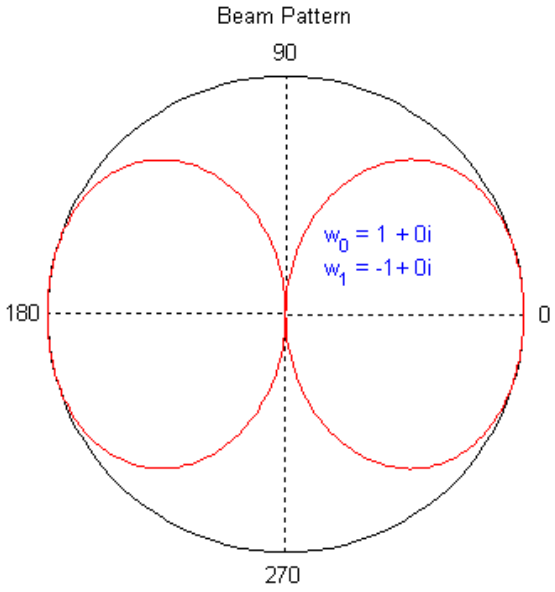


Figure 2-2 A typical beampattern for a two element antenna array pointing towards $0^0$.

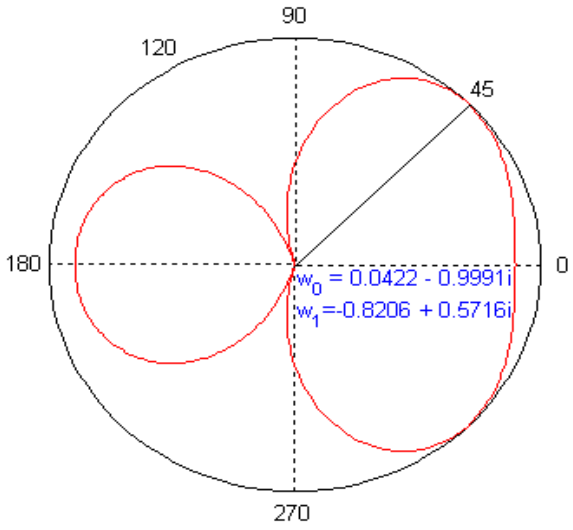


Figure 2-3 A typical beampattern for a two element antenna array pointing towards $45^0$.

Thus by manipulating the complex weights, an antenna array can be made to point towards any desired direction. In actual implementation an adaptive algorithm controls the weight manipulation. This algorithm updates the weights of the antenna array depending it's cost criteria. Since such algorithms are capable of adapting to the mobile scenario of the network and the varying nature of the wireless channel, they are called adaptive antenna array algorithms. The weight vector "w" is adapted / updated to maximize the quality of the signal at the input of the demodulator. The weight vector is usually determined such that it minimizes a cost function. This cost function is usually inversely associated with the quality of the signal at the antenna array output. Thus by adapting a weight vector, which minimizes the cost, the algorithm maximizes the quality (e.g. Signal to Noise Ratio) of the received signal. In our simulation we have considered three algorithms: LMS (Least Mean Squares), CMA (Constant Modulus Algorithm) and a fast constrained null steering algorithm. A description of each algorithm along with the explanation of their cost function is provided below.

### 2.2.1 LMS (Least Mean Squares)

The LMS algorithm is one of the most widely used algorithms for iteratively updating the adaptive arrays. It is a derivative of a Minimum Mean Square Error (MMSE) optimal beamforming technique. In MMSE algorithms the weight vector is determined as to minimize a cost function. The cost function is chosen to be inversely proportional to the quality of the signal at the array output. Equation 2-4 gives the concise form of the LMS algorithm.

$$w_{k,i} = w_{k,i-1} - mu_{i-1}\left(u_{i-1}^{H} w_{k,i-1} - d_{k,i-1}^{*}\right) \qquad \textbf{Equation 2-4}$$

where $w$ is the weight vector, $i$ is the current sampling instant, $k$ is the signal number, $m$ is the convergence factor, $u$ is the received sample vector and $d$ is the locally constructed symbol. $H$ denotes the "Hermitian transpose" and * denotes the conjugate operation. A detailed derivation for equation 2-4 is presented in [8]. The determination of the correct value of $m$ is heavily dependent on the environment and is usually an art rather than science. We implemented the LMS algorithm on the TMSC67XX based VT-

STAR communication system and found out the typical value of $m$ for an indoor office environment. The results of the implementation are presented in sub-section 2-6.

### 2.2.2 CMA (Constant Modulus Algorithm)

The CMA algorithm belongs to the group of blind adaptive algorithms that attempt to restore some know property of the received signal (e.g. modulus). The CMA algorithm tries to restore the modulus of the received signal to a known constant. The cost function for the CMA algorithm is presented in Equation 2-5

$$J(w_k) = E\left[\left|\left|w_k^H u_i\right|^p - \left|a\right|^p\right|^q\right] \qquad \textbf{Equation 2-5}$$

Where $a$ is the desired signal amplitude at the antenna array output. The exponents $p$ and $g$ are used to control the convergence behavior of the CMA algorithm. Their value is usually taken as 1 or 2. We implemented the CMA adaptive beam forming algorithm on the TMSC67XX based VT-STAR communication system and found out the typical value of $a$ for an indoor office environment. The results of the implementation are presented in sub-section 2-6.

### 2.2.3 Fast Constrained Null Steering Algorithm

The fast-constrained null steering algorithm is based on the LMS technique. Since the convergence of LMS is heavily dependent on the noise environment, it can be slow in converging under severe noisy environments. The fast-constrained null steering algorithm uses a simplified cascade structure of weight coefficients to null and adapt to certain interference environments. Equation 2-6 gives the fast null constrained algorithm

$$w_i = P\left[w_{i-1} - \Delta_s R_{aa} w_{i-1}\right] + f \qquad \textbf{Equation 2-6}$$

$$P = I - c\left(c^T c\right)^{-1} c^T$$

$$f = c\left(c^T c\right)^{-1} c^T$$

$$c = \left[1 \ldots 1\right]^T$$

where $I$ is the "$n \times n$" identity matrix, "$n$" is the number of antenna elements, "$c$" is $1 \times n$ ones vector, $R_{aa}$ is the correlation matrix of the received signal. "$T$" denotes the transpose operation, "-1" denotes the matrix inverse operation. "f" is the constraint for the algorithm and is decided by the designer. It is represented as

$$c^T w = f \qquad \textbf{Equation 2-7}$$

The detailed derivation for the fast null constrained algorithm is provided in reference [9].

## 2.3 Wireless Ad-Hoc Network

A wireless mobile ad-hoc network is an autonomous system of mobile nodes with compatible air interfaces. The nodes are capable of transmitting to and receiving from any other nodes within their antenna coverage area. In order to communicate with nodes that are not in their antenna coverage area they may route their transmission packet through an intermediate node. This type of communication is called multi-hop communication and its performance is heavily dependent on the routing protocols. In this thesis we will consider communication between nodes that are in each other's direct antenna coverage area. We will consider single hop traffic our analysis and simulation. We have chosen an IEEE 802.11b based wireless Local Area Network (LAN) system to investigate the effect of smart antennas on wireless ad-hoc networks. Typically the nodes, in wireless a LAN, are assumed to be equipped with a single antenna having isotropic (Omni-directional) beampattern as shown in Figure 2-4.

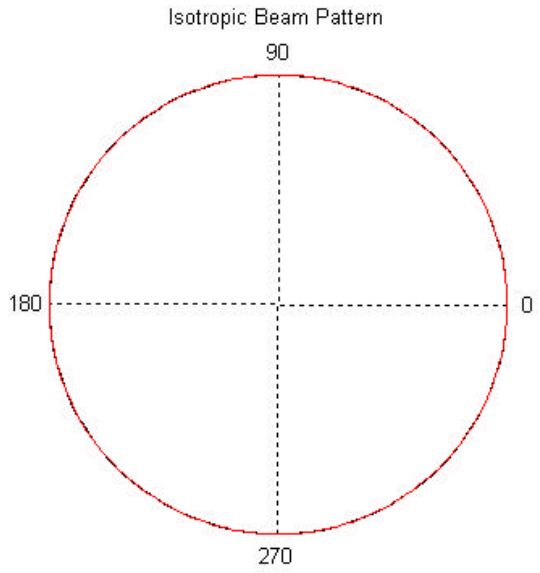


Figure 2-4 A typical isotropic (omni-directional) beampattern for a single element antenna.

As is apparent from Figure 2-4 the antenna gain is constant in all directions in azimuth (horizontal) plane. A constant gain in every direction at the receiver results in each signal being amplified by the same amount whether it is a desired signal or co-channel interference from other nodes or jammers. At the transmitter an omni directional beampattern implies that the transmitter is transmitting in the direction of the desired node as well as other non-desired directions with equal power, thus spending more power than is needs and thus increasing the interference levels of the wireless network.

The nodes in a wireless LAN employ an RTS-CTS protocol at the MAC layer for accessing the channel and eliminating the hidden terminal problem. An illustration diagram of the RTS-CTS protocol is presented in Figure 2-5 to 2-8. A typical wireless LAN distribution of four Nodes “A”, “B”, “C”, “D” is shown in Figure 2-5. Node “A” wants to communicate with Node “B” while Node “C” is in the antenna range of Node “A”. An antenna range is defined as the longest distance from which a node can successfully transmit to the receiver. Hence if both Node “C” and Node “B” transmit simultaneously to Node “A” then their transmission packets will collide at Node “A” and the transmission will be garbled. Since Node “C” is not in the antenna range of Node “B” it is a hidden terminal to Node “B”. To avoid the problem associated with hidden

terminals the IEEE 802.11 standard has adopted an RTS-CTS Medium Access Protocol (MAC). In this protocol a node wishing to initiate communication (Node "A") transmits an RTS packet as shown in Figure 2-6. Both nodes C and B receive this packet. Since the packet is addressed to Node "B", it replies with a CTS packet as shown in Figure 2-7 while Node "C" holds off any further transmission of its own. Node "A" and any other node in the vicinity of Node "B" receive the CTS packet sent by Node "B". Since the packet is addressed to Node "A", other nodes will hold off their transmission. After receiving the CTS packet from Node "B", communication between Node "A" and Node "B" commence without any interference from Node "C" and Node "D" as shown in Figure 2-8.

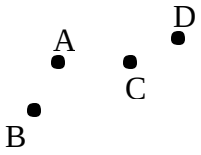


Figure 2-5 A typical Wireless LAN distribution of four Nodes A, B, C, D where Node "A" wants to communicate with B.

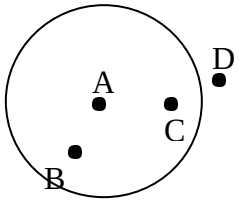


RTS by
Node "A"

Figure 2-6 Node "A" transmits a RTS packet to Node "B". Node "B" and Node "C" receive this packet. Node "C" holds off any transmission.

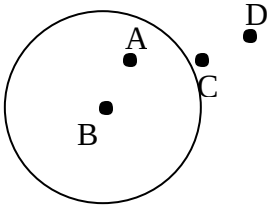


Figure 2-7 Node "B" responds with a CTS packet.

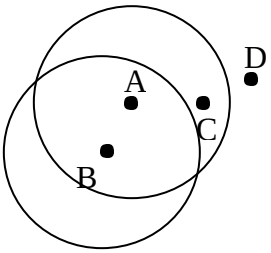


Figure 2-8 Node "A" and Node "B" are communicating with each other while Node "C" is waiting for the communication to finish before it can start transmitting.

## 2.4 Smart Antenna in Wireless Ad-Hoc Network

We propose to use smart antenna arrays at the physical layer to improve the channel access efficiency of the nodes in a wireless LAN. As can be observed from Figures 2-5 to 2-8, where all the nodes are using omni directional antennas, the channel access efficiency deteriorates due to omni directional transmission and reception of the Radio Frequency (RF) energy. For example, consider the scenario depicted in Figure 2.5-2.8, if Node "A" and Node "B" are communicating then Node "C" cannot communicate with Node "D" due to transmission hold imposed by the RTS CTS protocol. Now consider all the nodes to have smart antennas and beamforming capability. In the new scenario, when Node "A" wants to initiate communication with Node "B" it sends an RTS packet to Node "B" with the antenna beampattern pointing (having the maximum gain) towards Node "B" as shown in Figure 2-9. Notice that since all (ideally) the RF energy of the Node "A" is directed toward the Node "B", only Node "B" receives the RTS packet and Nodes C which is also in the omni directional antenna range of Node "A", does not receive any packet due to lower antenna gain towards it. Node "B" then replies with a CTS packet as shown in Figure 2-10.

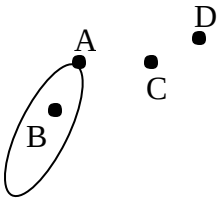


Figure 2-9 Node "A" sends an RTS packet to Node "B" using smart antenna with a beam pattern pointing towards Node "B".

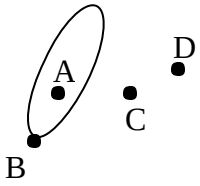


Figure 2-10 Node "B" responds with a Clear To send (CTS) packet using smart antenna with a beam pattern pointing towards Node "B".

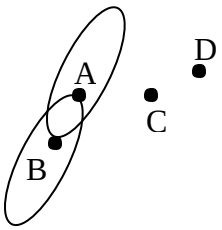


Figure 2-11 Node "A" and Node "B" are communicating with each other with beam pattern pointing toward each other.

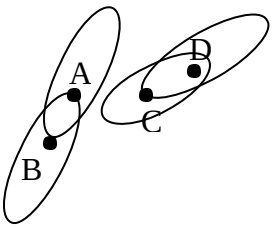


Figure 2-12 Node "D" and Node "C" are communicating with each other without interfering with the communication between Node "A" and Node "B".

Now Node "A" and Node "B" start to communicate with each other. Since Node "C" and Node "D" have not received either an RTS or an CTS packet they are free to initiate their own communication with their antenna's beam-pattern's pointing toward each other as shown in Figure 2-12. Thus, by employing smart antenna the throughput of the network has improved because of improved channel access efficiency. This is a simple example but it shows the dramatic effect that the smart antenna technology can have on the throughput of a wireless ad hoc network by allowing higher number of simultaneous transmissions. The above example is a simple solution to the exposed node problem. Figure 2-13 shows the smart antenna subsection in the protocol stack of wireless LAN with reference to the OSI layer. Notice that the smart antenna subsection or the smart antenna controller software interacts both with the upper layer and the physical layer for beamforming and with baseband layer for receiving the data.

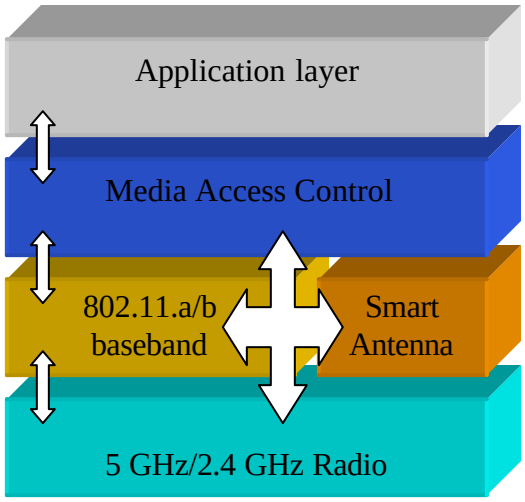


Figure 2-13 A conceptual OSI based model for the smart antenna integration with wireless LAN protocol stack.

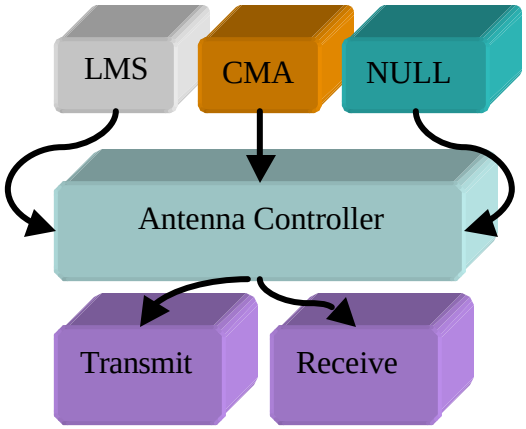


Figure 2-14 Smart Antenna Subsection

There are various flavors of smart antenna algorithms (as described in section 2.2) that can be used in conjunction with each other or just by themselves to improve the network throughput. Figure 2-14 presents a conceptual diagram of the smart antenna section. We have selected the following scenarios to investigate and study the effect of smart antennas on an ad-hoc networks.

### 2.4.1 Transmit Beamforming with Positional Awareness

Smart antennas can be implemented both at the receiver and at the transmitter in a node. In order to utilize the smart antenna for transmission, the position information of the target node should be available to the smart antenna subsection of the physical layer. The position information could be in terms of the angle with reference to the node's antenna axis or with reference to some global coordinate system as provided by a Global Positioning System (GPS). The nodes in an ad-hoc network can acquire the positional information of the surrounding nodes as they communicate with each other. Section 2.4.3 further explains this mode of operation. If positional information of the target node is available to the transmitting node, then it can be utilized by the antenna arrays to improve the transmission efficiency and lower co-channel interference in the network. Whenever a transmitter has to initiate a communication it will transmit an RTS packet towards the

target node using the directed beam pattern. Since the beam pattern will be pointing towards the desired node, fewer nodes will receive this packet. The target node will respond with a CTS packet utilizing a beam pattern that is pointing towards the original node. Since this transmission is also directed, fewer nodes will receive this packet than compared to omni directional antenna case. Figure 2-15 presents the above-described scenario for 100 nodes in a 100x100 $m^2$ area. Figure 2-16 presents same network scenario with omni directional antennas. The network throughput is also shown in Figure 2-15 and 2-16. The network throughput is defined as the average number of packets being transmitted at the same time in that packet slot (For simulation purpose we have divided the time in packet slots). It can be observed that the network throughput is much higher in the smart antenna scenario than in the omni directional antenna scenario. The increase in network throughput is the result of improved space division multiple accesses enabled through smart antennas.

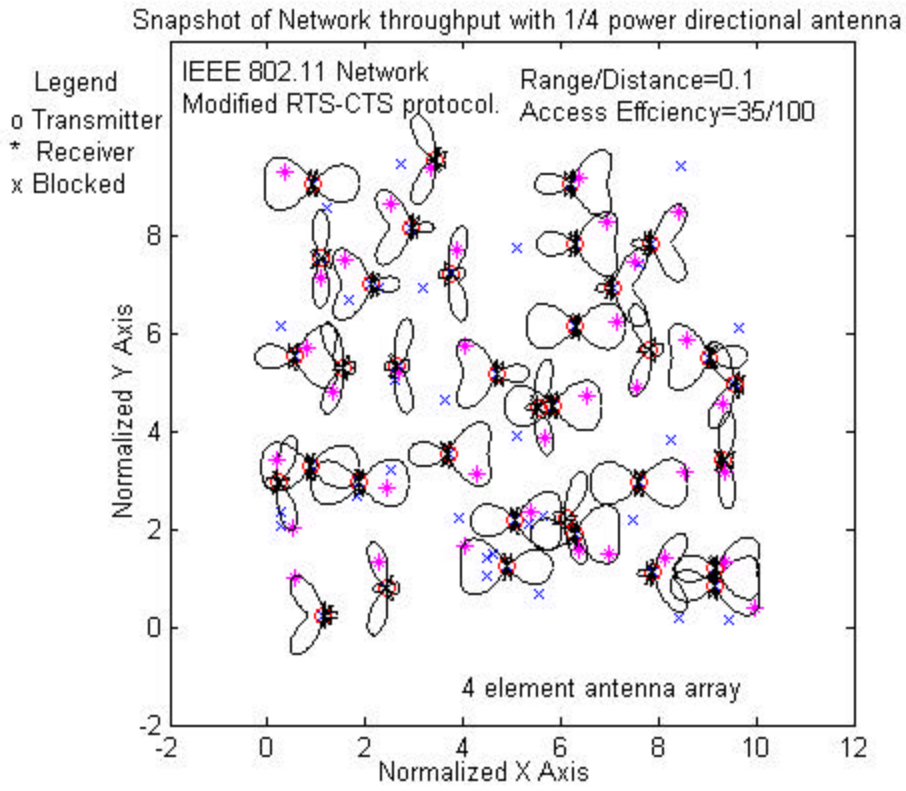


Figure 2-15 Network throughput with smart antenna, x and y axis varies between 0 to100 meters.

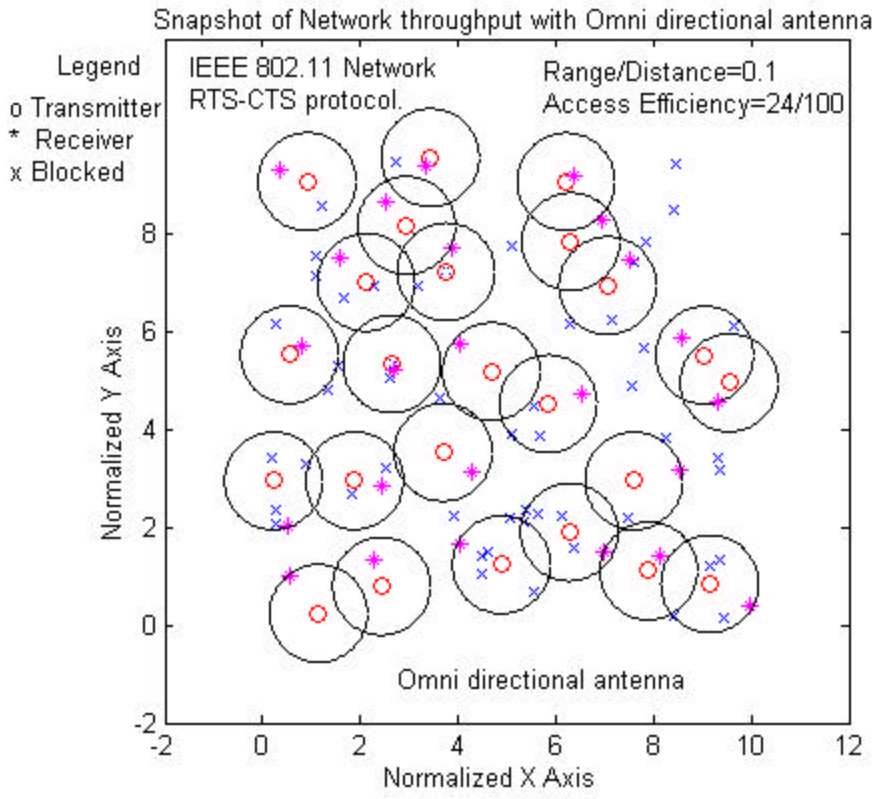


Figure 2-16 Network throughput with omni directional antenna, x and y axis varies between 0 to 100 meters.

The results presented above are heavily dependent on the traffic pattern and node distribution. But for a network with high node density and high traffic load for each node the average throughput with smart antennas would, on the average, be better than the omni directional scenario.

### 2.4.2 Adaptive Beamforming/Null Steering at Receivers

The smart antenna technology at the receiver takes the form of an antenna array with different adaptive array algorithms. There are two types of adaptive antenna algorithms

a) Beamforming

b) Null Steering

A beamforming algorithm at the receiver tries to steers the maximum of the antenna beam pattern towards the desired transmitter and nulls towards the undesired transmitters, referred to as interferers. By directing its receiver antenna beampattern towards the

desired transmitter it increases the desired signal strength and attenuates the RF energy from undesired transmitters, thus substantially increasing the signal to noise ratio (SNR) of the received signal. Subsections 2.2.1 and 2.2.2 present the two beamforming algorithms considered in this thesis: LMS and RLS.

Null steering algorithms are very useful in the presence of a high-energy interference sources. The null steering algorithm tries to steer a very deep null (very low gain in the antenna beam pattern) towards the source of interference and maintains a constant gain (referred to as a constraint) towards the desired direction or node. An example could be a microwave oven sending high RF energy in the wireless LAN 802.11b spectrum. To minimize this interference, nodes in the network can use the null steering algorithm to stem out the interfering signal at the receiver. Some of the null steering algorithms do require positional information of the desired nodes. Subsection 2.2.3 provides the description of the fast constraint null steering algorithm considered in this thesis.

When smart antennas are implemented using adaptive array algorithms no position location information of the transmitter is necessary. An excellent aspect of the adaptive beamforming algorithm is that it can track the transmitter's motion and or channel condition and update the weight vector to correctly point the antenna beampattern towards the desired transmitter.

### 2.4.3 Combined Approach

It is possible to make the MAC protocol to utilizes both of the approaches described in subsections 2.4.1 and 2.4.2. In the mixed approach both the transmitter and the receiver of a given node will use smart antenna techniques. The advantage of this approach would be considerable in terms of better SNR at the receiver, reduced overall co-channel interference and better network throughput.

The antenna sub section of the MAC protocol can be made smart enough to use one of the above described approaches or to use the combined approach, depending on the network scenario. The MAC layer can choose between the best adaptive algorithm and the best approach (transmit beamforming, receive beamforming or a combination of both) in a given network scenario. We present a modified RTS-CTS protocol for the IEEE 802.11b wireless LAN standard to incorporate the smart antenna technology. The

proposed modification can be extended to any ad-hoc network to accommodate smart antennas.

### 2.4.4 Modified Medium Access Protocol (MAC)

The Medium Access Control protocol in a wireless network such as the 802.11b wireless LAN performs the challenging task of resolving contention amongst the competing nodes while sharing the common wireless channel for transmitting packets. To integrate the smart antenna technology in 802.11b networks, we propose a modified version of the RTS- CTS protocol based on the concept presented in [3]. The MAC protocol proposed in [3] used M directional antennas per node. They divided the azimuth plane into M sectors, with each sector covering 360/M degrees. While the idea of the MAC protocol is innovative, it suffers from the practical difficulty of implementing more than four antenna elements. In our proposed MAC we use the adaptive beam forming technique to steer the beampattern of the antenna array, thus extracting better performance even with two or four antenna elements. We also incorporate a method by which a node can use smart antennas for transmit beamforming. The proposed MAC protocol for accessing the channel is presented in the flowchart of Figure 2-17 and 2-18. The flow chart is divided into a transmit section and a receive section. A detailed explanation of the flow chart is presented in following sections.

#### 2.4.4.1 Transmitter Node

Figure 2-17 presents the flow chart of the modified RTS and CTS protocol that runs on the node initiating the communication. It starts with an omni directional beam pattern and as the node starts to communicate with other nodes the algorithm builds up a weight vector look up table to use for transmit beamforming. Initially the transmit lookup table would be empty. Whenever a node receives a packet, its adaptive receive beamforming algorithm will update the receive weight vector. This weight vector will result in a beampattern that is pointing towards the desired transmitter. The same weight vector can be used by the transmitter to point the transmit beampattern towards the desired node. As the network communication proceeds every node will start to update it's transmit weight

vector table. Gradually all the communication will be via directed transmit beampattern and adaptive receive beampattern.

#### 2.4.4.2 Receiver Node

Figure 2-18 presents the flow chart of the modified RTS and CTS protocol that runs on the receiving node. The receiver initializes the receive weight vector to omni directional beampattern and starts the adaptive beam forming algorithm. Whenever it receives an RTS packet, the node will store the converged weight vector in the transmit look up table for the transmitter. The transmitter will use this stored weigh vector to transmit the packet. The receiving algorithm will continue to update the look up table every time it receives a packet. If a node has previously received an RTS or a CTS packet and is holding off its transmission, then it will determine the free directional splice that is available to it for transmission without interfering any on going communication around it. The determination of directional splice will depend on the number of antenna elements and structure of the antenna array. For LES array with two elements there are two directional splices. Splice one covers direction from zero to one hundred and eighty degrees and splice two covers direction from one hundred and eighty one to three hundred and sixty degrees. For circular antenna array structure the number of directional splices are be directly proportional to the number of antenna elements.

Figure 2-17 MAC Protocol state diagram when the node receives a request for communication

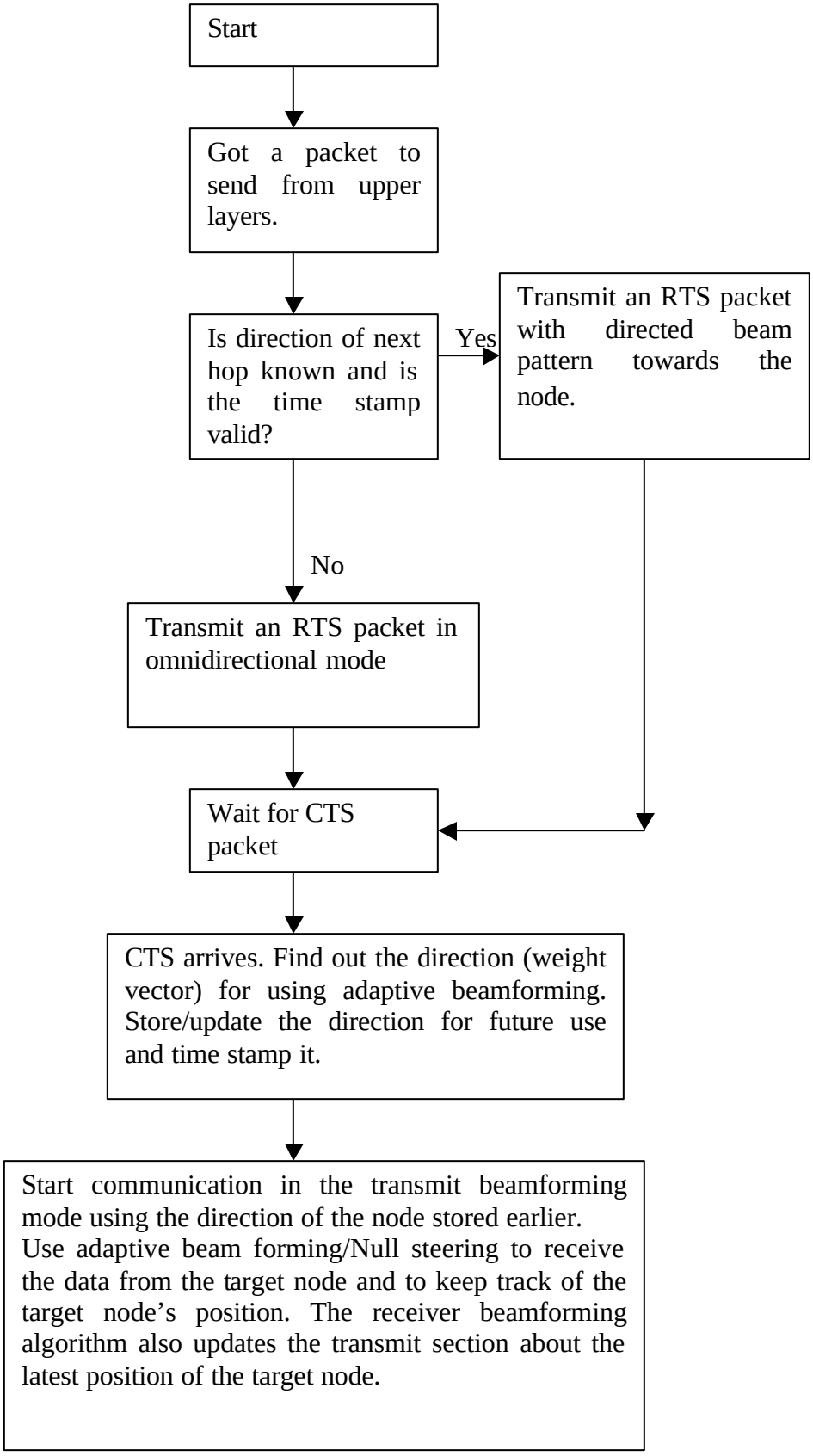

Figure 2-18 MAC Protocol state diagram when the node receives a request for communication.

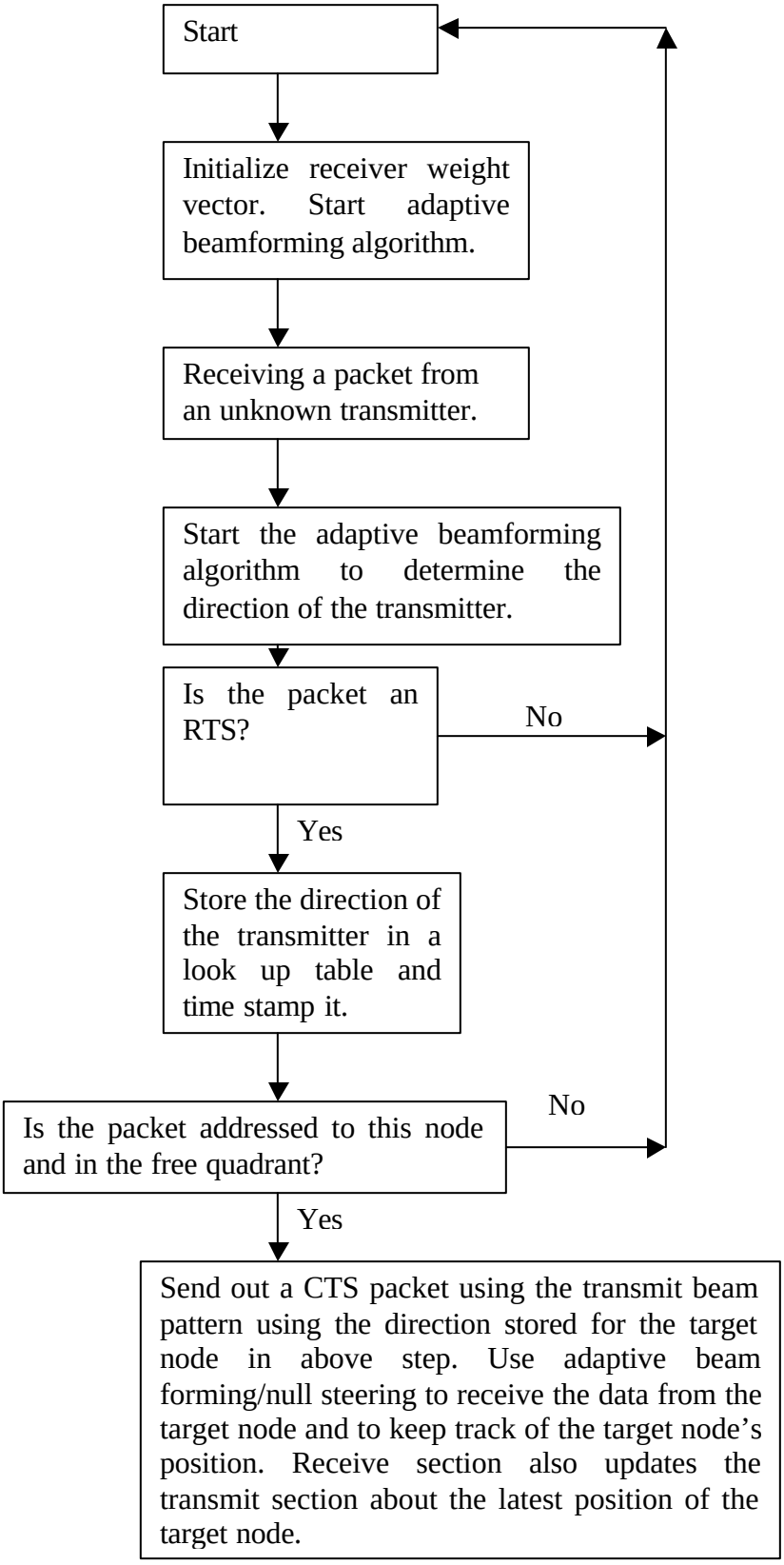

## 2.5 System Model

The objective of this section is to explain the characteristics of the simulation model we have developed. We use this simulation model to study the feasibility and the performance characteristics of our proposed smart antenna and power management algorithms. The aim of the proposed algorithms is to optimize the channel access efficiency and minimize the required power needed to transmit a packet in an 802.11b based wireless ad-hoc network using smart antennas. We needed a simulation model that incorporated spatial diversity. We assumed a strong line of sight signal component with multi-path delay spread less than the chip duration [16]. A Rician flat fading channel model fulfills the criteria. In this section we develop and explain a suitable simulation system model, implemented in MATLAB, which satisfies all the requirements while keeping complexity and simulation run time to a practical level.

### 2.5.1 Simulation Model Outline

Figure 2-19 shows the basic diagram and flow of the simulation model. We will go through each of the blocks in more detail in the following sections. The simulation commences by distributing the nodes in a square network area of dimension NxN. For every node a traffic load is defined at the start of the simulation. Each node that has a packet to transmit, contend for the channel via a simplified 802.11b MAC protocol. The implementation includes the RTS-CTS protocol. Upon accessing the channel, the nodes then transmit the packet. The flat fading Rician channel affects the transmitted data. The receiver receives the data and processes it according to the simplified MAC protocol. Various network statistics are collected for later analysis and presentation. A simplified version of the 802.11b MAC was implemented to make the simulation tractable and keep the simulation time reasonable. We incorporated the RTS and CTS collision avoidance mechanism, collision back off and an acknowledgement for every received data packet.

Figure 2-19 Simulation System Model.

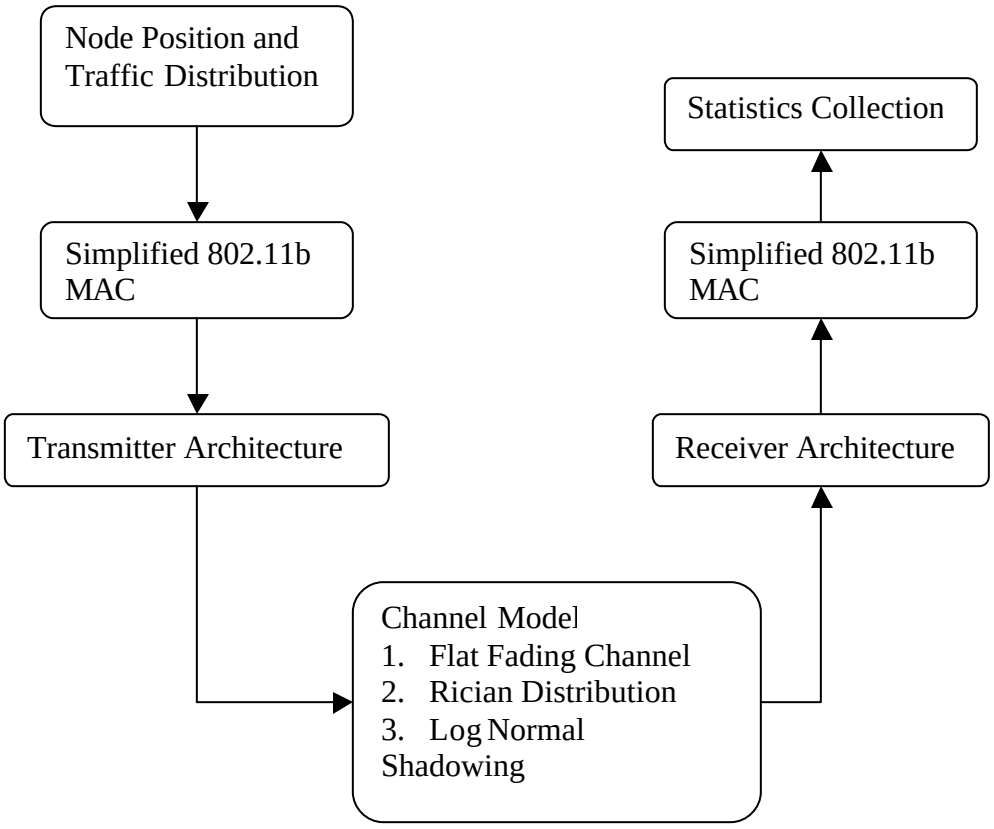


### 2.5.2 Transmitter/Receiver Architecture & Specification

The transmitter and the receiver specification were taken from commercially available wireless LAN products to make the simulation model resemble a real world scenario as closely as possible. Table 2-1 provides the specification for the implemented transmitter and the receiver characteristic.

**Table 2-1 Transmitter/Receiver Specification**

| | *Characteristic* | *Specification* |
|---|---|---|
| **Transmitter** | | |
| | Maximum Transmit Power | 20dBm |

| | | |
|---|---|---|
| | Minimum Transmit Power | 1dBm |
| | Spreading Gain | 11 |
| | Chip Duration | 4.08 e-10 sec |
| | Center Frequency | 2.45GHz |
| **Receiver** | | |
| | Sensitivity | -80dBm |
| | Operating SNR | 12dB |
| | Antenna Array | LES, Circular |
| | Number Of Elements | 1,2,4 |
| | System Loss | 2dB |

### 2.5.3 Node Position & Traffic Distribution

The nodes were distributed in a square network area having a dimension of NxN. The network dimension was varied between 10 m to 200 m to study the performance of the proposed algorithm on the network throughput under different network area. Table 2-2 presents the random distributions of nodes in the network that were considered

**Table 2-2 Node position & traffic distribution specification**

| *Distribution Type* | *Characteristic* | *Specification* |
|---|---|---|
| Uniform | The x and y coordinates were distributed uniformly in the network area. | x = uniform(10,N)<br>y = uniform(10,N) |
| Gaussian | The x and y coordinates were distributed with Gaussian distribution around the center of the network. | Mean = 0<br>Variance =3 |

### 2.5.4 Channel Model

To accurately investigate the effect of smart antenna on the ad hoc networks, a realistic channel model was needed. The convergence behavior of the adaptive algorithm and the corresponding antenna beampattern are heavily dependent of the channel environment. For our simulation model we have considered a quasi-indoor environment (a big hall type

indoor environment without many objects to block the line of sight (LOS) communication, e.g. airport lounge, hotel lounge, and malls). For our environment the multipath delay is less than the chip duration [16] of the waveform. Consequently the received signal amplitude will undergo flat fading. We are assuming at least a strong LOS component, hence we implemented a Rician flat fading channel. The various channel properties are listed in table 2-3.

**Table 2-3 Channel model specification**

| | *Characteristic* | *Specification* |
|---|---|---|
| Chip Duration | | 0.408 *ns* |
| Mean Multipath Delay | Average time of arrival of multipath component. | $34 \pm 10ns$ |
| Fading | Flat Fading as Chip duration < Mean multipath delay | Path loss exponent=3.5 |
| Rician Distribution | Line of sight assumed | $k = 6dB$ |
| Log Normal Shadowing | | Variance = 8dB |

## 2.6 Throughput Results for Wireless LAN 802.11 b

In this section we present the performance of the proposed MAC layer for an IEEE 802.11b based wireless LAN system. The performance metrics is network throughput in terms of number of simultaneous transmissions, number of blocked nodes and average maximum delay of the network. The performance of the smart antenna system is heavily affected by the transmit power. To accurately analyze and study the network performance with a smart antenna system we ran two different types of simulations:

- ***Constant EIRP****:* In this type of simulation we defined the maximum effective isotropic radiated power (EIRP) for each node in the wireless network. By defining the maximum EIRP, we characterized the maximum transmit power from a node including the gain in any direction from the antenna subsystem. In other words we equated the transmit power of the omni directional antenna to

that of the transmit power of the smart antenna system in the direction of the maximum gain. By defining a maximum for the EIRP we defined a common maximum distance that both the antenna subsystems can effectively reach.

- ***Constant power to antenna subsystem:*** In this type of simulations we defined a constant power that should be applied to both antenna systems (omni directional and smart). The result of defining a constant power is different maximum range achieved by the two antenna systems. The maximum range of the smart antenna system would depend on the gain in that direction, hence the maximum distance covered by the smart antenna subsystem can be greater than the omni directional scenario.

Figures 2-15 and 2-16 represent the constant EIRP scenario as the maximum transmit range for both the antenna systems are same. We found that the network throughput performance varies considerably between these two scenarios.

### 2.6.1 Test Scenario I

The simulation parameter for this test scenario is presented in table 2-4. This test scenario presents a wireless network with nodes distributed uniformly along both X and Y coordinates. The simulation was run for enough packet slots so that the weight tables get updated and nodes can start communicating using smart antennas.

**Table 2-4 Simulation Parameter Test Scenario I**

| *Characteristic* | *Specification* |
|---|---|
| Simulation Type | Constant EIRP |
| Node Distribution | Uniform along X,Y |
| Number of Nodes | 50 |
| Number of Antenna Element | 4 |
| Adaptive Algorithm | LMS |
| Transmit Power | 15.48dBm (35.4mWatts) |
| Antenna Structure | LES |

Figure 2-20 presents the throughput of the network with and without the use of smart antennas. The x-axis is the time axis divided in packet slots. The y-axis is the number of packets transmitted in that slot. It can be observed that the network throughput is better when modified MAC with smart antenna is adopted at the physical layer. This result is

clearer by comparing the average throughput in the two scenarios. The average throughput of the network with smart antennas is 7.624 packets/slot while the throughput achieved with the conventional MAC is 6.856 packet/slot. Even though the actual numbers of transmitted packets are heavily dependent on the traffic model and node distribution, Figure 2-20 illustrates that for the same traffic load and same node distribution the throughput of the network is higher when smart antennas are employed. The graphs seem very irregular because of the bursty nature of the network traffic.

Figure 2-21 presents the number of nodes that are holding off their transmission due to receiving either an RTS or a CTS packet destined for other nodes. It can be observed that at the start of the simulation, when the all nodes are building their look up table (for storing the weights), the number of nodes in the BACKOFF state is approximately same for smart antenna and omni-directional scenario. As nodes communicate more with each other the look up table start to build up. The nodes begin to use the smart antenna (by using the weight lookup table) to transmit the packets. The spatial efficiency of the smart antenna takes over and the number of nodes in BACKOFF state in smart antenna scenario starts to drop as compared to the omni-directional scenario.

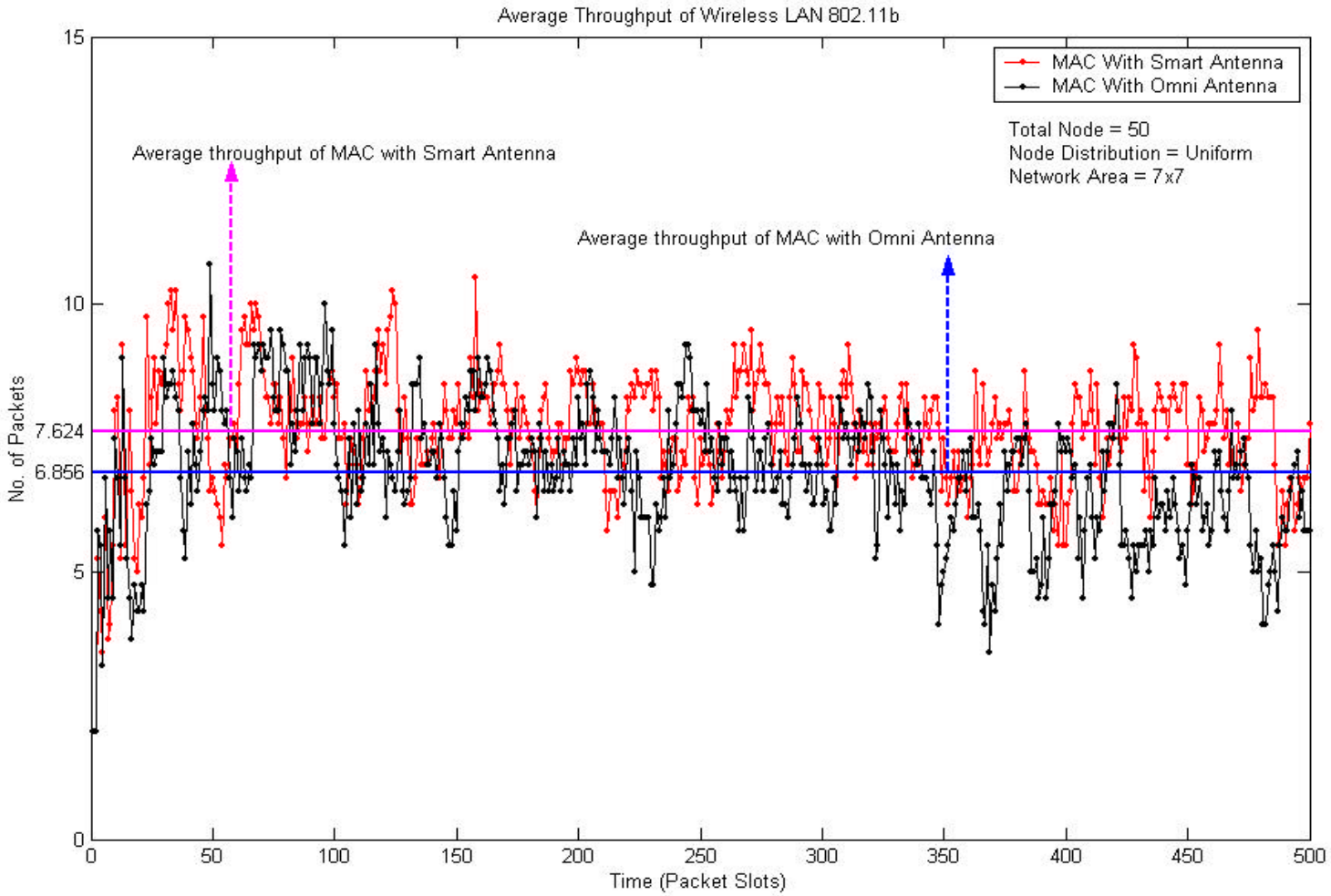


Figure 2-20 Network throughput comparison in single hop uniformly distributed nodes.

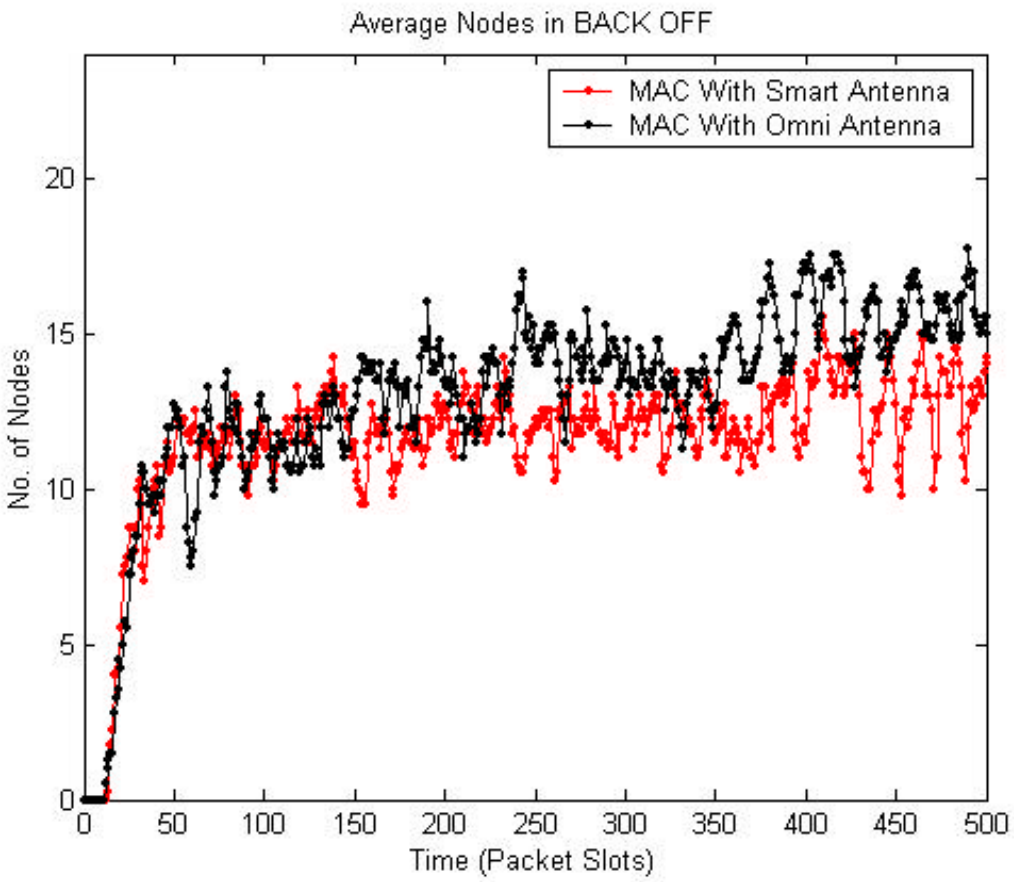


Figure 2-21 Number of nodes in RTS-CTS Backoff state.

### 2.6.2 Test Scenario II

This simulation is the same as in section 2-6-1. Since the throughput of the network is heavily dependent on the node position and the network area, we present the throughput comparison between with MAC using smart antennas and network with MAC using omni directional antenna.

**Table 2-5 Simulation Parameter Test Scenario II**

| *Characteristic* | *Specification* |
|---|---|
| Simulation Type | Constant EIRP |
| Node Distribution | Uniform |
| Number of Nodes | 50 |
| Number of Antenna Element | 4 |

| | |
|---|---|
| Adaptive Algorithm | LMS |
| Transmit Power | 15.48dBm (35.4mWatts) |
| Antenna Structure | LES |

Figure 2-22 presents the average network throughput represented as a percentage with respect to the omni directional case. It can be observed that the network throughput is very low when nodes are distributed in a small area because the nodes are in back off mode due to RTS CTS protocol. As the network area is increased the throughput increases for both the smart and omni directional antenna scenarios. But it can be observed that the performance of network with MAC using smart antenna is consistently better than the network with MAC using omni directional antenna.

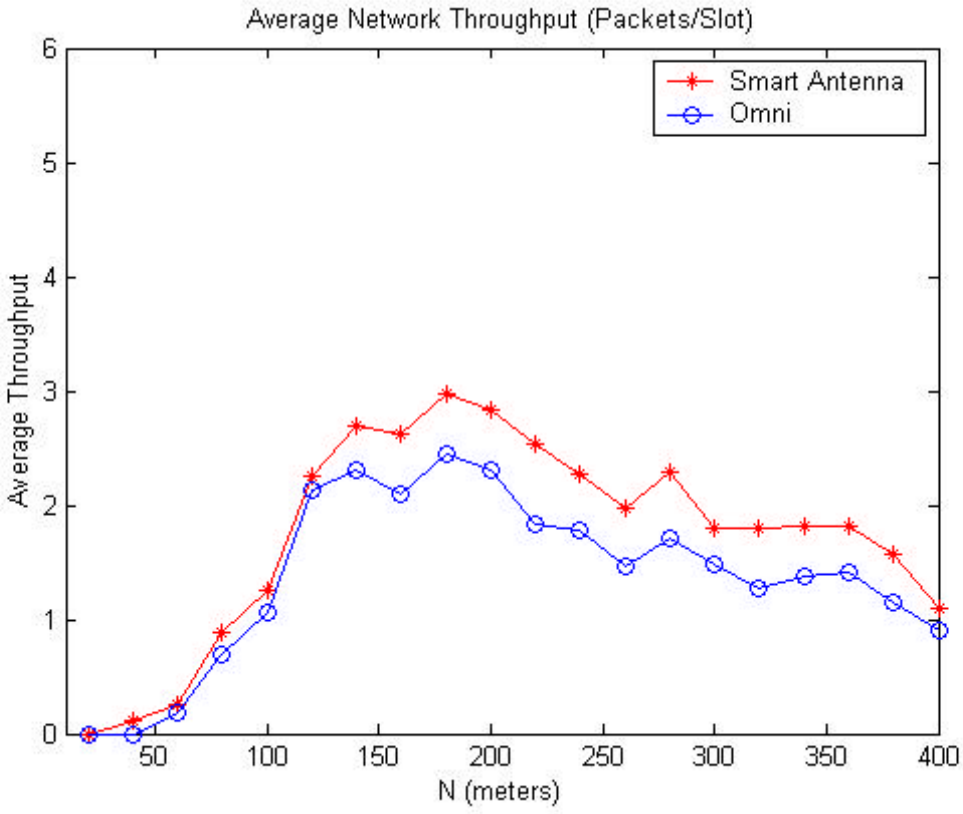


Figure 2-22 Average network throughput with varying network area. Four element array, constant EIRP.

### 2.6.3 Test Scenario III

In this scenario the power supplied to antenna subsystem is kept constant, which results in varying transmit power depending on the gain of the smart antenna. The network throughput is heavily dependent on the ratio of the antenna range and the network dimension. If the network dimension is small then all the nodes would be in the transmit range of a given node. Hence even if one node were transmitting most of the nodes would go into RTS-CTS back off. The throughput represented as percentage of to the omni directional scenario is presented in Figure 2-23. It can be observed that the network with smart antenna performs consistently better in this scenario.

**Table 2-6 Simulation parameter Test Scenario III**

| *Characteristic* | *Specification* |
|---|---|
| Simulation Type | Constant Power |
| Node Distribution | Uniform |
| Number of Nodes | 50 |
| Number of Antenna Element | 4 |
| Adaptive Algorithm | LMS |
| Transmit Power | 15.48dBm (35.4mWatts) |
| Antenna Structure | LES |

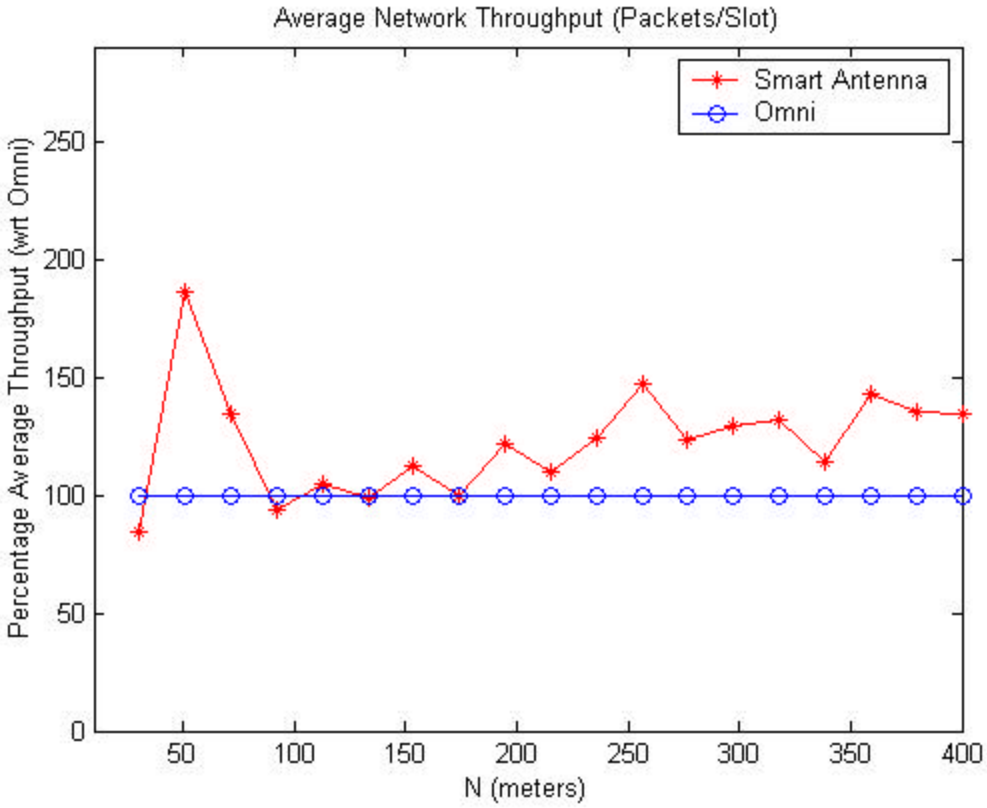


Figure 2-23 Average network throughput with varying network area. Four element array , constant power.

It is interesting to note that the smart antenna system is not performing much better than the omni directional scenario at lower to medium network area, while for larger network area the throughput increases in the network using the smart antennas compared to network using omni direction al antenna. This is due the fact that, with its high gain the smart antenna is able to reach nodes that are further than the unidirectional antenna. The directional beam also provides more efficient space division multiplexing hence better channel access efficiency and higher network throughput.

### 2.6.4 Test Scenario IV

In this scenario the number of antenna elements has been reduced to two. The results for constant power scenario are presented in Figure 2-24. The same trend is visible in this scenario. For lower network area the smart antenna case is not necessarily performing better that the omni directional case. But for larger network area the performance

improvement is considerable in network using smart antenna as compared to network using omni directional antenna.

**Table 2-7 Simulation Parameter Test Scenario IV**

| *Characteristic* | *Specification* |
|---|---|
| Simulation Type | Constant Power |
| Node Distribution | Uniform along axis X , Narrow along axis Y |
| Number of Nodes | 50 |
| Number of Antenna Element | 2 |
| Adaptive Algorithm | LMS |
| Transmit Power | 15.48dBm (35.4mWatts) |
| Antenna Structure | LES |

The performance of the two-element smart antenna system is better for lower network area than the four-element system in constant power scenario. The reason for this seemingly contradicting result is that with four elements the gain can be very high (up to 6dB) whereas for two elements the maximum gain is low (up to 3dB). With higher gain the four element smart antenna system is able to affect (reach) more nodes with its transmission, thus blocking them, while the two-element smart antenna system does not block as many nodes, hence achieves better performance. With a larger network area, the smart antenna system with four elements is able to reach more nodes, which are sparsely distributed, and hence achieves better network throughput. The two-element smart antenna system is not able to reach as many nodes; hence network through performance is inferior to the four element case.

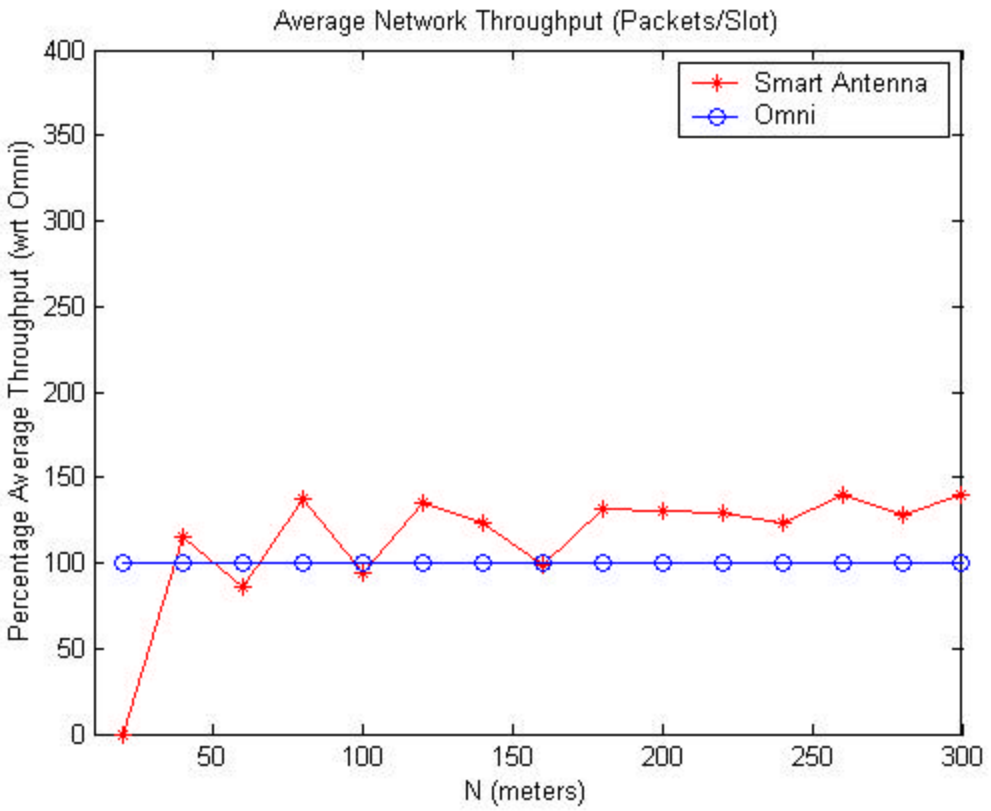


Figure 2-24 Average network throughput with varying network area. two element array , constant power scenario.

### 2.6.5 Test Scenario V

For the constant EIRP scenario the results are presented in Figure 2-25. In this scenario the smart antenna system has achieved a network throughput improvement of 40-50% compared to the omni directional case. It can be observed that with constant EIRP the smart antenna system consistently performs better than the omni directional scenario.

**Table 2-8 Simulation Parameter Test Scenario V**

| *Characteristic* | *Specification* |
|---|---|
| Simulation Type | Constant EIRP |
| Node Distribution | Uniform along axis X , Narrow along axis Y |
| Number of Nodes | 50 |
| Number of Antenna Element | 2 |
| Adaptive Algorithm | LMS |
| Transmit Power | 15.48dBm (35.4mWatts) |
| Antenna Structure | LES |

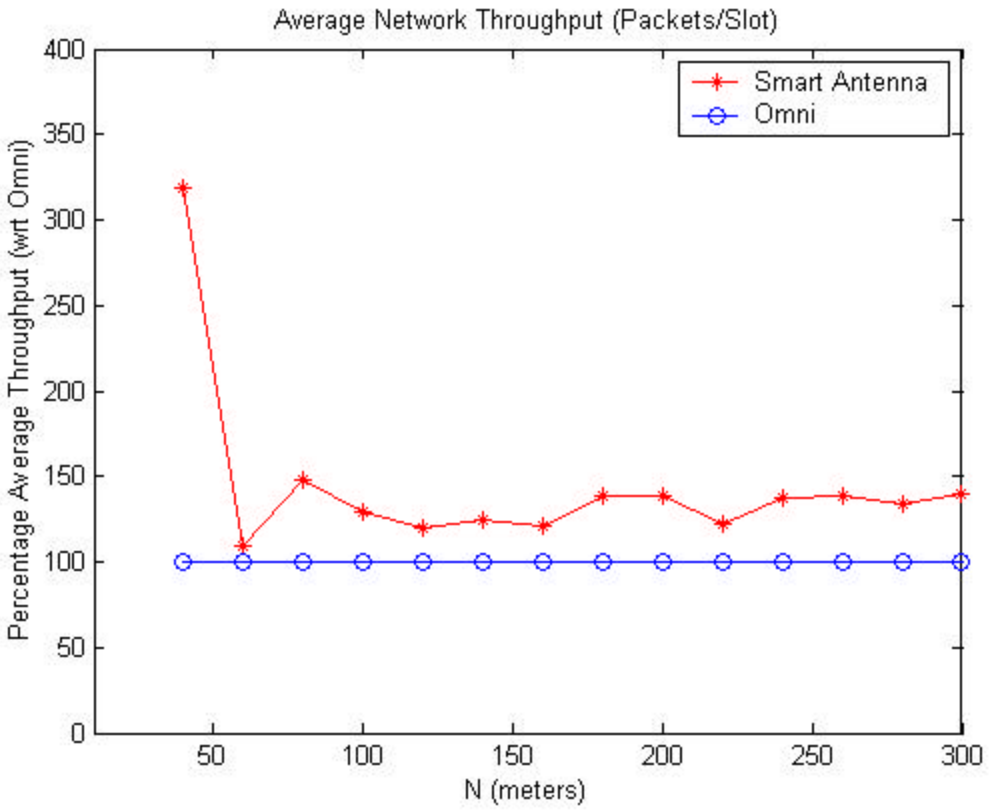


Figure 2-25 Average network throughput with varying network area. Two element array, constant EIRP .

## 2.7 Test Scenario VI

In this test scenario we have considered a narrow hall environment, which is small in breadth and long in length. All the nodes are distributed along this narrow hall. The network throughputs for the three scenarios (constant EIRP, constant power, omni directional) considered are presented in Figure 2-26. The x-axis is the different simulation run with same network area and traffic distribution. It can be observed that the network with smart antenna and constant EIRP consistently perform better than the omni directional scenario. But the same conclusion is not true for the constant power (varying EIRP) scenario. Since all the nodes are distributed along a narrow network area, sometimes the higher antenna gain of the constant power scenario blocks more nodes

than the omni directional case. This results in lower network throughput of the constant power case as compared to the omni directional case.

| *Characteristic* | *Specification* |
|---|---|
| Node Distribution | Uniform (Hall) |
| Simulation Type | Comparison |
| Number of Nodes | 50 |
| Number of Antenna Element | 4 |
| Adaptive Algorithm | LMS |
| Transmit Power | 16.94 dBm (~= 49.5 mWatts) |
| Antenna Structure | LES |

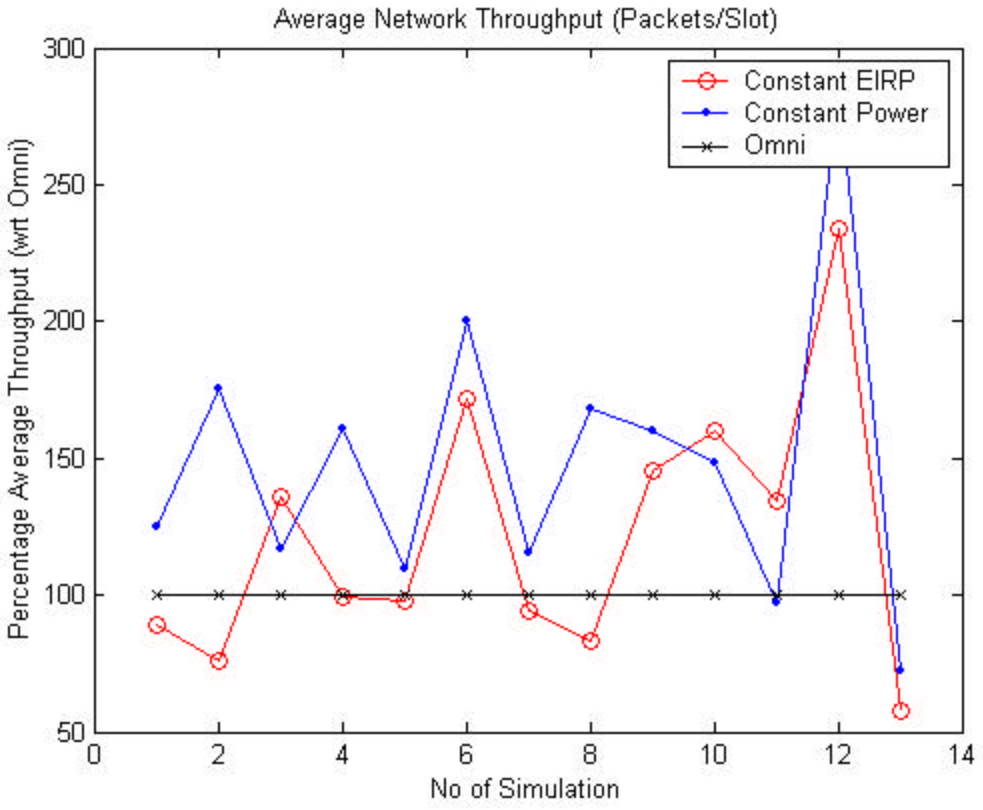


Figure 2-26 Average transmit power / packet starting power level 16.94 dBm (~= 49.5 mW).

## 2.8 Implementation Issues- An Implementation on Real Time TI-C6701 DSP Based System

To investigate the performance of the adaptive antenna array algorithms in indoor wireless environments, we implemented some of the algorithms that we considered in our simulation on a VT-STAR communication system. VT-STAR is a real time wireless communication system based on Texas Instrument TMS C6701 Digital Signal Processor (DSP). The system specifications are provided in Table 2-9.

**Table 2-9 Specification of VT-STAR**

| | |
|---|---|
| Carrier Frequency | 2.050 GHz. |
| Number of Transmitting Antenna | 1 |
| Number of Receiving Antenna | 2 |
| Antenna Element Spacing | 0.071 Meters |
| Wavelength | 0.146 Meters |
| Individual Element Beam Pattern (Approximation) | Omni-Directional |
| Processor | Texas Instrument@ TMS C6701 |

A simplified functional block diagram of the VT-STAR system is presented in Figure 2-26. The workstation was a Windows based computer with a Pentium-2 processor running at 300 MHz. The following adaptive antenna algorithms were implemented on the VT-STAR system:

- Least Mean Squares;
- Constant Modulus Algorithm;
- Recursive Least Squares.

The algorithms were implemented in the baseband section of the system as shown in Figure 2-27. This figure also presents the software code structure of the smart antenna subsection.

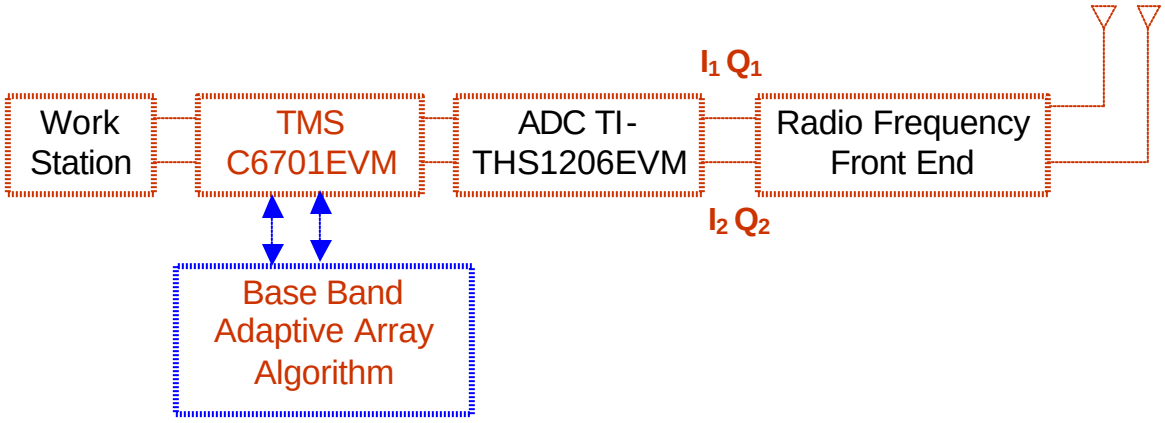


Figure 2-27 VT-STAR Architecture, a TMS C6701EVM DSP based real time wireless communication system.

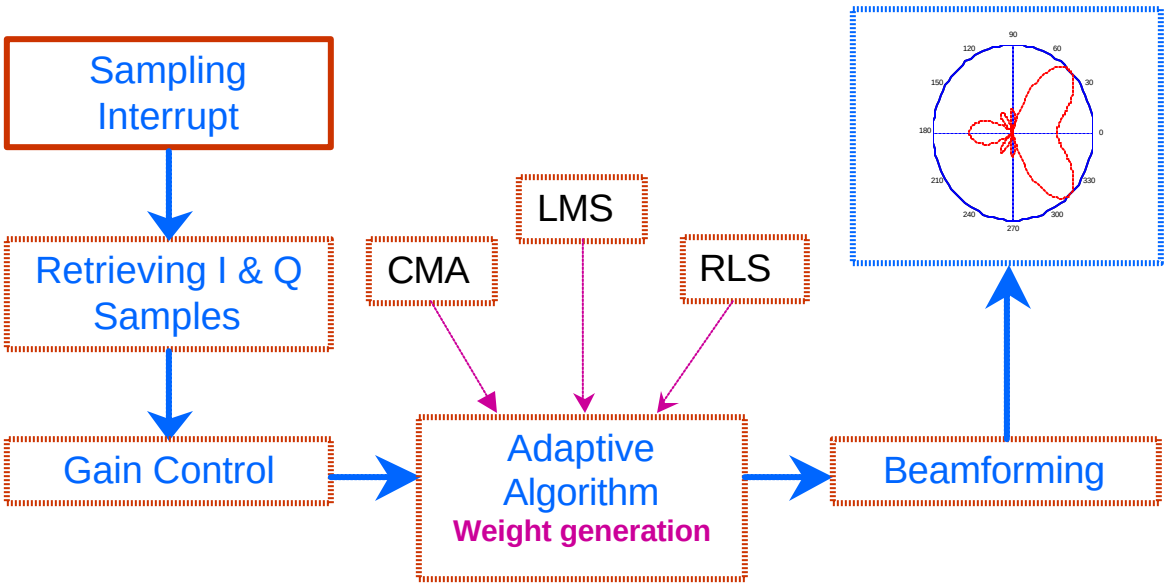


Figure 2-28 Software Code Structure of the smart antenna sub-section.

A detailed explanation and working of VT-STAR is provided in [12].

### 2.8.1 Profiling & Optimization

**Table 2-10 Profiling & Optimization on VTSTAR**

| *ALGORITHM* | *CYCLES ( "c" )* | *CYCLES OPTIMIZED (ASM)* | *% Reduction In Cycles* |
|---|---|---|---|
| LMSE | 4039 | 2001 | 50.46 |
| CMA | 5050 | 2536 | 49.78 |
| RLS | 8904 | - | - |
| BEAM-PATTERN | 1414500 | 456570 | 67.72 |
| MATRIX MULTIPLICATION | 715 | 320 | 55.24 |

To compare the implemented algorithms, we profiled their performances on the VT-STAR system. Table 2-10 provides profiling results. We found that the RLS algorithm was the fastest algorithm to converge and the LMS algorithm was the slowest. In terms of implementation complexity the RLS algorithm was the most complex and the LMS algorithm was the least complex. The performance of the CMA algorithm was intermediate in both speed of convergence and implementation complexity. The RLS algorithm took the maximum number of CPU cycles and the LMS algorithm took the least. We also present the reduction in number of cycles achieved after optimizing the software code by writing the algorithms in assembly language. In most of the cases the reduction in number of cycles was almost 50% as compared to the original code (written in "c"). Figure 2-28 presents a snapshot of the beam pattern of the antenna array as formed by the CMA algorithm. The desired angle of arrival is $90^0$. It can be observed that the CMA algorithm has converged properly and the beam pattern is pointing towards $90^o$. Another property to observe is the symmetry of the beam pattern with respect to $180^0$. This is consistent with the property of the LES arrays whose beam patterns are symmetrical with respect to $180^0$.

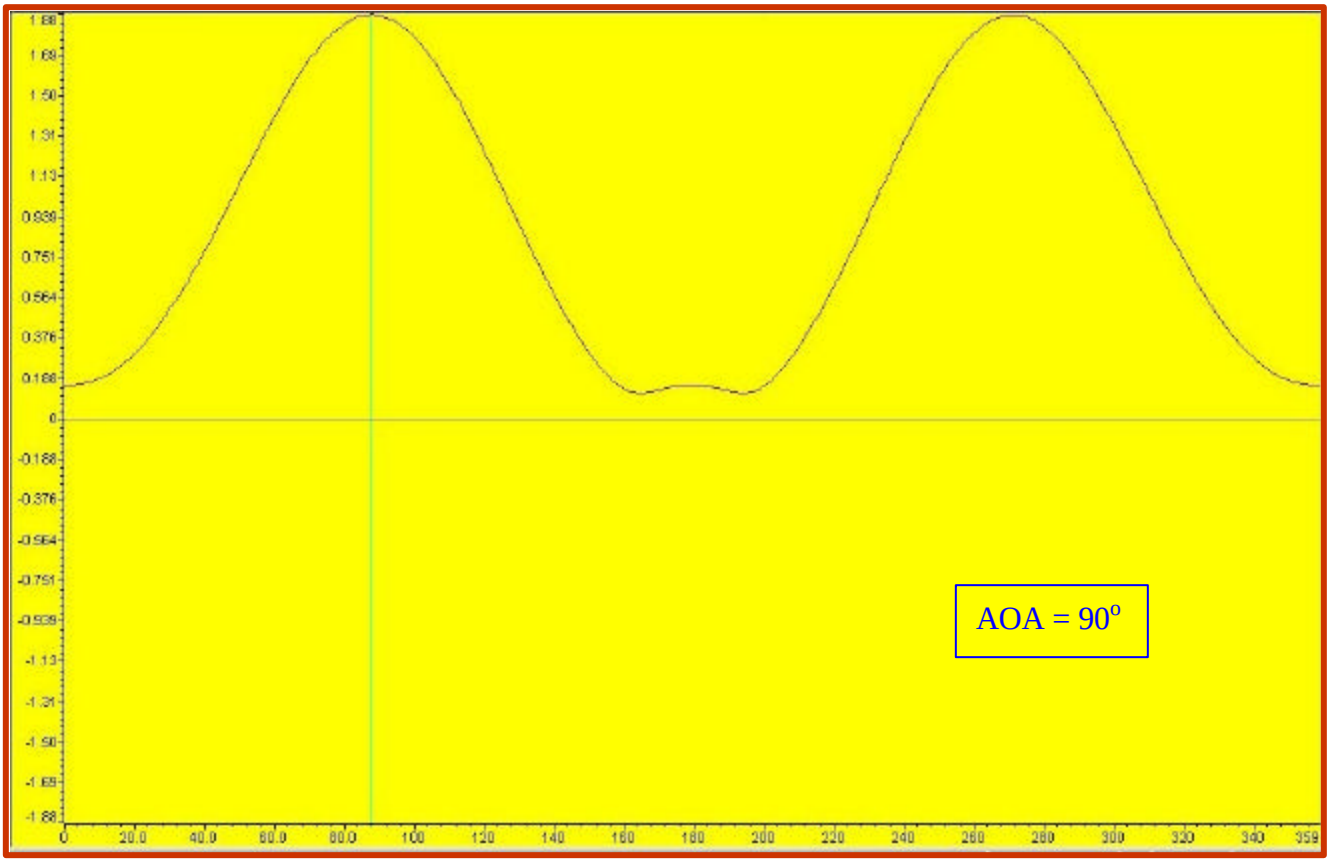


Figure 2-29 Snapshot of the antenna Beam pattern formed by the CMA algorithm on VT-STAR.

### 2.8.2 Issues & Approaches

- All the adaptive algorithm implementations required extensive complex (real & imaginary) operations. There were no built-in commands or functions available in the code composer studio (provided by Texas Instrument for C67XX DSP). We wrote our own functions both in "C" and later in assembly language for the optimization of the code. We also needed several matrix manipulation utilities to perform operations such as conjugation, inverse, Hermitian transpose, and matrix multiplication with complex data types.
- The convergence behavior of each adaptive algorithm under consideration was heavily dependent on the recursive step parameter. Determination of the step parameter for each algorithm was more of an art than a science. By experimenting

we came up with the following optimal values for the algorithm in an office-like indoor environment.

**Table 2-11 Algorithm Convergence Parameter Values**

| *Algorithm* | *Step Parameter (Delta)* |
|---|---|
| CMA | 0.03 |
| LMS | 0.015 |
| RLS | 1.111 ( $F^{-1}$ ) |

- Array calibration was a major concern. A correction table was created for known Angle of Arrivals to train the adaptive antenna algorithm response. This correction table was necessary to mitigate the imbalance present in the I and Q chain of the transreceiver section.

## 2.9 Chapter Conclusion

In this chapter we proposed a simple modification to the existing wireless LAN 802.11b MAC to incorporate the smart antennas. We presented simulation result showing the improvement in the network throughput if smart antennas are employed. We defined two different scenarios in which smart antenna systems can be used and showed the performance of network under each scenario. The result of section 3-4 shows that the implementation of smart antenna would not always bring better throughput performance. The throughput performance would depend on the mode in which smart antenna is being operated, the node and the traffic load distribution of the nodes. For smaller network area the constant EIRP mode gives better performance than the constant power and omni directional modes. As the network area increases and node density becomes less the constant power mode performs better than other two modes.

We also presented the practical implementation issues we faced while implementing the smart antenna algorithm on VT-STAR real time communication system. We present the values of various step parameters for implemented algorithms in an indoor environment.

# Chapter 3 Power Management in Ad-Hoc Networks

## *3.1 Introduction*

The transmitting range or antenna power of the nodes in a wireless ad-hoc network has tremendous impact on the battery life and the uptime of the wireless node. Transmit power may also affect the throughput of the network. In conventional wireless 802.11b network with omni directional antennas, the transmit power determines the antenna range, which determines the number of nodes in a backoff state by virtue of receiving RTS or CTS packets meant for different nodes. The higher the transmit power of a node, the higher the number of nodes affected by its transmission. It is apparent that a node should not transmit at a power higher than necessary to reach it's destination. Some results have been reported in the literature on the impact of transmit range or transmit power on the throughput performance in mobile ad hoc networks. Dutkiewicz [6] investigated the optimum range of a node in IEEE 802.11 based wireless networks employing RTS-CTS virtual carrier sensing mechanism. The author(s) reported that, under a wide set of network and local conditions; multi-hop networks have lower performance than single hop networks. According to them, data throughput is maximized when all the nodes are in the communication range of each other and the addition of relay nodes does not significantly improve throughput performance of multi hop networks.

Elbatt et al. [17] have presented initial results for distributed power management through the concept of 'minimum power,' which essentially means that a node should not use higher power than necessary to communicate with other node. Though the scheme is similar to what we propose they have not considered the effect of smart antennas and imperfect antenna patterns. In this chapter we will investigate the network throughput performance for single hop networks and battery life consumption with variable transmit power and smart antennas. We have carefully implemented the channel characteristics such as fading, interference and lognormal shadowing to accurately account for the impact of realistic channel conditions. Various parameters like receiver sensitivity,

maximum transmit power and minimum transmit power have been modeled on actual commercial wireless LAN 802.11b devices [10, 11]. We will compare performance of the network incorporating smart antenna and power management scheme with that of network with only omni directional antenna. We will propose a distributed algorithm to be embedded at the MAC layer, which will enable the nodes to find an optimum transmit power (antenna gain) for transmitting and receiving. The power management algorithm would on link-by-link basis. We will also incorporate the power management scheme with the smart antenna to show that it is possible to improve the network throughput and simultaneously reduce the average transmit power per packet in a wireless ad-hoc network.

## *3.2 Network Throughput, Interference & Battery Life*

We will consider only the single hop networks based on 802.11b MAC with RTS CTS protocol. For analyzing the performance of the proposed scheme we define the network throughput as the number of successful packet transmissions per packet slot. The unsuccessful packet transmissions are not included in the throughput calculations. In order to make the simulation modeling tractable and simulation time realistic we have divided the time into packet slotted time. A node can transmit or receive a packet (of fixed length) in one time slot only. Subsection 2.5 gives a detailed explanation of the simulation model. To understand the impact of transmit power the reader should observe Figure 3-1. It shows the scenario of the network throughput being low due to sub-optimum transmit power.

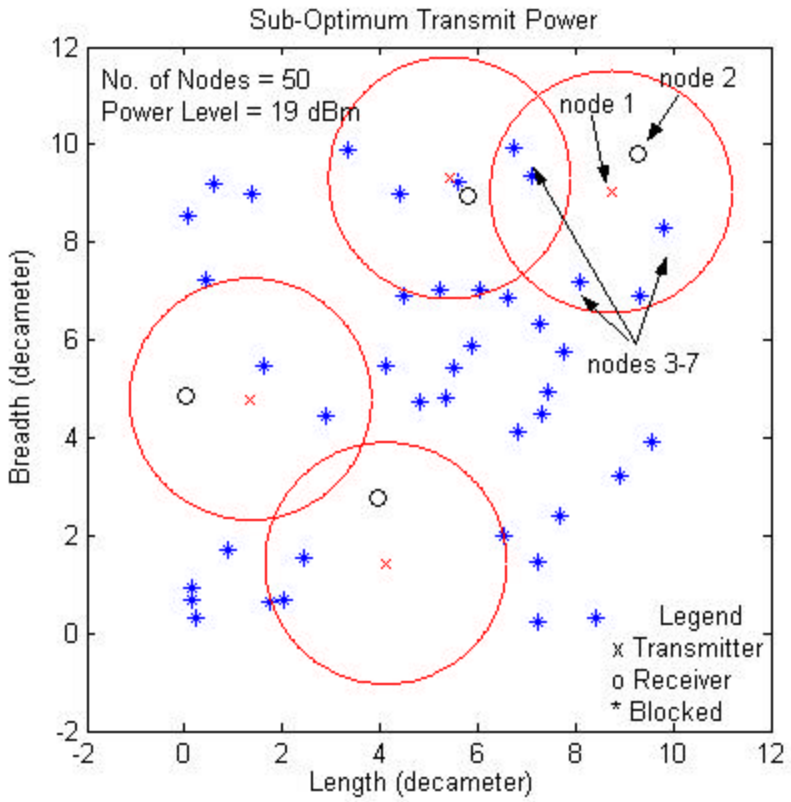


Figure 3-1 Sub-Optimum Transmit Power, Lowering the Network Throughput.

Node 1 (Red star) has transmitted an RTS packet to Node 2 (Black Star). Since the transmit power of node 1 is higher than it is necessary to reach node 2, it has blocked nodes 3-to-7 (Blue Stars). Had node 1 been transmitting at the optimum power level it would not have blocked all the nodes. By reducing the transmit power of node 1, the other nodes would not be blocked and are free to commence their own transmission. Also, by reducing the excess power of the nodes the average power consumption of the network can be lowered substantially. The other effect of reducing the transmit power from an un-necessarily high value to an optimum lower values is the reduced co-channel interference experienced by other nodes. If the average transmit power of every node in the network is reduced considerably the average bit error rate (BER) of the network will also reduce due to reduced interference. This may help the nodes to increase the data rate (due to lower BER the nodes can choose higher modulation schemes). This lowering of

power consumption is a very important consideration because the devices in a wireless 802.11b network have a limited battery power and any reduction in the usage of battery directly maps to higher up time. Next section explains our proposed algorithm to reduce the transmit power of the nodes in a wireless ad-hoc network.

## 3.3 The Concept of Power management in Ad-Hoc Network

We power management algorithm is presented in Figure 3-2. We use the existing 802.11b MAC protocol's acknowledgement mechanism for each packet to update the transmit power of the transmitter. By embedding a power control bit in the header of all the packets the nodes in a wireless network can perform link-to-link power management. For each received packet, the receiver will calculate the average SNR of the packet. If the average SNR of the packet is higher than a threshold (determined by the link budget calculation) by a certain value then in the acknowledgement for the packet, the receiver will indicate the sender to reduce its transmit power by one step value. Similarly, if the received SNR is near or slightly less than the threshold then the receiver can indicate the sender to increase the transmit power by a power step. The exact magnitude of the power step is heavily dependent on the wireless environment, interference and the network structure. To show the reduction in the average power consumption of the wireless nodes using our proposed scheme we ran Monte Carlo simulation for the specific environment. The analysis and discussion of the simulation results are presented in next the section.

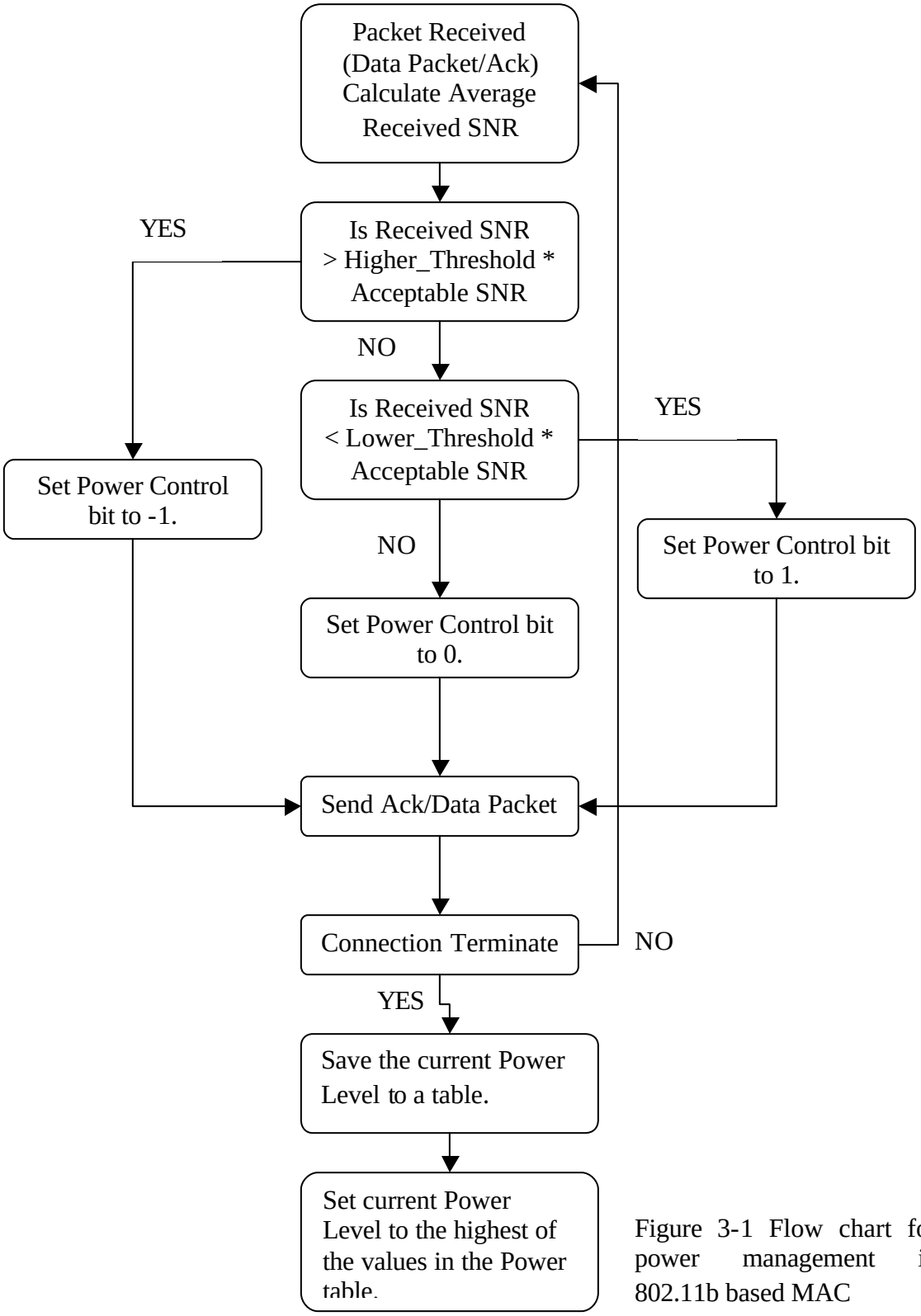


Figure 3-1 Flow chart for power management in 802.11b based MAC

## *3.4 Throughput & Power Simulation Results for Wireless LAN 802.11 b*

To compare the performance of the proposed algorithm in terms of the average transmit power and network throughput we considered the following two cases.

- Omni directional antenna without power control;
- Smart antenna with power control.

We will run simulations with different starting power to investigate the performance of the power management algorithm as compared to the omni directional scenario. In the simulations for the omni directional antenna without power management algorithm, the transmit power will remain same (equal to starting level) throughout the simulation. For the case where the power management algorithm is incorporated the transmit power will be adjusted link by link and the power level table will be updated as nodes starts to communicate with each other. The average transmit power would then be compared presented with the omni directional scenario.

### 3.4.1 Test Scenario I

**Table 3-1 Simulation Parameter Test Scenario I**

| *Characteristic* | *Specification* |
|---|---|
| Node Distribution | Uniform |
| Simulation Type | Constant EIRP |
| Number of Nodes | 50 |
| Number of Antenna Elements | 4 |
| Adaptive Algorithm | LMS |
| Transmit Power | 13.26 dBm (22 mW) |
| Antenna Structure | LES |

In Figure 3-3 we present the average power required to transmit a packet for the case when starting power is equal to 22mW. The average power is calculated by summing the power used to transmit each packet (by every node) and then dividing by the number of transmitted packets. This would be the average power required to transmit a packet in the wireless network.

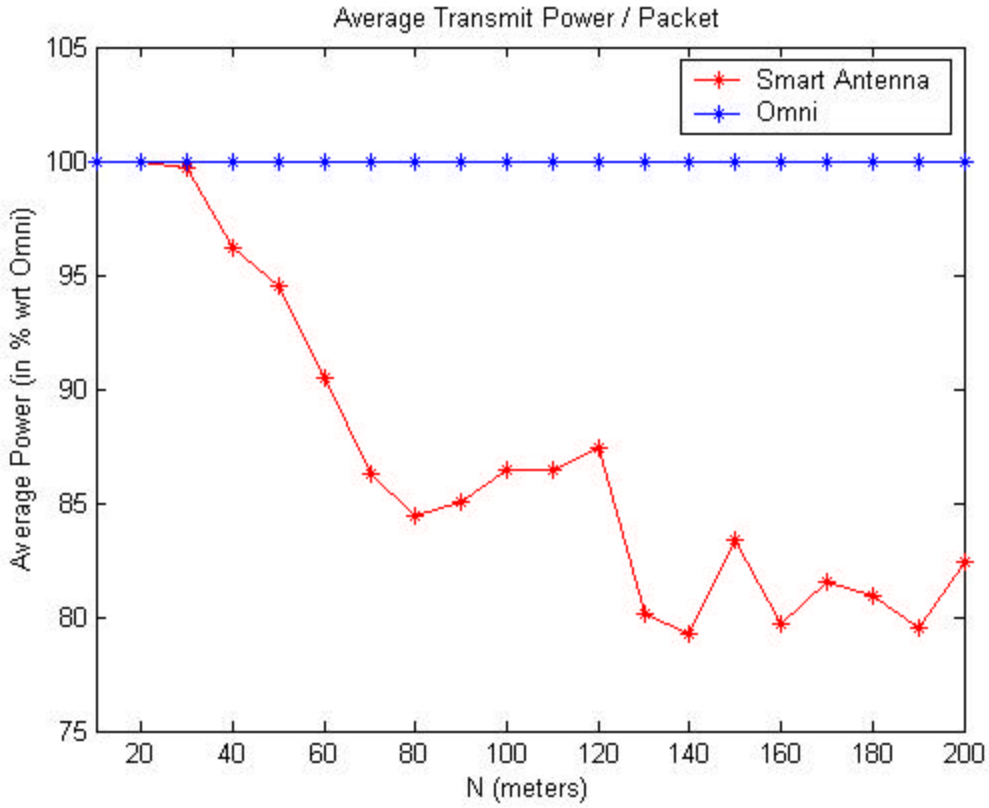


Figure 3-2 Average transmit power / packet starting power level 13.26 dBm (22 mW).

The average transmit power is plotted as percentage values with respect to the omni directional antenna scenario without power management. It can be observed that considerably less average power is required to transmit a packet when power management scheme is employed. The average power required to transmit a packet is approximately 15-18 percent lower when power control mechanism is employed as compared to the omni directional scenario. For small network areas (N=10 to N=40) the average power required for MAC with power management is closer to the MAC without power management because very few transmissions and receptions are being carried out. This happens because all the nodes are closely packed in the small network area and are blocked due to the RTS CTS protocol. Since communication occurrences between the nodes are low, the power tables do not get updated and the nodes keep transmitting at higher values. But as network area increases, more nodes are able to communicate, consequently the power tables gets updated in network employing MAC with power

management and average power required to transmit a packet drops to about 80-85% as compared to the network employing MAC without power management.

### 3.4.2 Test Scenario II

In this test scenario we start with a higher power level. The effect of higher transmit power on the average power consumption is interesting

**Table 3-2 Simulation Parameter Test Scenario II**

| *Characteristic* | *Specification* |
|---|---|
| Node Distribution | Uniform (Hall) |
| Simulation Type | Constant EIRP |
| Number of Nodes | 50 |
| Number of Antenna Element | 4 |
| Adaptive Algorithm | LMS |
| Transmit Power | 15.48 dBm ( 35.3mWatts) |
| Antenna Structure | LES |

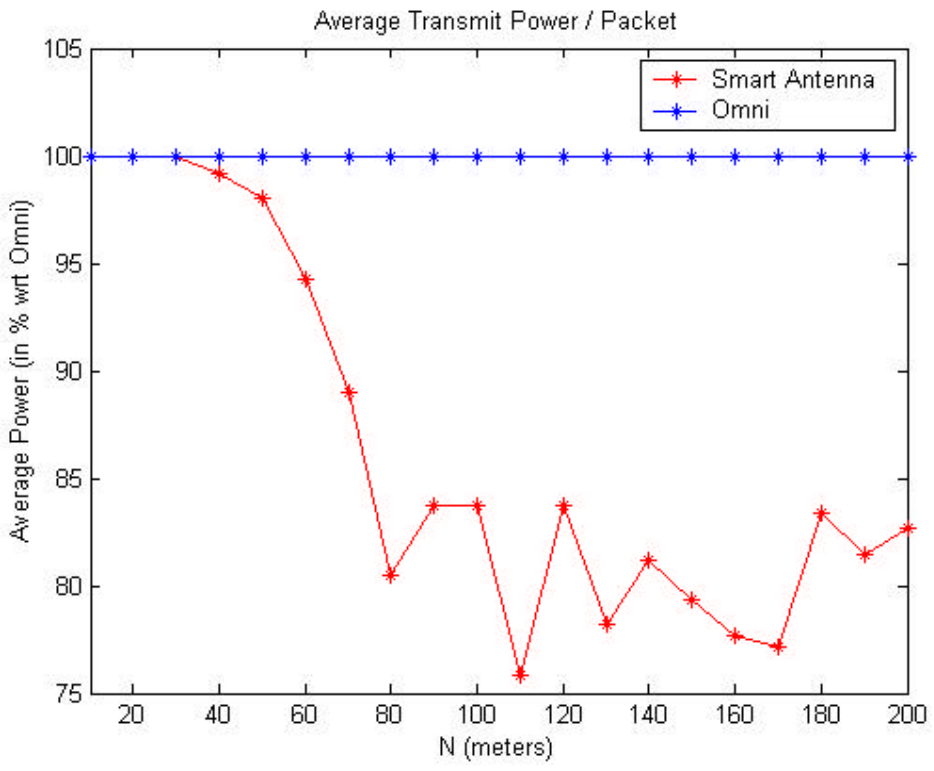


Figure 3-3 Average transmit power / packet starting power level 15.48 dBm ( 35.3mWatts).

Figure 3-4 presents the average power required to transmit a packet in networks with and without power management. The results are similar to the previous section. The average power required by the network with power management falls by 15-20 % as compared to the network without power management case. Figure 3.5 presents a snapshot of the average transmit power during a simulation run. Actual average transmit power per packet per slot is plotted in red. The overall average of the transmit power per packet is plotted in blue. The black curve represents the continuous average transmit power per packet. Notices that at the beginning of the simulation the average transmit power are high (near the starting power level). But as the simulation proceeds, the power table gets updated and nodes begin to use the updated transmit power values. As the simulation goes on, the continuous average transmit gradually drops to an optimum value.

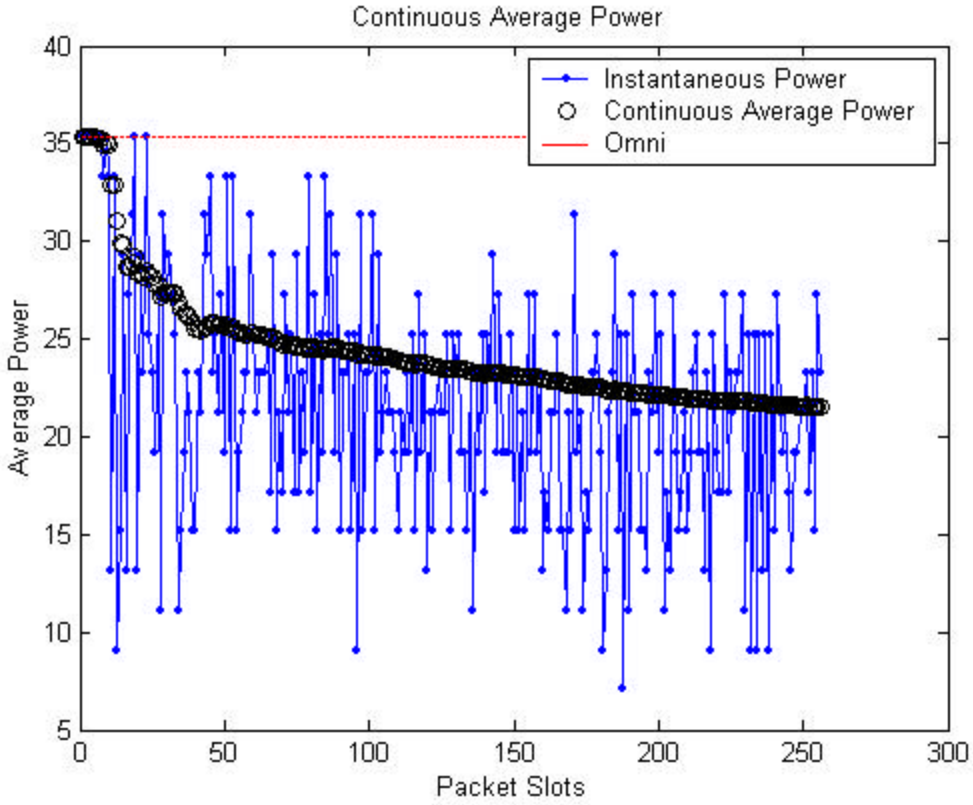


Figure 3-4 Snapshot of average transmit power. The figure shows continuous average transmit power in black starting power level 15.48 dBm ( 35.3mWatts)

### 3.4.3 Test Scenario III

To investigate the effect of different mode of smart antenna operation (constant power and constant EIRP) we ran simulations with same node and traffic distribution for both the cases. The average power consumption of both modes are presented with respect to omni directional scenario in Figure 3-5.

**Table 3-3 Simulation parameter Test Scenario III**

| *Characteristic* | *Specification* |
|---|---|
| Node Distribution | Uniform |
| Number of Nodes | 50 |
| Number of Antenna Element | 4 |
| Adaptive Algorithm | LMS |
| Transmit Power | 15.48 dBm |
| Antenna Structure | LES |

Although both the mode with power control algorithm performs better than the omni directional MAC without power control, the performance of the constant power mode is better by 10% as compared to the constant EIRP mode. This interesting behavior can be explained by the fact that, in constant power mode the EIRP of the transmitter is varying depending on the gain of the antenna section. If nodes are communicating with optimum beam pattern then they would able to reduce their transmit power by a higher degree than the constant EIRP case. This extra degree of freedom in controlling the transmit power results in better performance for the constant power case.

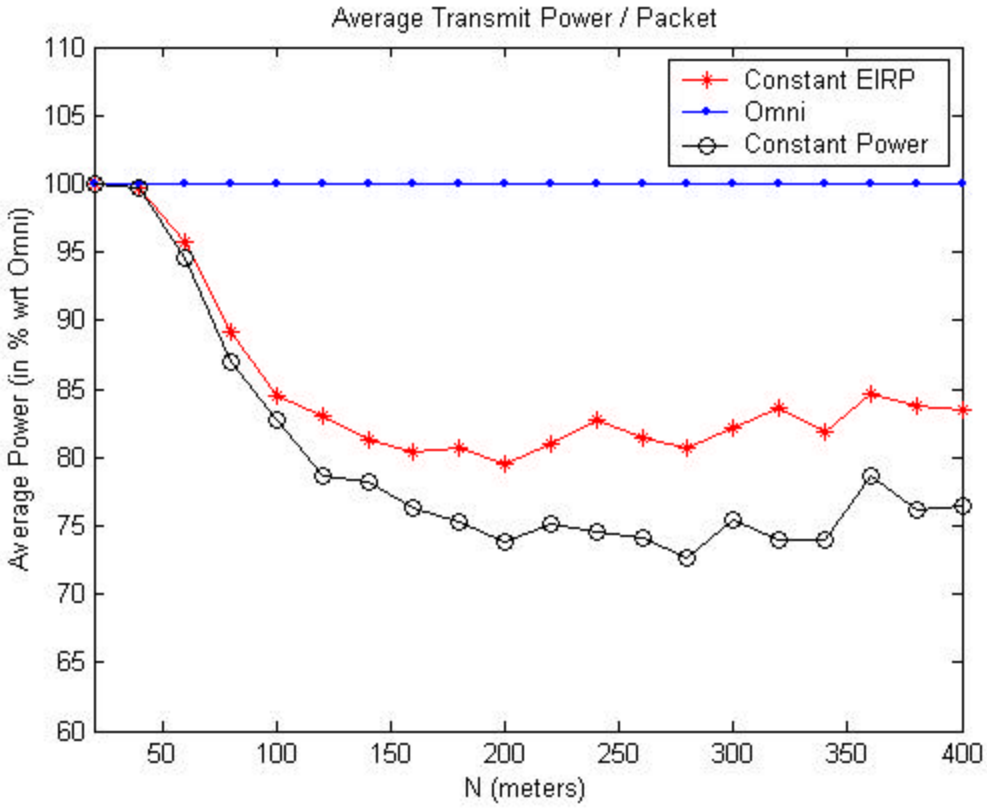


Figure 3-5 Power consumption comparison of constant EIRP and constant power mode.

## 3.5 Chapter Conclusion

In this chapter we proposed a link-by-link power management algorithm to improve the transmit power efficiency of the IEEE 802.11b based wireless ad hoc networks. We have presented the simulation results which shows that significant transmit power can be saved if power management scheme is adopted in every node of the network. The network throughput may or may not be better than the omni directional antenna case. The power consumption of the constant power mode is lower than the constant EIRP case as nodes are able to utilize the higher antenna gain in reducing their transmit power levels.

# Chapter 4 Cellular Communication System Design Using Smart Antenna

## *4.1 Introduction*

Spectral utilization efficiency of cellular radio networks can be improved by reducing the cluster size (i.e., by lowering the co-channel reuse factor) but at the expense of increased co-channel interference (CCI) [25]. This penalty, however, may be recovered by implementing some sort of CCI mitigation technique (such as power management, cell sectorization, diversity mechanisms or space-time array processing) and to some extend, through use of dynamic channel allocation strategies. Unlike the dynamic channel allocation approaches, deployment of smart antennas (for steering nulls towards the CCI signals) in a cellular network does not necessitate a significant increase of the task of system resource manager. Unfortunately, the capabilities of smart antennas will be limited by size, complexity and cost considerations. This is particularly true for small, low-power, and light-weight hand-held mobile terminals. As such, practical adaptive array for portable terminals will typically be restricted to a few antenna elements [27]. In general, a smart antenna with $D$-elements can effectively suppress $D-1$ near equal power co-channel interferer signals that impinge on the adaptive array simultaneously using linear array processing techniques (e.g., digital beam-forming or adaptive interference nulling)[28] –[29]. When the number of co-channel interferers $N_I$ is larger than $D-1$ , the array with $D$ elements is said to be overloaded. To cope with this situation, one may either resort to a linear array processing technique by shaping the antenna beampattern such that the gain in the direction of the desired user signal is maximized while placing nulls in the directions corresponding to the angles of arrival of the $(N_I - N)$ strongest CCI signals (where $N$ denotes the number of uncancelled CCI signals), or alternatively develop a new overloaded array processing technique. In this chapter, we will consider the first approach and develop a theoretical framework for

calculating the outage probability of the system under consideration in a cellular mobile radio environment. It is apparent that in this case, the outage probability will be dictated by the $N$ remaining "weakest" CCI signals and/or the receiver noise.

Related studies on selective or partial co-channel interference cancellation (SIC) using smart antenna include References [27, 30-32]. The capacity of a narrowband TDMA system in which only the strongest CCI is cancelled is simulated in References [30,31]. In Reference [27], several closed form expressions for the outage probability of cellular mobile radio system in interference limited and minimum signal power constraint cases are derived by assuming that the $(N_I - N)$ strongest independent and identically distributed (i.i.d) Rayleigh-faded CCI signals are cancelled. The key to their derivation is the knowledge of the probability distribution function (PDF) of the sum of $N$ exponential random variables (arranged in an ascending order) in closed-form [33]. In Reference [32], the author derived the PDF of signal-to-interference ratio (SIR) with SIC, again assuming i.i.d Rayleigh faded CCI signals. In this case they have utilized a well known result involving the sum of ordered exponential random variables (RV) as a linear combination of standard unordered exponential RVs with an appropriate weighting [34-36] to compute the PDF of total CCI power. Subsequently, an outage probability expression for the interference limited case was obtained.

Different form [27] and [32], in this chapter we first outline a simple numerical approach for computing the probability of outage metric, which only requires the knowledge of the moment generating function (MGF) of the sum of ordered (uncancelled) interferer power $\Phi_I(s)$ (In case of basic outage definition) or both $\Phi_I(s)$ and the marginal MGF of the desired signal power (is a minimum signal power constraint is imposed to take into account of the receive noise). Specifically we point out how the general framework for computing outage probability of mobile radio system developed in References [37] and [38] can be modified so that it enables us to investigate the effect of SIC (using smart antenna) on the spectral efficiency and the coverage performance. This framework is applicable to any fading environment and works as long as $\Phi_I(s)$ is available or easily computable. Based on a novel formulation for evaluating the sum of ordered RVs [39], we were able to generalize the results presented in References [27] and [32] by

considering Nakagami-m faded CCI signals. In addition a number of new closed form formulas for the outage probability are derived given that the CCI signal amplitudes are subject to Nakagami-m fading with positive integer fading index or Rayleigh fading. In fact these closed form formulas are sufficiently general because they can treat all common fading statistics for the desired user signal amplitude (including Rayleigh, Nakagami-m and Nakagami-q models).

The remainder of this paper is organized as follows. In Section 4.2.2, we discuss a generic numerical approach for computing the probability of outage with SIC by exploiting the knowledge of the marginal MGF of the desired user signal and $\Phi_I(s)$ Section 3 deals with the derivations of closed-form formulas for the outage given that the CCI signal amplitudes follow Nakagami-m (positive integer fading index) distribution. An alternative, simpler derivation for $\Phi_I(s)$ while the i.i.d CCI signals experience Rayleigh fading is also discussed in Appendix B. Section 4 provides selected numerical examples to illustrate the application of the theory for mobile cellular radio design. Section 5 summarizes our ongoing investigations in this area.

## 4.2 Outage Analysis

The probability of outage is one of the most important statistical measure of cellular mobile radio performance in the presence of CCI. In an interference-limited system, satisfactory reception is assumed to be achieved as long as the short-term SIR exceeds the CCI power protection ratio $q$, thereby neglecting the receiver background noise. Hence, the outage event is given by

$$P_{out(N,N_I)} = P_r\{p_0 < qI\} = P_r\left\{\frac{p_0}{q} - \sum_{k=1}^{N} p_{k:N_I} < 0\right\} \qquad \textbf{Equation 4-1}$$

$$\equiv P_r\{\Delta < 0\}$$

where the instantaneous signal powers $p_i\,(i = 0,1,2,...,N_I)$ are modeled as RV with mean $p_i$ (subscript $i = 0$ corresponds to the desired user signal and $i = 1,2,...,N_I$ are for the interfering signals), $N \le N_I$ denotes the number of remaining (uncancelled) CCI signals out of a total of $N_I$ interferers, $q$ is the CCI power protection ratio (which is fixed

by the type of modulation, transmission scheme employed and the quality of service), the ordered statistics $p_{k:N_I}$ are obtained by arranging the interfering signal powers in ascending order and $I = \sum_{k=1}^{N} p_{k:N_I}$ is a sum of the uncancelled "weakest" CCI signal powers. In practice, however, thermal noise and receiver threshold always exists which may be of concern particularly in macro-cells. In the literature, this effect is considered either by imposing an additional minimum desired signal power requirement for satisfactory reception [26] or by treating the receiver noise as CCI [25].

### 4.2.1 Treating receiver Noise as CCI

To incorporate the effect of receiver noise, the outage event (1) can be redefined as $P_r\{p_o < qI + \Lambda\}$ [1], where $\Lambda$ (constant) is a product of the total noise power $h$ and the noise power protection margin $r$ Consequently, the computation of outage simply requires the cumulative distribution function (CDF) of $\Lambda$ (defined in (1)) evaluated at $\Lambda / q$, viz , $P_{out(N,N_I)} = F_{\Delta}\left(\frac{\Lambda}{q}\right)$. It is also apparent that specifying a receiver noise threshold will cause a floor on the outage probability regardless of whether CCI is present or not because the deep fades will result in signal power level below the specified minimum level. In fact, this floor level dictates the outage performance in a noise-limited case. Recognizing that $\Delta$ is a linear sum of random powers, its moment generating function (MGF) can be expressed as

$$\Phi_{\Delta}(s) = \Phi_0\left(s/q\right)\Phi_I(-s) \qquad \textbf{Equation 4-2}$$

where notations $\Phi_i(.)$ and $\Phi_I(.)$ have been used to denote the MGF of $p_i$ and $I$ respectively. Therefore, an integral expression with finite integration limits for the outage follows at once from the Laplace inversion formula :

$$P_{out(N,N_I)} = \frac{1}{2p}\int_{-\infty}^{\infty}\frac{\Phi_\Delta(c+jw)}{c+jw}\exp\left[(c+jw)\Lambda/q\right]dw$$
$$= \frac{1}{p}\int_{0}^{p/2}\tilde{\Phi}_\Delta(q)dq \qquad \textbf{Equation 4-3}$$
$$= \frac{1}{2n}\sum_{i=1}^{n}\tilde{\Phi}_\Delta\left[\frac{(2i-1)p}{4n}\right]+R_n$$

where $j=\sqrt{-1}$, $R_n$ is the remainder term (due to series truncation), $\Phi_\Delta(.)$ is defined by

$$\tilde{\Phi}_\Delta(q) = \text{Real}\left\{(1-j\tan q)\,\Phi_\Delta\left[c(1+j\tan q)\right]\exp\left[(1+j\tan q)\frac{\Lambda c}{q}\right]\right\} \qquad \textbf{Equation 4-4}$$

and $0<c<a_{\min}=\min(a_i)$ with $a_i>0$ being the i'th pole of $\Phi_\Delta(.)$ in the left half plane. While the optimal choice for coefficient c may be determined via a numerical search (i.e., at saddle point $s=c, \Phi_\Delta(s)e^{sx}/s$ achieves its minimum on the real axis), it is sufficient to use a rule of thumb $c=a_{\min}/2$ for all practical purposes [12]. It should be emphasized that in arriving to [3] , we do not impose any restrictions on the fading amplitude distributions of both the desired user signal and the CCI signals, except that they are independent. Since a closed-form expression for $\Phi_0(.)$ is known (see Table 1) when the fading amplitude of the desired user signal is assumed to be flat Rayleigh, Rician, Nakagami-m

**Table 4-1 PDF and MGF of signal power for several common fading channel models.**

| *Channel Model* | *PDF* $f_i(x)$ *and MGF of the* $k^{th}$ *instantaneous fading signal power* |
|---|---|
| Rayleigh | $f_k(x)=\frac{1}{\bar{p}_k}\exp\left(\frac{-x}{\bar{p}_k}\right), x\geq 0$<br>$\Phi_k(s)=\frac{1}{1+s\bar{p}_k}$ where $\bar{p}_k=E[p_k]$=average SNR per symbol |
| Rician | $f_k(x)=\frac{1+K_k}{\bar{p}_k}\exp\left(-K_k-\frac{(1+K_k)x}{\bar{p}_k}\right)I_0\left[2\sqrt{\frac{K_k(K_k+1)x}{\bar{p}_k}}\right], x\geq 0$ |

| | |
|---|---|
| | $\Phi_k(s) = \frac{1+k_k}{1+k_k+s\overline{p}_k}\exp\left(\frac{-sk_k\overline{p}_k}{(1+k_k+s\overline{p}_k)}\right) k \geq 0$ where $k \geq 0$ is a rice parameter |
| Nakagami-*q* | $f_k(x) = \frac{1}{\overline{p}_k\sqrt{1-b_k^2}}\exp\left[\frac{-x}{(1-b_k^2)\overline{p}_k}\right] I_0\left[\frac{b_k x}{(1-b_k^2)\overline{p}_k}\right], x \geq 0$ where $-1 \leq b_k = \frac{1-q_k^2}{1+q_k^2} \leq 1$<br>$\Phi_k(s) = \frac{1}{\sqrt{\left[s\overline{p}_k(1+b_k)+1\right]\left[s\overline{p}_k(1-b_k)+1\right]}}$ where $0 \leq q_k \leq \infty$ is the fading parameter |
| Nakagami-*m* | $f_k(x) = \frac{1}{\Gamma(m_k)}\left(\frac{m_k}{\overline{p}_k}\right)^{m_k} x^{m_k-1}\exp\left(\frac{-m_k x}{\overline{p}_k}\right), x \geq 0$<br>$\Phi_k(s) = \left(\frac{m_k}{m_k+s\overline{p}_k}\right)^{m_k}$ Where $m_k \geq 0.5$ is the fading figure. |
| Lognormal | $f_k(x) = \frac{1}{\sqrt{2p}\,s_k x}\exp\left[\frac{-\ln^2(x/m_k)}{2s_k^2}\right], x \geq 0$<br>$\Phi_k(s) = \frac{1}{\sqrt{p}}\sum_{i=1}^{H} w_i \exp\left[-sm_k\exp\left(\sqrt{2}s_k x_i\right)\right] + R_H$<br>$s_k$ is the logarithmic standard deviation of shadowing<br>$m_k$ is the local mean power<br>$x_i$ and $w_i$ are abscissa and weight of the i[th] root of an H[th] order Hermite polynomial<br>$R_H$ is a remainder term |
| Suzuki | $f_k(x) = \int_0^\infty \frac{1}{\Omega}\exp\left(-\frac{x}{\Omega}\right) \times \frac{1}{\sqrt{2p}\,s_k\Omega}\exp\left[\frac{-\ln^2(\Omega/m_k)}{2s_k^2}\right] d\Omega, x \geq 0$<br>$\Phi_k(s) = \frac{1}{\sqrt{p}}\sum_{i=1}^{H}\frac{w_i}{1+sm_k\exp\left(\sqrt{2}s_k x_i\right)} + R_H$ |
| Lognormal Rice | $f_k(x) = \int_0^\infty \frac{1+K_k}{\Omega}\exp\left[-K_k - \frac{(1+K_k)x}{\Omega}\right] I_0\left[2\sqrt{\frac{K_k(1+K_k)x}{\Omega}}\right] \times \frac{1}{\sqrt{2p}\,s_k\Omega}\exp\left[\frac{-\ln^2(\Omega/m_k)}{2s_k^2}\right.$<br>$\Phi_k(s) = \frac{1}{\sqrt{p}}\sum_{i=1}^{H}\frac{w_i(1+K_k)}{1+K_k+sm_k\exp\left(\sqrt{2}s_k x_i\right)}\exp\left[\frac{-sK_k m_k\exp\left(\sqrt{2}s_k x_i\right)}{1+K_k+sm_k\exp\left(\sqrt{2}s_k x_i\right)}\right] + R_H$ |

| | |
|---|---|
| Lognormal Nakagami -*m* | $f_k(x)=\int_0^{\infty}\left(\frac{m_k}{\Omega}\right)^{m_k}\frac{k^{m_k-1}}{\Gamma(m_k)}\exp\left(\frac{-m_k x}{\Omega}\right)\times\frac{1}{\sqrt{2p}\,s_k\Omega}\exp\left[\frac{-\ln^2(\Omega/m_k)}{2s_k^2}\right]d\Omega, x\geq 0$<br>$\Phi_k(s)=\frac{1}{\sqrt{p}}\sum_{i=1}^{H}\frac{w_i}{\left[1+sm_k\exp\left(\sqrt{2}s_k x_i/m_k\right)\right]^{m_k}}+R_H$ |

or Nakagami-q fading, only the the knowledge of $\Phi_I(s)$ is further required to compute the probability of outage. When $N=N_I$, it is straight-forward to show that

$$\Phi_I(s)=\prod_{k=1}^{N_m}\Phi_k(s)$$

**Equation 4-5**

because in this case, the ordering of $p_k$ does not alter the statistic of I. Substituting (2) and (5) in (3), we obtain [12, eq. (3)] as expected. However, if $1\leq N<N_I$ a general solution for $\Phi_I(.)$ in closed-form similar to (5) is not available in the existing literature for an ordered RV (other than the special case of exponential RV) because finding the joint distribution of ordered RVs is generally much more difficult than for the unordered RVs. The primary difficulty stems from the fact that the uncancelled CCI powers $p_{1:N}\leq p_{2:N}\leq\ldots\leq p_{N:N}$ because of the inequalities among them are necessarily dependent. Nevertheless, it is possible to derive a closed-form formula for the linear combination of ordered exponential RVs - and ordered Gamma RVs [33]-[36] (using the procedure discussed in [39]) for both identical and nonidentical fading cases. For instance, assuming that all the $N_I$ independent CCI signals have the same average power $\overline{p}$ and subject to slow nonselective Rayleigh fading, we obtain (see Appendix B).

$$\Phi_I(s)=\prod_{k=1}^{N}\left[1+s\overline{p}\left(\frac{N-k+1}{N_I-k+1}\right)\right]^{-1},1\leq N<N_I$$

**Equation 4-6**

Development of $\Phi_I(.)$ that takes into account of the effect of power imbalance among the CCI signals is beyond the scope of this paper and will be reported in a future report. However, it should be stressed that equation (3) still holds even in this case, with an

appropriate substitution for $\Phi_I(.)$. Also, the interference-limited case can be treated directly by letting $\Lambda = 0$ in (3). Before concluding this subsection, we would like to point out that it is also possible to express $P_{out}$ in terms of an inverse Fourier transform integral similar to [12, eq. (5)]. However, numerical computations reveal that (3) is much more efficient and stable in comparison to the inverse Fourier transform integral counterpart, specifically at lower values of $P_{out}$.

### 4.2.2 Minimum Signal Power Requirement Scenario

By formulating the outage problem in the framework of hypothesis-testing [25], it is also possible to compute the probability of outage with a minimum desired signal power constraint using an inverse Laplace transform integral (whose integrand is composed of only the MGF of the sum of uncancelled CCI signals and the marginal MGF of desired signal power):

$$P_{out(N,N_I)} = F_0(\Lambda) + \frac{1}{2p}\int_{-\infty}^{\infty} \frac{G_0(c+jw,\Lambda)}{c+jw}\Phi_I(-c-jw)\,dw$$

$$= F_0(\Lambda) + \frac{1}{p}\int_0^{p/2} \Phi_g(q)dq \qquad \textbf{Equation 4-7}$$

$$= F_0(\Lambda) + \frac{1}{2n}\sum_{i=1}^{n} \Phi_g\left[\frac{(2i-1)p}{4n}\right] + R_n$$

where $F_o(x)$ denotes the CDF of the desired signal power RV evaluated at x, $\Lambda$ corresponds to the minimum desired signal power level for satisfactory reception (due to receiver noise), $\Phi_g(q)$ is defined as

$$\Phi_g(q) = \mathrm{Re}al\left[(1-j\tan q)G_0(c+jc\tan q,\Lambda)\Phi_I(-c-jc\tan q)\right] \qquad \textbf{Equation 4-8}$$

and the marginal MGF $G_0(s,x) = \int_x^{\infty} \exp\left(-sp_0/q\right) f_0(p_0)\,dp_0$ is convergent. When the desired signal amplitude is subject to Rayleigh, Rician, Nakagami-m or Nakagami-q fading, $G_0(s,x)$ can be expressed in terms of familiar mathematical functions. These results, originally derived in [37], are summarized below for the sake of clarity and convenience of the readers:

#### 4.2.2.1 Rayleigh

$$G_0(s,\Lambda)=\frac{\exp\left[-\Lambda\left(s/q+1/\overline{p}_0\right)\right]}{1+s\overline{p}_0/q} \qquad \textbf{Equation 4-9}$$

where $\overline{p}_0$ denotes the average desired signal power.

#### 4.2.2.2 Rician

$$G_0(s,\Lambda)=\frac{1+K_0}{s\overline{p}_0/q+1+K_0}\exp\left[\frac{-K_0\, s\overline{p}_0/q}{s\overline{p}_0/q+1+K_0}\right]Q\left(\sqrt{\frac{2K_0(1+K_0)}{s\overline{p}_0/q+1+K_0}},\sqrt{\frac{2\left(s\overline{p}_0/q+1+K_0\right)\Lambda}{\overline{p}_0}}\right)$$

**Equation 4-10**

where $Q\left(\sqrt{2a},\sqrt{2b}\right)=\int_b^\infty \exp(-t-a)\,I_0\left(2\sqrt{at}\right)dt$ denotes the first-order Marcum Q-function and $K_0$ is the Rice factor of the desired user signal.

#### 4.2.2.3 Nakagami-m

$$G_0(s,\Lambda)=\frac{1}{\Gamma(m_0)}\left(\frac{m_0}{m_0+s\overline{p}_0/q}\right)^{m_0}\Gamma\left[m_0,\Lambda\left(s/q+m_0/\overline{p}_0\right)\right] \qquad \textbf{Equation 4-11}$$

Where $\Gamma[a,x]=\int_x^\infty \exp(-t)\,t^{a-1}dt$ is the complementary incomplete Gamma function. If the fading index of the desired user signal $m_0$ assumes a positive integer value, (11) may be simplified as

$$G_0(s,\Lambda)=\left(\frac{m_0}{m_0+s\overline{p}_0/q}\right)^{m_0}\exp\left(-s\Lambda/q-m_0\Lambda/\overline{p}_0\right)\sum_{k=0}^{m_0-1}\frac{\left[\Lambda\left(s/q+m_0/\overline{p}_0\right)\right]^k}{k!}$$

**Equation 4-12**

### 4.2.2.4 Nakagami-q

$$G_0(s,\Lambda)=\frac{q}{\sqrt{[s\overline{p}_0+q]^2-[s\overline{p}_0 b_0]^2}}-\frac{q}{s\left(1-b_0^2\right)\overline{p}_0+q}I_e\left(\frac{b_0 q}{s\left(1-b_0^2\right)\overline{p}_0+q},\frac{\Lambda\left(1-b_0^2\right)\overline{p}_0 q}{s\left(1-b_0^2\right)\overline{p}_0+q}\right)$$

**Equation 4-13**

where $|b_0|\le 1$ is the fading parameter and Rice's $I_e$-function is related to the first-order Marcum Q-function as $I_e\left(V/U,U\right)=\frac{U}{W}\left[Q\left(\sqrt{U+W},\sqrt{U-W}\right)-Q\left(\sqrt{U-W},\sqrt{U+W}\right)\right]$ while $W=\sqrt{U^2-V^2}$.

Furthermore, $F_0(x)$ may be computed directly from $G_0(s,x)$ via relation $F_0(x)=1-G_0(s,x)$. It is therefore apparent that the outage probability calculation equation 7 only requires an evaluation of a single integral expression with finite integration limits if $\Phi_I(.)$ can also be expressed in closed-form. While $\Lambda=0$, equation 7 agrees with equation 3 since $G_0(s,0)=\Phi_0\left(\frac{s}{q}\right)$. Also, when $N=N_I$, in conjunction with reverts back to [12, eq. (9)], as anticipated.

In subsections 2.1 and 2.2, we have demonstrated that the mathematical framework for computing the outage probability of cellular mobile radio systems developed in [37] without SIC is still applicable in the present analysis with an appropriate substitution for $\Phi_I(.)$. In fact, these results are much more general to that of [27] and [32] because they are not restricted to i.i.d Rayleigh-faded CCI signals alone. Rather, this approach works as long as $\Phi_I(.)$ is computable (preferably in closed-form). As an example, MGF

$$\Phi_I(s)=\frac{N}{(m-1)!}\binom{N_I}{N}\sum_{n=0}^{(N_I-N)(m-1)}b(n,N_I-N,m)\left(\frac{m}{p}\right)^{n+mN}\sum_{v=0}^{N-1}(-1)^v\binom{N-1}{v}\sum_{k=0}^{v(m-1)}b(k,v,m)\frac{(m+n+k-1)!}{\left(s+\frac{m}{p}\right)^{m(N-1)-k}\left[s(v+1)+\frac{m}{p}(N_I-N+v+1)\right]^{m+n+k}}$$

$1\le N\le N_I$ of a sum of $N$ "weakest" among $N_I$ i.i.d Nakagami-faded (positive integer fading index) CCI signals is derived in Appendix A:

**Equation 4-14**

Where the coefficients $b(...)$ may be computed using multinomial theorem,

$$b(z,k,d)=\sum_{i=z-d+1}^{z}\frac{b(i,k-1,d)}{(z-i)!}I\left[0,(k-1)(d-1)\right](i) \qquad \textbf{Equation 4-15}$$

while , $b(0,0,d)=b(0,k,d)=1, b(z,1,d)=\frac{1}{z!}$ , and $b(1,k,d)=k$ .Substituting equation 14 into equation 3 or equation 7, one may investigate the impact of fade statistics of the interfering signals on the outage performance of a mobile radio system equipped with a smart antenna, in both interference-limited and noise-limited cases. Also, neither [27] nor [32] treat the case when the desired signal amplitude is subject to Nakagami-q fading or the refined outage criterion as discussed in Section 2.1.

## *4.3 Closed Form Expression for Outage Probability*

In this section, a few exact closed-form formulas for the probability of outage are derived by assuming that the desired signal amplitude is subject to Rayleigh or Nakagami-m fading (positive integer *m*) or when the fading amplitudes of the i.i.d interferers follow Nakagami-m distribution with positive integer fading severity index or the Rayleigh distribution. The underlying principle of the derivation is that if $F_0(.)$ (or $F_I(.)$) is of the form $1-\sum y^k\exp(-y), P_{out}$ can be directly expressed in terms of the derivatives of $\Phi_I(s)$ (or $\Phi_0(s)$) through use of a Laplace derivative formula:

$$\int_0^\infty y^k e^{-ay} f_I(y)\,dy=(-1)^k\frac{d^k}{ds}\left[\Phi_I(s)\right]\Big|_{s=a}=(-1)^k\Phi^{(k)}{}_I(a) \qquad \textbf{Equation 4-16}$$

### 4.3.1 Interference Limited case

$$\int_0^\infty y^k e^{-ay} f_I(y)\,dy=(-1)^k\frac{d^k}{ds}\left[\Phi_I(s)\right]\Big|_{s=a}=(-1)^k\Phi^{(k)}{}_I(a) \qquad \textbf{Equation 4-17}$$

$$P_{out}\left(N,N_I\right)=\int_0^{\infty} f_0\left(p_0\right)F_I^{(c)}\left(\frac{p_0}{q}\right)dp_0$$

Where $F_I^{(c)}\left(x\right)=1-F_I\left(x\right)$ denotes the complementary CDF. If all the CCI signal amplitudes are i.i.d and subject to Rayleigh fading, equation 17 can be evaluated in closed-form by substituting equation B8 in equation 17, viz.,

$$P_{out}\left(N,N_I\right)=\sum_{k=1}^{N}h_k\Phi_0\left(\frac{k+N_I-N}{qk\bar{p}}\right),\left[1\le N\le N_I\right] \qquad \textbf{Equation 4-18}$$

while $\Phi_0\left(.\right)$ is tabulated in Table 1 for a variety of fading environments. If the i.i.d CCI signal amplitudes experience Nakagami-m fading (positive integer fading severity index *m*), then it is also not very difficult to show that (with the aid of equation (A14) ,(A15) ,(A16) and equation 16 ):

$$\begin{aligned}
P_{out}\left(N,N_I\right)&=\frac{N}{\Gamma\left(m\right)}\binom{N_I}{N}^{(N_I-N)(m-1)}\sum_{n=0}^{}b\left(n,N_I-N,m\right)\left(\frac{m}{p}\right)^{mN+n}\\
&\times\sum_{v=0}^{N-1}\left(-1\right)^v\binom{N-1}{v}\sum_{k=0}^{v(m-1)}b\left(k,v,m\right)\\
&\times\left\{\sum_{r=1}^{m(N-1)-k}A_r\left(\frac{\bar{p}}{m}\right)^r\sum_{z=0}^{r-1}\frac{1}{z!}\left(\frac{-m}{q\bar{p}}\right)^z\Phi_0^{(z)}\right.\\
&\times\left(\frac{m}{q\bar{p}}\right)+\sum_{r=1}^{m+n+k}B_r\left[\frac{\bar{p}\left(v+1\right)}{m\left(N_I-N+v+1\right)}\right]^r\\
&\times\sum_{z=0}^{r-1}\frac{1}{z!}\left[\frac{m\left(N_I-N+v+1\right)}{-q\bar{p}\left(v+1\right)}\right]^z\\
&\left.\times\Phi_0^{(z)}\left(\frac{m\left(N_I-N+v+1\right)}{q\bar{p}\left(v+1\right)}\right)\right\}\\
&\times\frac{\Gamma\left(m+n+k\right)}{\left(v+1\right)^{m+n+k}},\left[1<N<N_I\right]
\end{aligned} \qquad \textbf{Equation 4-19}$$

$$P_{out}\left(N,N_I\right)=\sum_{z=0}^{mN_I-1}\frac{1}{z!}\left(\frac{-m}{q\bar{p}}\right)\Phi_0^{(z)}\times\left(\frac{m}{q\bar{p}}\right),\left[N=N_I\right] \qquad \textbf{Equation 4-20}$$

$$P_{out}\left(1,N_I\right)=\frac{N_I}{\Gamma(m)}\sum_{n=0}^{(N_I-1)(m-1)}b\left(n,N_I-1,m\right)\times\frac{\Gamma(m+n)}{N_I^{\,m+n}}\sum_{z=0}^{m+n-1}\frac{1}{z!}\left(\frac{-mN_I}{q\bar{p}}\right)^z\Phi_0^{(z)}\left(\frac{mN_I}{q\bar{p}}\right),\left[N=1\right] \qquad \textbf{Equation 4-21}$$

where the $z$-th order derivative of MGF of the desired signal power is tabulated in Table 2 for several fading channel models.

### 4.3.2 Minimum Signal Power Requirement Scenario

If an additional minimum signal power constraint is imposed for satisfactory reception, then the probability of outage is given by

$$P_{out}\left(N,N_I\right)=1-\int_{\Lambda}^{\infty}f_0\left(p_0\right)F_I\left(\frac{p_0}{q}\right)dp_0=F_0\left(\Lambda\right)+\int_{\Lambda}^{\infty}f_0\left(p_0\right)F_I\left(\frac{p_0}{q}\right)dp_0 \qquad \textbf{Equation 4-22}$$

Where the CDF of the desired user signal power is related to its marginal MGF as $F_0\left(\Lambda\right)=1-G_0\left(0,\Lambda\right)$ and $G_0\left(s,\Lambda\right)$ (in closed-form) is defined in equation (9) through (13) through for different fading channel models. While the i.i.d CCI signals are subject to Rayleigh fading, we may simplify equation (22) as

$$P_{out}\left(N,N_I\right)=F_0\left(\Lambda\right)+\sum_{k=1}^{N}h_kG_0\left(\frac{k+N_I-N}{k\bar{p}},\Lambda\right),\left[1<N<N_I\right] \qquad \textbf{Equation 4-23}$$

using equation (B8) Further simplifications of equation (22) (similar to our treatment of the interference-limited case in subsection 3.1) appears not possible except for the case of both the desired user signal and the CCI signals are subject to Nakagami-m fading. These results are summarized below:

$$P_{out}(N,N_I)=\frac{N}{\Gamma(m)}\binom{N_I}{N}\sum_{n=0}^{(N_I-N)(m-1)}\beta(n,N_I-N,m)\left(\frac{m}{\bar{p}}\right)^{mN+n}\sum_{v=0}^{N-1}(-1)^v\binom{N-1}{v}\sum_{k=0}^{v(m-1)}\beta(k,v,m)$$

$$\times\left\{\sum_{r=1}^{m(N-1)-k} A_r\left(\frac{\bar{p}}{m}\right)^r \sum_{z=0}^{r-1}\frac{1}{z!}\left(\frac{m}{q\bar{p}}\right)^z \varnothing\left(\Lambda, \frac{m}{\bar{p}q}, z\right) + \sum_{r=1}^{m+n+k} B_r\left[\frac{\bar{p}(v+1)}{m(N_I-N+v+1)}\right]^l \right.$$

$$\left. \times \sum_{z=0}^{r-1}\frac{1}{z!}\left[\frac{m(N_I-N+v+1)}{q\bar{p}(v+1)}\right]^z \varnothing\left(\Lambda, \frac{m(N_I-N+v+1)}{q\bar{p}(v+1)}, z\right)\right\} \frac{\Gamma(m+n+k)}{(v+1)^{m+n+k}}, \quad [1 < N < N_I]$$

**Equation 4-24**

$$P_{out}(N_I, N_I) = \sum_{z=0}^{mN_I-1}\frac{1}{z!}\left(\frac{m}{\bar{p}q}\right)^z \varnothing\left(\Lambda, \frac{m}{\bar{p}q}, z\right) \quad [N = N_I]$$

**Equation 4-25**

$$P_{out}(1, N_I) = \frac{N_I}{\Gamma(m)} \sum_{n=0}^{(N_I-1)(m-1)} \beta(n, N_I-1, m)\frac{\Gamma(m+n)}{N_I^{m+n}} \sum_{z=0}^{m+n-1}\frac{1}{z!}\left(\frac{mN_I}{\bar{p}q}\right)^z \varnothing\left(\Lambda, \frac{mN_I}{\bar{p}q}, z\right), \quad [N = 1]$$

**Equation 4-26**

where

$$\varnothing(\Lambda, \Omega, z) = \left(\frac{m_0}{\bar{p}_0}\right)^{m_0} \frac{\Gamma(z+m_0, \Lambda(\Omega + m_0/\bar{p}_0))}{\Gamma(m_0)(\Omega + m_0/\bar{p}_0)^{z+m_0}}$$

**Equation 4-27**

It is important to note that while $m$ is restricted to a positive integer value in the above expressions, $m_0$ may assume any real number that is greater than or equals to ½.

**Table 4-2 n$^{th}$ order derivative of the MGF of the signal power $f_k^{(n)}(.)$**

| Fading environment | n$^{th}$ order derivative of the MGF of the signal power |
|---|---|
| Rayleigh | $f_k^{(n)}(s) = \frac{(-\bar{p}_k)^n n!}{(1+s\bar{p}_k)^{1+n}}$ |
| Rician | $f_k^{(n)}(s) = \frac{(-\bar{p}_k)^n (n!)^2 (1+K_k)}{(1+K_k+s\bar{p}_k)^{1+n}} \exp\left(\frac{-sK_k}{1+K_k+s\bar{p}_k}\right) \sum_{i=0}^{n} \frac{1}{(i!)^2 (n-i)!}\left(\frac{K_k(1+K_k)}{1+K_k+s\bar{p}_k}\right)^i$ |
| Nakagami-$q$ | $f_k^{(n)}(s) = \frac{n!}{2^{2n}\sqrt{[1+s\bar{p}_k(1+b_k)][1+s\bar{p}_k(1-b_k)]}}\left[\frac{-\bar{p}_k(1+b_k)}{1+s\bar{p}_k(1+b_k)}\right]^n \times \sum_{w=0}^{n}\frac{(2w)![2(n-w)]!}{[w!(n-w)!]^2}\left[\frac{(1-b_k)[1+s\bar{p}_k(1+b_k)]}{(1+b_k)[1+s\bar{p}_k(1-b_k)]}\right]^w$ |

| | |
|---|---|
| Nakagami-*m* | $f_k^{(n)}(s) = \dfrac{(-\bar{p}_k)^n m_k^{m_k} \Gamma(m_k + n)}{(m_k + s\bar{p}_k)^{m_k+n} \Gamma(m_k)}$ |

### 4.3.3 Treating receiver Noise as CCI

Suppose the effect of receiver noise is taken into account in a cellular system design by treating it as CCI, we can show that the probability of outage is

$$P_{out}(N, N_I) = F_0(\Lambda) + \int_{\Lambda}^{\infty} f_0(p_0) F_I^{(c)}((p_0 - \Lambda)/q) dp_0$$

**Equation 4-28**

For the special case of i.i.d Rayleigh-faded CCI signal amplitudes, equation (28) may be evaluated in closed-form as

$$P_{out}(N, N_I) = F_0(\Lambda) + \sum_{k=1}^{N} \eta_k \exp\left(\frac{k + N_I - N}{q k \bar{p}/\Lambda}\right) G_0\left(\frac{k + N_I - N}{k\bar{p}}, \Lambda\right), \quad [1 \le N < N_I]$$

**Equation 4-29**

Development of a generic closed-form formula similar to equation (29) appears to be impossible for any other distribution besides the Rayleigh statistic for the CCI signal amplitudes. Nevertheless, it is possible to derive a closed-form formula for the outage probability given that the CCI signal amplitudes follow the Nakagami-m distribution (positive integer fading index) and the desired user signal is subject to either Rayleigh or Nakagami-m fading. Next, we will derive a concise expression for the probability of outage while both the desired user signal and the CCI signal amplitudes experience Nakagami-m fading (positive integer fading index). In this case, it is advantageous to restate equation (28) as

$$P_{out}(N, N_I) = \int_0^{\infty} f_I(I) F_0(qI + \Lambda) dI$$

**Equation 4-30**

so that the final solution may be expressed in terms of only the derivatives of $\Phi_I(.)$. Substituting equation (A5) into equation (30), and then simplifying the resultant expression using equation (16), we obtain

$$P_{out}(N, N_I) = 1 - \exp\left(\frac{-m_0\Lambda}{\bar{p}_0}\right) \sum_{n=0}^{m_0-1} \frac{1}{n!}\left(\frac{m_0\Lambda}{\bar{p}_0}\right)^n \sum_{k=0}^{n} \binom{n}{k} (-q/\Lambda)^k \phi_I^{(k)}\left(\frac{m_0 q}{\bar{p}_0}\right)$$

**Equation 4-31**

while $\Phi_I^{(k)}(.)$ is computed from equation (14) using the Leibniz's derivative rule of a product [16, Eq. (0.42)]. The above formula holds for all values of $1 < N < N_I$. It is also interesting to note that for the specific case of $m_0 = 1$, equation (31), simplifies into an extremely simple expression that allows one to predict the refined outage performance given that the desired user signal power random variable follows an exponential distribution:

$$P_{out}(N, N_I) = 1 - \exp(-\Lambda/\bar{p}_0)\ \phi_I(q/\bar{p}_0)$$

**Equation 4-32**

## *4.4 Computational Results*

In the following, we present selected numerical curves for outage probability of cellular mobile radio systems by assuming that the number of CCI signals is fixed. Subsequently, the effect of traffic loading (to account for random number of interferers) on the outage performance is investigated. The usefulness of the probability of outage metric (derived in Sections 2 and 3) in a cellular mobile radio design is also discussed. Specifically, we highlight the benefits of deploying a smart antenna in a cellular radio architecture — in terms of its ability to significantly reduce the co-channel reuse distance factor, and therefore, realizing a much higher spectral efficiency compared to a system which only deploys a conventional receiver (i.e., without CCI cancellation).

### 4.4.1 Outage Probability with Fixed Number of Interferers

Fig. 5.1 illustrates the outage probability with selective interference cancellation for both Rayleigh and Rician faded desired user cases in an interference-limited environment. It is apparent that about 0.8 dB gain can be realized by cancelling only the strongest CCI signal over the average SIR/q (i.e., $\frac{p_0}{\bar{p}q}$) requirement for satisfying a prescribed grade-of-service (GoS) with no CCI cancellation. The relative improvement gets larger as additional CCI signals are cancelled. For instance, a gain of 4.8 dB is obtained using an

adaptive array with 5-elements. This observation in turn suggests that it is desirable to use an adaptive array with a higher number of antenna elements so as to achieve a significantly better performance if size, cost and complexity considerations are not major factors in the design.

In Fig. 5.2, we compare the outage probability of a mobile radio system while $N_I - N$ CCI signals are cancelled using two different interference nulling algorithms. It is apparent that the outage probability of a cellular system which uses a smart antenna to suppress $N_I - N$ "strongest" CCI signals is always lower than that of a cellular system with $N$ CCI signals but no interference cancellation. To explain this trend, let us assume that $N_I = 6$ and an adaptive array with 2-elements is used to suppress a single CCI signal.

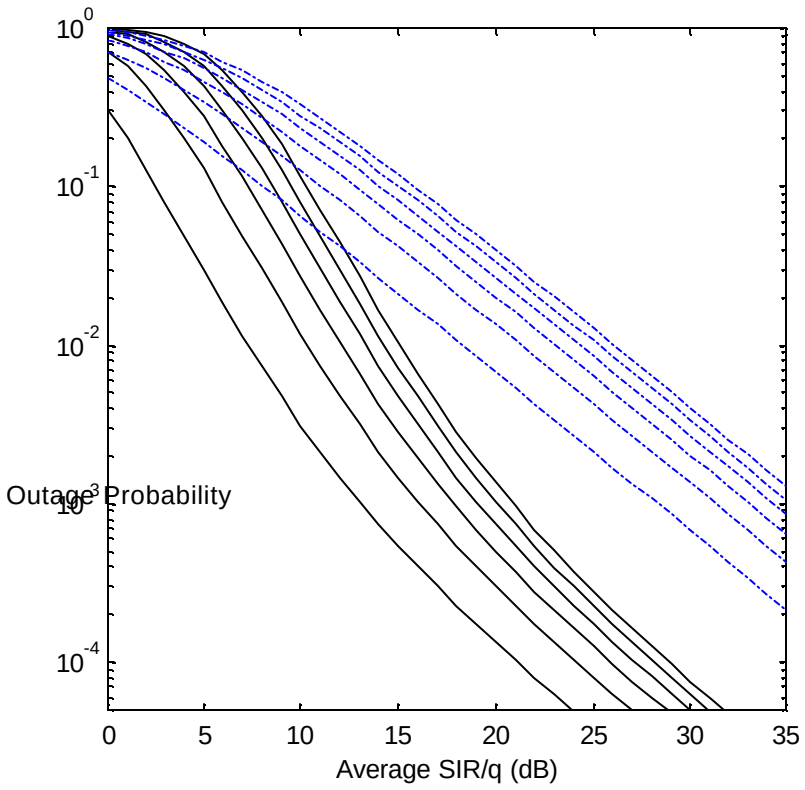


Figure 4-1 Outage probability $P_{out}$ versus average SIR/$q$ $\overline{p}_0/\overline{p}q$ curves for a cellular mobile radio system that employs an adaptive array with $D = N_I - N + 1$ elements (to cancel the "strongest" $(N_I - N)$ CCI signals) in an interference-limited Rician (desired

user)/Nakagami-*m* (interferers) fading channel model.

If the adaptive array randomly cancels one out of the six i.i.d CCI signals, then the outage performance of the system will be equivalent to that of a mobile radio system with $(N_I = 5)$ and no interference cancellation. However, if the adaptive array rejects the CCI signal having the strongest instantaneous signal power, then the probability of outage will be governed by the remaining $(N = 5)$ "weakest" CCI signals. As such, we can expect the latter algorithm (which exploits the ordered statistic of instantaneous CCI signal powers) to outperform the former (which cancels the CCI signals randomly without any ranking). From Fig. 5.2, we also observe that the discrepancy between these two curves becomes more pronounced as $N$ decreases while $N_I$ is fixed, as anticipated. Using the above argument, we can also expect the adaptive array to yield a larger performance improvement when the mean CCI signal powers are not uniformly distributed (or more generally, when the CCI signals are subject to nonidentical fading). As well, if the ranking of CCI instantaneous signal powers is not done perfectly (owing to outdated or noisy estimates), then the outage probability of the cellular system will be upper bounded by the outage curve generated using the random cancellation assumption.

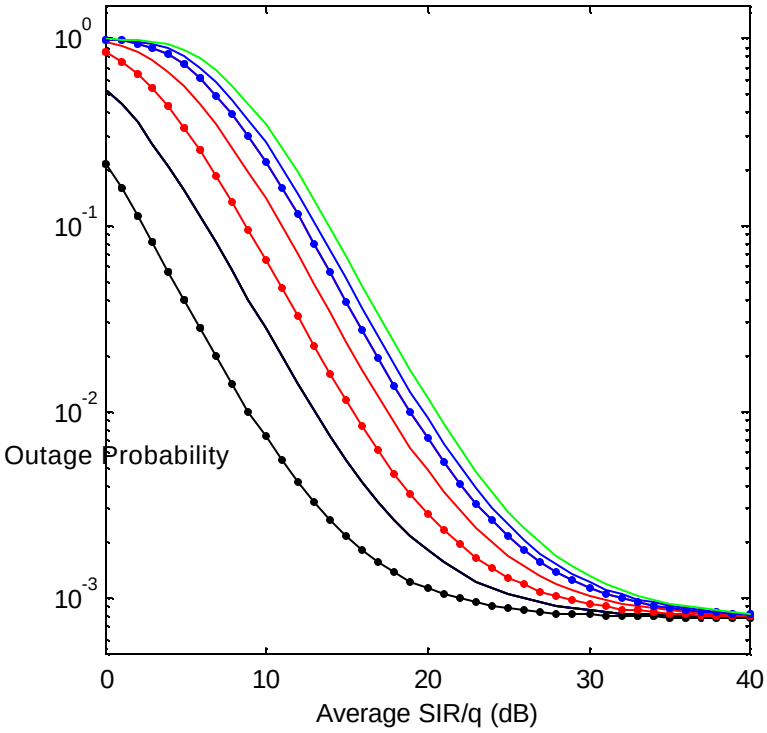


Figure 4-2 Comparison of outage probability of a mobile radio network (a minimum signal power requirement is imposed to consider the effect of receiver noise) which uses a smart antenna either to suppress the "strongest" $(N_I - N)$ CCI signals or to simply reject $N_I - N$ interfering signals randomly (i.e., without ordering/ranking the instantaneous CCI signal powers).

Fig. 5.3 reveals that a floor on outage probability will occur at high average SIR/q range when receiver noise is considered, regardless of whether the CCI signals are present or not, because the deep fades will result in signal power level below the specified minimum. While the system performance is interference-limited at lower average SIR/q values, it becomes noise-limited as the average SIR/q is increased to a sufficiently large value. As such, we would expect that the system performance gain realized using a smart antenna in practical cellular systems will diminish beyond a certain average SIR/q value. This trend has been validated in Fig. 5.2. Our computational experiments also reveal that equation 3 is stable as long as $\Lambda$ is not very large. In fact, the remainder term $R_n$ declines rapidly as $\Lambda \to 0$. From Fig. 5.3, we also observe that the outage probability predicted by treating receiver noise as CCI tends to be slightly pessimistic compared to

minimum signal power constraint approach, and their discrepancy is largest at the knee of the curves. Moreover, the difference between these two curves becomes more pronounced as the fading index of the desired user signal gets larger.

### 4.4.2 Outage Probability with Random Number of Interferers

In Sections 2 and 3, we have derived analytical expressions for computing the probability of outage by assuming that that all of the co-channel interferers $N_I$ are active all the time, and therefore $L = N_I$ is fixed, where *L* denotes the number of active CCI signals. In practice, however, this may not be the case because not all the CCI signals will be active at any given time. This is particularly true if the offered traffic load in the co-channel cells is not heavy or when a discontinuous transmission scheme is implemented to improve the spatial efficiency. Outage calculation in these situations can also be handled quite easily by letting L be a random variable (which may take any of the values $\{0,1,...,N_I\}$ where $N_I$ denotes the total number of co-channel interferers) and considering all the possibilities for the number of active co-channel interferers, viz.,

$$P_{out} = \sum_{L=0}^{N_I} \Pr\{L\} P_{out}(N, L)$$

**Equation 4-33**

where $P_{out}(N, L)$ is interpreted as the conditional probability of outage given that there are *N* remaining (uncanceled) "weakest" CCI signals out of *L* active CCI signals, and $\Pr\{L\}$ is the probability of having *L* active co-channel interferers. Suppose an adaptive array with D elements is used to suppress the "strongest" (D-1) CCI signals, then equation (33) may be conveniently rewritten as

$$P_{out} = F_0(\Lambda) \sum_{L=0}^{D-1} \Pr\{L\} + \sum_{L=D}^{N_I} \Pr\{L\} P_{out}(L - D + 1, L)$$

**Equation 4-34**

because $P_{out}(N, L) = F_0(\Lambda)$ if $L \le D - 1$.

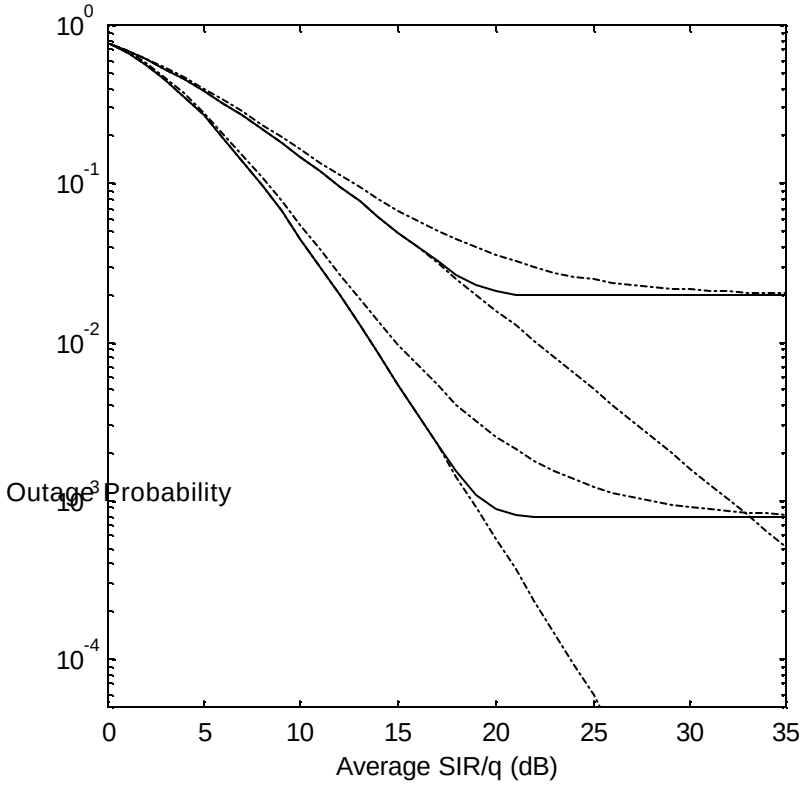


Figure 4-3 Outage probability versus the average SIR/q in a Nakagami-*m* (desired)/Nakagami-m (interferer) fading channel model: (a) treating receiver noise as CCI; (b) receiver noise is considered by imposing a minimum signal power constraint; (c) interference-limited case (ignoring the receiver noise).

Assuming uniform traffic loading across cells and that each of the $N_I$ i.i.d co-channel cells have $N_c$ different frequency voice channels with blocking probability B, reference [41] has shown that $\Pr\{L\}$ can be described by a binomial distribution:

$$\Pr\{L\} = \binom{N_I}{L}(p_A)^L(1-p_A)^{N_I-L} = \binom{N_I}{L}B^{L/N_c}(1-B^{1/N_c})^{N_I-L} \qquad \textbf{Equation 4-35}$$

since the status of whether a co-channel interferer in a given cell is active or not is given by a Bernoulli PDF and $p_A$ is the probability that a voice channel is active. The effect of nonidentical blocking probability for different co-channel cells (to reflect the nonuniform traffic loading conditions) can also be treated by replacing the standard binomial PDF in equation (35) with a generalized binomial PDF.

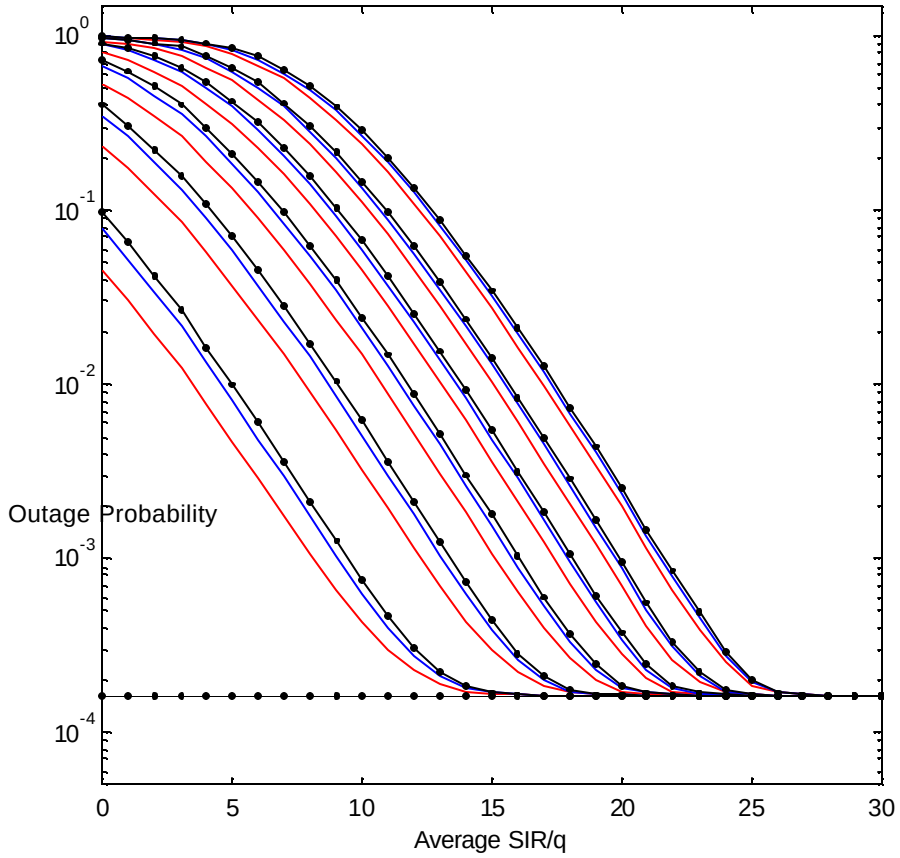


Figure 4-4 Outage probability (minimum signal power constraint case) versus average SIR/q for different blocking probabilities $\left(B \in \{0.5, 0.2, 0.02\}\right)$ while a smart antenna with $D$-elements is used to suppress the strongest $D-1$ CCI signals.

Fig. 5.4 illustrates the outage probability of a cellular mobile radio system when both the desired user signal and CCI signal amplitudes are subject to Nakagami-m fading with $m_0 = 2.5$ and $m = 2$, for different values of blocking probabilities. It is evident that increasing the number of elements D in adaptive array translates into a considerable reduction in the probability of outage. The relative improvement gets larger as D increases, until all of the CCI signals are cancelled. Similarly, the dependence of outage probability on blocking probability becomes more pronounced when SIC is applied (i.e., the spread between the curves corresponding to different blocking probabilities increases).

### 4.4.3 Spectral Utilization Efficiency

Spectral efficiency is of primary concern to cellular system planners, and is measured in terms of the spatial traffic density per unit bandwidth. Spectral efficiency of a cellular system that consists of a uniform deployment of hexagonal cells is given by [42]

$$\eta = \frac{G_c}{N_c W_c C A_{cell}} \text{ Erlang/MHz/km}^2$$

**Equation 4-36**

where $G_c$ is defined as the offered traffic per cell, $N_c$ corresponds to the number of channels per cell, $W_c$ is the bandwidth per channel (MHz), C denotes the cluster size and $A_{cell}$ is the area per cell ($km^2$). Using geometric arguments, we can show that $A_{cell} = 3\sqrt{3}R^2/2$ and the co-channel reuse factor $R_f$ is related to the cluster size $C$ as $R_f = D/R = \sqrt{3C}$ for a regular hexagonal cell deployment while R is the distance from the center to the corner of a cell (i.e., cell radius) and D denotes the co-channel reuse distance (distance between the centers of the nearest neighboring co-channel cells). Hence, equation (36) may be restated as

$$\eta = \frac{2G_c}{\sqrt{3}N_c W_c R^2 R_f^2} \text{ Erlang/MHz/km}^2$$

**Equation 4-37**

Considering a two-slope path loss model, reference [19] has shown that the average SIR (i.e., $\frac{p_0}{\bar{p}}$) in the worst-case scenario (in which the desired user is near the edge of its cell and the interfering users are on the cell edges closest to the desired user cell) is given by

$$\frac{\bar{p}_0}{\bar{p}} = \left(\frac{D-R}{R}\right)^a \left(\frac{1+(D-R)/g}{1+R/g}\right)^b = (R_f - 1)^a \left(\frac{g/R + R_f - 1}{g/R + 1}\right)^b$$

**Equation 4-38**

where a and b are the path loss exponents, and parameter g denotes the breakpoint range (typically, in the range of 150-300 meters). Therefore, using equation (37) and/or equation (38) in conjunction with the analytical expressions for the outage probability (with/without receiver noise) derived in Sections 2 and 3, the dependence of outage probability.

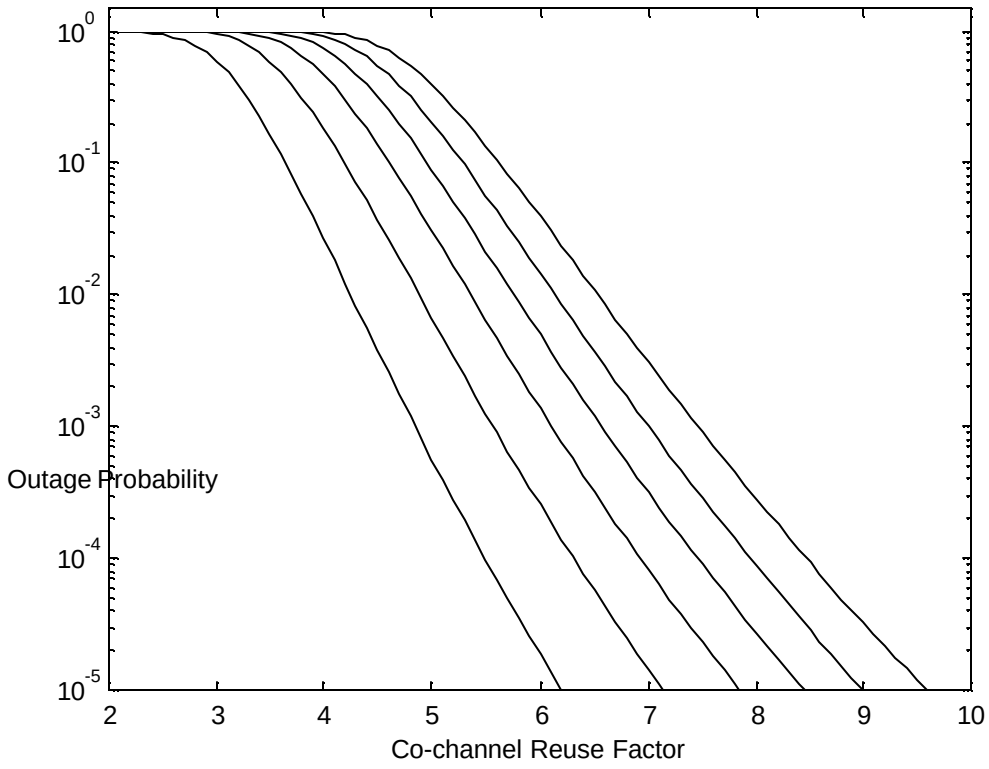


Figure 4-5 Outage probability (interference-limited case) dependence on the co-channel reuse factor $R_f$ in a Nakagami-*m* fading environment ( $m_0 = 3$ and $m = 2$ ).

on co-channel reuse factor and/or spectral efficiency can be investigated. As an example, Fig. 5.5 shows the outage probability of a microcellular system versus the co-channel reuse factor when $m_0 = 3, m = 2$ and $q = 9.5$ dB. For a fixed *N*, the outage probability declines rapidly with a higher co-channel reuse factor because of lesser co-channel interference (due to the attenuation or path loss effect of wireless medium). There is also a marked decrease in the outage probability for a given reuse distance when a SIC technique is implemented. As reuse distance is increased, the gain derived from the smart antenna system become more pronounced as can be observed by the widening of the curves at higher $R_f$. It is also clear that the use of a smart antenna lowers $R_f$ at a specified $P_{out}$, which in turn improves the spectral efficiency. The fact that a smaller $R_f$ translates into a higher spectral efficiency while other system parameters remain unchanged can be deduced from equation (37). The dependence of spectral efficiency on

the capabilities of SIC scheme is illustrated in Fig. 5.6 for $K_0 = 3.5$ (i.e., Rician-faded desired user signal) and $m = 2$. When $h$ is large, then the outage probability is also high as expected, owing to the smaller reuse distance. But it can be observed that the degradation is less severe when some sort of CCI cancellation scheme has been employed.

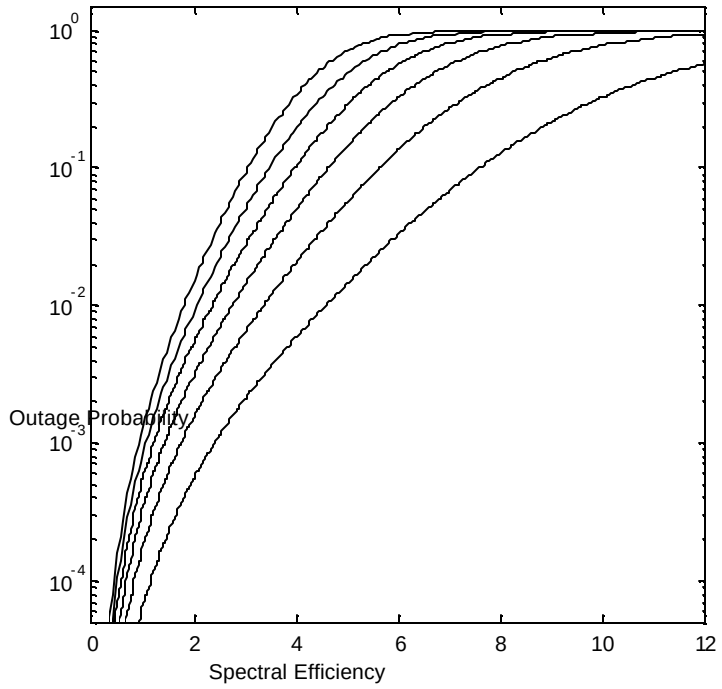


Figure 4-6 Effect of an adaptive interference nulling technique on the spectral efficiency of an interference-limited cellular mobile radio system.

Before concluding this section, we would like to point out that the cluster size C for a prescribed $P_{out}(N, N_I)$ may be determined with the aid of the outage probability versus co-channel reuse factor curves similar to that of Fig. 5.5. Since a tessellating reuse cluster of size C can be constructed if $C = (u + v)^2 - uv$ where $u$ and $v \le u$ are non-negative integers, it follows that the allowable cluster sizes are $C = 1,3,4,7,9,12...$ and so on. Therefore, once the value of $R_f$ has been interpolated from the above figure, we may

then choose the smallest value from the set of allowable $C$ values which exceeds $R_f^2/3$ to be the cluster size.

### 4.4.4 Outage Probability with Rician Faded Interferers

Equation (3) can be used to generate along with table 1 can be used to generate the probability of outage for any of the fade distribution of the desired user signal and interferer signal. Figure 4.7 presents the scenario where desired user signal's fading is Rayleigh distributed and interfere signal fading is Rician distributed.

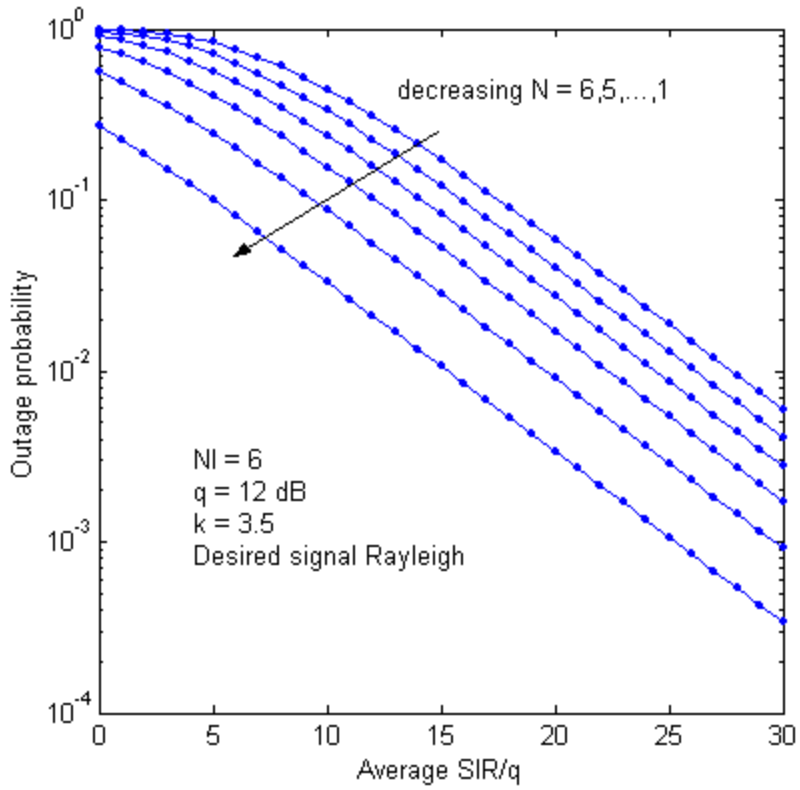


Figure 4-7 Probability of Outage $P_{out}$ versus average SIR/q curves for a cellular mobile radio system employing adaptive array with D antenna element ($D = N_I - N + 1$) cancel the strongest $(N_I - N)$ CCI signals in an interference limited scenario with Rayleigh (Desired User) / Rician (Interferers) fading channel model.

It can be observed that the outage probability of a cellular system which uses a smart antenna to suppress $N_I - N$ 'strongest' CCI signals is always lower than that of cellular system with N CCI signals but no interference cancellation.

## 4.5 Practical Considerations

The theoretical results in above sections were derived by assuming the perfect cancellation of the strongest co-channel interferes by the smart antenna system. In practical system perfect cancellation or perfect steering of the deep nulls towards interfering signal is hard to achieve. There are several factors that effect the null steering of the smart antenna system such as phase imbalance antenna branches, non convergence of the adaptive algorithm, thermal noise and calibration of the smart antenna system. In practical system the all the strongest $N_I - N$ interferes would not be cancelled completely and would appear at the receiver as residual interference along with the N remaining interferes The effect of above mentioned imperfection in the resulting antenna beam pattern and it's effect on the outage probability is almost impossible to characterize in the theoretical treatment because the amount of non convergence of the antenna algorithm and the amount of imperfection in the beam pattern due to any reason is completely random and it's distribution is difficult predict.

How ever the theoretical results presented in this chapter do provides a strong upper bound for the system employing smart antenna under the assumed conditions. They provided a very reliable, accurate and convenient method of comparing and/or analyzing the system performance under various conditions without running time consuming Monte Carlo simulations.

## 4.6 Concluding Remarks

This article presents a theoretical framework for evaluating the outage performance of a cellular mobile radio system in overloaded array environments. Selected design examples are provided to show the benefits of a "selective interference cancellation" scheme (in terms of communication link quality improvement without compromising the spectrum utilization efficiency and extended battery life) for cellular mobile radio communications.

The impact of fade statistics and traffic loading on the probability of outage are also studied. The extension of this work that examines the effect of power imbalance among all the independent Nakagami-m or Rician faded CCI signals (including the real-valued fading severity index case) on the outage probability and the average symbol error rate performance of a multitude digital modulation schemes is currently being studied.

## 4.7 Appendix A

If the i.i.d random variables $p_{1,}p_{2,}...,p_{N_I}$, each with PDF $f(x)$ and CDF $F(x)$, are arranged in an ascending order of magnitude and then written as $p_{1:N_I} \le p_{2:N_I} \le ... \le p_{N_I:N_I}$, we call $p_{k:N_I}$ the -th order statistic. From Section 2, we know that only the knowledge of MGF of $I = \sum_{k=1}^{N} p_{k:N_I}$ is further required for calculating the probability of outage of mobile cellular radio systems with SIC. Therefore, in this appendix, we first develop a general procedure for deriving $\Phi_I(s)$ for any $1 \le N \le N_I$ and subsequently apply this result to derive the MGF, PDF and the CDF of the sum of N "weakest" CCI signals in a Nakagami-m fading environment. From reference [35], we know that the joint density function of $p_{1:N_I} \le p_{2:N_I} \le ... \le p_{N_I:N_I}$ to be

$$f_{1,\ldots,N:N_I}(x_1,\ldots,x_N) = N!\binom{N_I}{N}[1-F(x_N)]^{N_I-N}\prod_{k=1}^{N} f(x_k) \qquad \textbf{A 1}$$

where $0 < x_1 < ... < x_N < \infty$. Then the MGF of I may be computed as

$$\begin{aligned}\phi_I(s) &= \int_0^{\infty} e^{-sx_N}\int_0^{x_N} e^{-sx_{N-1}}\ldots\int_0^{x_2} e^{-sx_1} f_{1,\ldots,N:N_I}(x_1,\ldots,x_N)\,dx_1\ldots dx_{N-1}\,dx_N \\ &= N!\binom{N_I}{N}\int_0^{\infty} e^{-sx_N} f(x_N)[1-F(x_N)]^{N_I-N} \\ &\times\left\{\int_0^{x_N} e^{-sx_{N-1}} f(x_{N-1})\ldots\int_0^{x_2} e^{-sx_1} f(x_1)\,dx_1\ldots dx_{N-1}\right\}dx_N \\ &= N\binom{N_I}{N}\int_0^{\infty} e^{-sx_N}[1-F(x_N)]^{N_I-N} f(x_N)\left(\int_0^{x_N} e^{-sx} f(x)\,dx\right)^{N-1} dx_N \end{aligned} \qquad \textbf{A 2}$$

since the $(N-1)$-fold nested integral in the second line of equation (A2) may be replaced by a product of $(N-1)$ integrals, viz.,

$$\int_0^{x_N} e^{-sx_{N-1}} f(x_{N-1}) \ldots \int_0^{x_2} e^{-sx_1} f(x_1)\, dx_1 \ldots dx_{N-1} = \left( \int_0^{x_N} e^{-sx} f(x)\, dx \right)^{N-1} / (N-1)! \quad \textbf{A 3}$$

To the best of the authors' knowledge, equation (A2) is new and has not been reported in the literature. It is also interesting to note that equation (A2) holds for all common fading distributions. For instance, if $p_k \, (k = 1,2,..., N_I)$ denote the instantaneous signal powers of the CCI signals, it can be shown that $\Phi_I(s)$ reduces to a single integral expression (whose integrand is composed of tabulated functions) while the fading amplitudes of the interfering signals follow Rician, Nakagami-m (real $m \geq 0.5$) or Nakagami-q distribution. This is attributed to the availability of a closed-form formula for the marginal MGF $\int_0^x e^{-sx} f(x)\, dx$ in the above cases . Moreover, if $p_1, p_2, \ldots, p_{N_I}$ are i.i.d exponential or Gamma variates, equation (A2) can also be evaluated in closed-form. A sketch of this derivation is provided next.

Assuming that the amplitudes of the CCI signals are subject to Nakagami-m fading with a positive integer fading severity index m, we have

$$f(x) = \frac{1}{\Gamma(m)} \left( \frac{m}{\bar{p}} \right)^m x^{m-1} e^{-mx/\bar{p}} \quad \textbf{A 4}$$

$$F(x) = 1 - e^{-mx/\bar{p}} \sum_{n=0}^{m-1} \frac{1}{n!} \left( \frac{mx}{\bar{p}} \right)^n \quad \textbf{A 5}$$

In order to simplify equation (A2) , we first rewrite as $\left[1 - F(x_N)\right]^{N_I - N}$

$$\left[ e^{-mx_N/\bar{p}} \sum_{n=0}^{m-1} \frac{1}{n!} \left( \frac{mx_N}{\bar{p}} \right)^n \right]^{N_I - N} = e^{-m(N_I - N)x_N/\bar{p}} \sum_{n=0}^{(N_I - N)(m-1)} \beta(n, N_I - N, m) \left( \frac{mx_N}{\bar{p}} \right)^n \quad \textbf{A 6}$$

while the coefficients $b(.,.,.)$ are defined in equation (15), and then substituting equation (A4) and equation (A6) in the second line of equation (A2) to yield

$$\phi_I(s) = \frac{N!}{[\Gamma(m)]^N}\binom{N_I}{N}\sum_{n=0}^{(N_I-N)(m-1)}\beta(n, N_I-N, m)\left(\frac{m}{\bar{p}}\right)^{n+mN}$$

$$\times G\left(s+\frac{m}{\bar{p}}, s+\frac{m}{\bar{p}}(N_I-N+1), m, m+n, N\right) \qquad \textbf{A 7}$$

where

$$G(a, b, m, d, N) = \int_0^{\infty} e^{-bx_N} x_N^{d-1}\int_0^{x_N} e^{-ax_{N-1}} x_{N-1}^{m-1}\cdots\int_0^{x_2} e^{-ax_1} x_1^{m-1}\, dx_1\ldots dx_{N-1}\, dx_N \qquad \textbf{A 8}$$

Using reference[40], Eq. (3.351.1) to evaluate the inner-most integral in equation (A8), we can show that $G(a,b,m,d,N)$ (for any $N \geq 2$) can be evaluated in closed-form via a recursion formula:

$$G(a, b, m, d, N) = \sum_{k=0}^{d-1}\frac{\Gamma(d)}{k!\, b^{d-k}} G(a, a+b, m, k+m, N-1),\ N \geq 2 \qquad \textbf{A 9}$$

and $G(.,b,.,d,1) = \dfrac{\Gamma(d)}{b^d}$.

Alternatively, by applying equation (A3) in equation (A8), $\Phi_I(s)$ reduces to

$$\phi_I(s) = \frac{N}{\Gamma(m)}\binom{N_I}{N}\sum_{n=0}^{(N_I-N)(m-1)}\beta(n, N_I-N, m)\left(\frac{m}{\bar{p}}\right)^{n+mN}\sum_{v=0}^{N-1}(-1)^v\binom{N-1}{v}\sum_{k=0}^{v(m-1)}\beta(k, v, m)$$

$$\times\frac{\Gamma(m+n+k)}{\left(s+\frac{m}{\bar{p}}\right)^{m(N-1)-k}\left[s(v+1)+\frac{m}{\bar{p}}(N_I-N+v+1)\right]^{m+n+k}},\quad [1 \leq N \leq N_I] \qquad \textbf{A 10}$$

after simplifications using the following two identities:

$$\int_0^u x^{n-1} e^{-\mu x}\, dx = \frac{\Gamma(n)}{\mu^n}\left[1 - e^{-u\mu}\sum_{k=0}^{n-1}\frac{1}{k!}(u\mu)^k\right]$$

$$\left[\sum_{k=0}^{m-1}\frac{1}{k!}(ax_N)^k\right]^v = \sum_{k=0}^{v(m-1)}\beta(k, v, m)(ax_N)^k$$

In Section 3, the PDF and the CDF of I are also needed so as to facilitate the derivation of $P_{out}$ in closed-form. A closed-form expression for the PDF of I can be readily obtained from equation (A10) by first expanding $\Phi_I(s)$ using partial fractions and then performing an inverse Laplace transformation of the resultant terms. The final result for $f_I(x)$ is summarized below:

$$f_I(x) = \frac{N}{\Gamma(m)}\binom{N_I}{N}\sum_{n=0}^{(N_I-N)(m-1)}\beta(n, N_I-N, m)\left(\frac{m}{\bar{p}}\right)^{mN+n}\sum_{v=0}^{N-1}(-1)^v\binom{N-1}{v}\sum_{k=0}^{v(m-1)}\frac{\Gamma(m+n+k)}{(v+1)^{m+n+k}}$$

$$\times\beta(k, v, m)\left\{\sum_{r=1}^{m(N-1)-k}\frac{A_r}{\Gamma(r)}x^{r-1}e^{-\frac{xm}{\bar{p}}}+\sum_{r=1}^{m+n+k}\frac{B_r}{\Gamma(r)}x^{r-1}e^{-\frac{xm}{\bar{p}}\left(\frac{N_I-N+v+1}{v+1}\right)}\right\},\ [1<N<N_I] \quad \textbf{A 11}$$

$$f_I(x) = \frac{1}{\Gamma(mN_I)}\left(\frac{m}{\bar{p}}\right)^{mN_I}x^{mN_I-1}e^{-mx/\bar{p}},\ [N=N_I] \quad \textbf{A 12}$$

$$f_I(x) = \frac{N_I}{\Gamma(m)}\sum_{n=0}^{(N_I-1)(m-1)}\beta(n, N_I-1, m)\left(\frac{m}{\bar{p}}\right)^{m+n}x^{m+n-1}e^{-xmN_I/\bar{p}},\ [N=1] \quad \textbf{A 13}$$

where $A_r$ and $B_r$ are coefficients of a partial fraction expansion and they are defined as

$$A_r = (-1)^{m(N-1)-k-r}\left[\frac{\bar{p}(v+1)}{m(N_I-N)}\right]^{mN+n-r}\binom{mN+n-r-1}{m+n+k-1}$$

$$B_r = (-1)^{m(N-1)-k}\left[\frac{\bar{p}(v+1)}{m(N_I-N)}\right]^{mN+n-r}\binom{mN+n-r-1}{m(N-1)-k-1}$$

The corresponding CDF

$$F_I(x) = 1-\int_x^{\infty}f_I(z)dz$$

can also be evaluated in closed-form as:

$$F_I(x) = 1-\frac{N}{\Gamma(m)}\binom{N_I}{N}\sum_{n=0}^{(N_I-N)(m-1)}\beta(n, N_I-N, m)\left(\frac{m}{\bar{p}}\right)^{mN+n}\sum_{v=0}^{N-1}(-1)^v\binom{N-1}{v}\sum_{k=0}^{v(m-1)}\beta(k, v, m)$$

$$\times \frac{\Gamma(m+n+k)}{(v+1)^{m+n+k}} \left\{ \sum_{r=1}^{m(N-1)-k} A_r \left(\frac{\bar{p}}{m}\right)^r e^{-xm/\bar{p}} \sum_{z=0}^{r-1} \frac{1}{z!}\left(\frac{mx}{\bar{p}}\right)^z \right.$$

$$\left. + \sum_{r=1}^{m+n+k} B_r \left[\frac{\bar{p}(v+1)}{m(N_I - N + v + 1)}\right]^r e^{-\frac{xm}{\bar{p}}\left(\frac{N_I - N + v + 1}{v+1}\right)} \sum_{z=0}^{r-1} \frac{1}{z!}\left[\frac{xm(N_I - N + v + 1)}{\bar{p}(v+1)}\right]^z \right\}, [1 < N < N_I]$$

**A 14**

$$F_I(x) = 1 - e^{-xm/\bar{p}} \sum_{z=0}^{mN_I - 1} \frac{1}{z!}\left(\frac{mx}{\bar{p}}\right)^z, [N = N_I]$$

**A 15**

$$F_I(x) = 1 - \frac{N_I}{\Gamma(m)} \sum_{n=0}^{(N_I-1)(m-1)} \beta(n, N_I - 1, m) \frac{\Gamma(m+n)}{N_I^{m+n}} e^{-xmN_I/\bar{p}} \sum_{z=0}^{m+n-1} \frac{1}{z!}\left(\frac{mN_I x}{\bar{p}}\right)^z, [N = 1]$$

**A 16**

It should be noted that the statistics of the sum of ordered exponential variates can be directly obtained from the above expressions by setting $m = 1$ . In addition to this direct proof, two alternative derivations for this special case are also discussed in the Appendix B.

## *4.8 Appendix B*

In this appendix, we discuss three different methods for deriving the statistic of $I = \sum_{k=1}^{N} p_{k:N_I}$ given that $p_1, p_2, \ldots, p_{N_I}$ are i.i.d exponential variates (i.e., fading amplitudes are subject to Rayleigh fading). These results would be useful for predicting

the probability of outage in a macro-cell environment because in this case, the availability of a direct line-of sight path is not very likely.

### 4.8.1 Method I

While $m=1$, equation (A10) simplifies to

$$\phi_I(s) = \frac{N\binom{N_I}{N}}{(s\bar{p}+1)^{N-1}} \sum_{v=0}^{N-1} \frac{(-1)^v \binom{N-1}{v}}{[s\bar{p}(v+1)+N_I-N+v+1]}, \; [1 \le N \le N_I] \qquad \textbf{B 1}$$

It should be noted that the derivation leading to the above formula is short and simple. In fact, substituting appropriate expressions for $f(x)$ and $F(x)$ in the last line of equation (A2), we immediately obtain equation (B1). The corresponding PDF and CDF of I may be obtained by letting $m=1$ in equations (A11)-(A16).

### 4.8.2 Method II

If $p_{1,}p_{2,}...,p_{N_I}$ are i.i.d exponential variates, then their spacing $p_{k:N_I} - p_{k-1:N_I} = p_k/(N_I-k+1), [k=1,...,N_I]$, are again exponential and, remarkably are independent [34]. It is only in the case of exponential RVs such spacing properties are encountered [35]. It can be observed from the above relation that

$$p_{k:N_I} = \sum_{r=1}^{k} \frac{p_r}{N_I - r + 1}, \; [k = 1, \ldots, N_I] \qquad \textbf{B 2}$$

which simply expresses the k-th order statistic in a sample of size $N_I$ from the standard exponential distribution as a linear combination of independent standard exponential variates with an appropriate weighting. Now it is straight-forward to show that

$$I = \sum_{k=1}^{N} p_{k:N_I} = \sum_{k=1}^{N} \sum_{r=1}^{k} \frac{p_r}{N_I - r + 1}$$
$$= \frac{p_1 N}{N_I} + \frac{p_2 (N-1)}{N_I - 1} + \ldots + \frac{p_N}{N_I - N + 1}$$
$$= \sum_{k=1}^{N} \left( \frac{N-k+1}{N_I - k + 1} \right) p_k \qquad \textbf{B 3}$$

Since the MGF of $p_k$ is given by $1/(1+s\bar{p})$, we immediately obtain equation (B4) by observation:

$$\phi_I(s) = \prod_{k=1}^{N} \left[ 1 + s\bar{p} \left( \frac{N-k+1}{N_I - k + 1} \right) \right]^{-1}, \quad [1 \le N \le N_I] \qquad \textbf{B 4}$$

Although reference [32] also discussed the use of the spacing property [34] for deriving the MGF of I , our approach, however, is slightly different and much more direct to get equation (B4).

### 4.8.3 Method III

When both m and d equal to unity, it is easy to show that

$$G(a, b, 1, 1, N) = \frac{1}{b(a+b)(2a+b)\ldots[(N-1)a+b]} = \prod_{k=1}^{N} \frac{1}{[(k-1)a+b]} \qquad \textbf{B 5}$$

using the recursion formula equation (A9).

While setting $m = 1$ and substituting equation (B5) into equation (A7), we obtain

$$\phi_I(s) = \frac{N!}{\bar{p}^N} \binom{N_I}{N} \left[ \prod_{k=1}^{N} \frac{\bar{p}}{k + N_I - N} \right] \prod_{k=1}^{N} \left[ 1 + \frac{k\bar{p}s}{k + N_I - N} \right]^{-1}$$
$$= \prod_{k=1}^{N} \left[ 1 + \frac{k\bar{p}s}{k + N_I - N} \right]^{-1} \qquad \textbf{B 6}$$

The PDF of I for any $N < N_I$ can be found to be a weighted sum of exponential functions by taking an inverse Laplace transformation of an argument involving a partial fraction expansion of the MGF, viz.,

$$f_I(x) = \sum_{k=1}^{N} \eta_k \left( \frac{k + N_I - N}{k\bar{p}} \right) e^{-x\left( \frac{k + N_I - N}{k\bar{p}} \right)}, \quad [1 \le N < N_I] \qquad \textbf{B 7}$$

where

$$\eta_k = \prod_{i=1, i \neq k}^{N} \frac{k(i + N_I - N)}{(N_I - N)(k - i)}$$

Finally, the CDF of I in this case is given by

$$F_I(x) = 1 - \sum_{k=1}^{N} \eta_k e^{-x\left( \frac{k + N_I - N}{k\bar{p}} \right)}, \quad [1 \le N < N_I] \qquad \textbf{B 8}$$

# Chapter 5 Conclusion & Future Work

## *5.1 Summary*

This research work study and analyze the effect of smart antennas and power management in 802.11b wireless LAN in ad-hoc mode. There has been a substantial demand for the wireless LAN technology in recent years. Wireless LAN has grown from being add on connection for cable based Ethernet to being the main backbone network carrying critical traffic. With the tremendous increase in its use the networks are reaching their limits in throughput and acceptable co-channel interference. We have proposed a modified to the existing MAC to accommodate the smart antennas for both transmit and receive beamforming.

The smart antenna algorithm uses the receive signal to converge and form beam towards the desired transmitter. The weight vector is then stored in a weight look up table to be used by the transmitter. When the node want to reply to its sender it looks up the desired weight from the weight vector table and forms transmits beam pointing towards the desired node. As more and more node communicates with each other their weight look up table gets filled and more communication occur via the smart antenna. The network throughput increases as channel access efficiency of the network improves.

We studied the effect of various channel conditions on the throughput of the network. The effect of proposed power management algorithm in realistic channel conditions is analyzed and studied. The conclusion drawn from the simulation results are presented in the next section.

## *5.2 Conclusion*

We proposed an algorithm to incorporate smart antenna to 802.11b based ad-hoc network. We presented simulation result showing the improvement in throughput if smart antennas are employed. We defined two different scenarios that affect the performance of the smart antenna system considerably.

- Constant EIRP: IN this case the effective transmit range of the transmitter is kept constant by imposing a limit on the maximum EIRP allowed for both omni and smart antenna system.

- Constant Power to antenna section: In this scenario we defined the maximum power that should be supplied to the antenna section. In effect this allowed the smart antenna section to vary it's EIRP depending on the gain in a given direction.

The performance of the smart antenna system was different for these two scenarios. For constant EIRP the smart antenna system consistently performed better that the omni directional antenna system. The reason is even though both omni and smart antenna had the same range the smart antenna was able to use space division multiplexing more efficiently with its directed beampatterns.

The performance of the smart antenna system in constant power (Varying EIRP) scenario was dependent on the network area. For smaller network area the performance of the smart antenna system was equivalent to the omidirectional case. But for larger network area the smart antenna system performed better as it was able to reach more nodes due it's higher gain.

We also presented the practical implementation issues we faced while implementing the smart antenna algorithm on VT-STAR real time communication system. We present the values of various step parameters for various algorithms under an indoor environment.

We also proposed a link by link power management algorithm to improve the transmit power efficiency of the wireless ad hoc network. We have presented our simulation results which shows that significant transmit power can be saved if power management scheme is adopted.

We proposed and derived various numerical methods to design cellular communication system employing smart antennas. We presented the practical use to the numerical in calculating outage probability under various fading conditions for interference and desired signal. We presented the numerical method to analyze effect of an adaptive interference nulling technique on the spectral efficiency and reuse distance of an ceellular mobile radio system.

## 5.3 Future research Directions

The impact of smart antennas and power management on the wireless ad-hoc networks is part of a larger research area which referred to as "C*ross Layer Optimization*". In its implementation and previous research both smart antennas and link to link power management has been considered as the physical layer issues. But as we have shown in our work the impact of both smart antennas and power management is substantial on the performance criteria of the upper layer e.g Network throughput.

To extract the maximum advantage from the under lying technology the upper layer (MAC, Routing Protocol) should be cognitive of the environment it is operating in and should control the lower layer. We feel following research areas have become extremely important in investigating the performance of cross layer optimization and/or the impact of smart antennas and power management on the wireless ad-hoc networks.

- The smart antenna control mechanism can be modified so that it can be controlled by the routing protocol via matrices like power, gain, interference environment and throughput.
- The power management algorithm should also be controlled by the routing protocol to maximize the wireless network performance. The matrices that would be considered by the routing protocol to control the power management algorithm could be connectivity (Higher power, more connectivity) Interference, network load distribution, delay.
- The power management and the smart antenna algorithm could be analyzed and simulations could be performed for non line of sight environment.
- The effect of different traffic load (HTTP, FTP, database queries) on the performance of smart antenna and power management algorithm can studied and analyzed.

## *Bibliography*


[1] T. Ohira, "Emerging Adaptive Antenna Techniques for Wireless Ad-Hoc Networks", *The 2001 IEEE International Symposium on Circuits and Systems, 2001. ISCAS 2001.*, Volume: 4 , 2001 Page(s): 858 -861.

[2] S. Bandyopadhyay, K. Hasuike, S. Horisawa, S. Tawara, "An Adaptive MAC Protocol for Wireless Ad Hoc Community Network (WACNet) Using Electronically Steerable Passive Array Radiator Antenna",*Global Telecommunications Conference, 2001. GLOBECOM '01. IEEE* , Volume: 5 ,2001 Page(s): 2896 -2900.

[3] C. E. Anderson and M.A. Wickert, " The performance of a wireless LAN Access Node Using Antenna BeamForming for Dynamic and Static Users.", *Radio and Wireless Conference*, 1999.RAWCON 99 Page(s): 27 -30.

[4] Kaixin Xu, Mario Gerla and Sang Bae ,"How Effective is the IEEE 802.11 RTS/CTS Handshake in Ad Hoc Networks?,".

[5] Antonis kalis and Theodore Antonakopolous ,"Relative Direction Determination in Mobile Computing Networks", Instrumentation and Measurement Technology Conference, 2001. IMTC 2001. Proceedings of the 18th IEEE, Volume: 3, 2001 Page(s) : 1479 -1484 vol.3

[6] Eryk Dutkiewicz, "Impact of Transmit Range on Throughput Performance in Mobile Ad-Hoc Network.", Communications, 2001. ICC 2001. IEEE International Conference on , Volume: 9 , 2001 Page(s): 2933 -2937 vol.9

[7] A. Nasipuri, S Ye, J. You and R.E. Hiromoto, "A MAC Protocol for Mobile Ad-hoc Networks Using Directional Antenna" , *Wireless Communications and Networking Confernce, 2000. WCNC. 2000 IEEE* , Volume 3 Page(s): 1214 - 1219.

[8] Joseph C. Liberti, Jr and Theodore S. Rappaport," Smart Antennas For Wireless Communications: IS-95 and Third Generation CDMA Applications", Prentice hall Communications, 1999.

[9] Hassan M. Elkamchouchi and Mohamed A. Elsalam," A new constrained fast

null steering algorithm", Seventeenth National Radio Science Conference, Feb 22-24, 2000,Egypt.

[10] Compaq Wireless LAN Multiport W200 Options. http://h18000.www1.hp.com/products/quickspecs/11391_na/11391_na.HTML

[11] Wireless LAN product information by Intersil for 2.45 GHz 2,11Mbps product, http://www.intersil.com/data/fn/fn8012.pdf.

[12] Ramesh Chembil Palat, "VT-STAR design and implementation of a test bed for differential space-time block coding and MIMO channel measurements", Master's Thesis, Virginia Tech 2002.

[13] Theodore S. Rappaport,"Wireless Communications Principles & Practice", Prentice Hall Communications 2002.

[14] Hans-Jurgen Zepernick, Tadeusz A. Wysocki ,"Multipath Channel Parameters for Indoor Radio at 2.4 GHz ISM Band", Vehicular Technology Conference, 1999 IEEE 49th , Volume: 1 , Jul 1999 Page(s): 190 -193 vol.1.

[15] Daeyoung Kim; Ingram, M.A.; Smith, W.W ," Small-scale fading for an indoor wireless channel with modulated backscatter", Vehicular Technology Conference, 2001. VTC 2001 Fall. IEEE VTS 54th , Volume: 3 , 2001 Page(s): 1616 -1620 vol.3

[16] Woodward, G.; Oppermann, I.; Talvitie, J.," Outdoor-indoor temporal and spatial wideband channel model for ISM bands **"**, Vehicular Technology Conference, 1999. VTC 1999 - Fall. IEEE VTS 50th ,Volume: 1 , 1999 Page(s): 136 -140 vol.1

[17] ElBatt T.A.; Krishnamurthy, S.V.; Connors D; Dao S," Power management for throughput enhancement in wireless ad-hoc networks", Communications, 2000. ICC 2000. 2000 IEEE International Conference on , Volume: 3 , 2000 Page(s): 1506 -1513 vol.3

[18] Bruce Tuch,"An IEEE 802.11 WLAN Primer," Communication Systems Design, Sept 1997

[19] P. Lehne, M. Pettersen,"an overview of smart antenna technology for mobile communications systems", IEEE communications surveys,

http://www.comsoc.org/~magazinees/surveys/4q99issue/lehne.htm.

[20] INTERNATIONAL STANDARD ISO/IEC 8802-11 ANSI/IEEE Std 802.11 First Edition 1999-00-00 Part 11: Wireless LAN Medium Access Control (MAC) and Physical Layer Specification (PHY). ISBN 07381-1658-0

[21] B. G. Agee, K Cohen, J. H. Reed and T.C. Hsia ,"Simulation Performance of a Blind Adaptive Array for a Realistic Mobile Channel",1993IEEE0-7803-1266-x

[22] PRISM chipset, Intersil Corp., http://www.intersil.com

[23] K. Gyoda et al.," Wacnet: Wireless ad-hoc community network ", IEEE ISCAS2001, Sydney, Nov. 1998.

[24] Andrew S. Tanenbaum ,"Computer Networks", Third edition,1999 ISBN-81-203-1165-5

[25] Linnartz J.P, "Narrowband Land-Mobile Radio Networks.", Artech MA 1993.

[26] Yao Y-D, Sheik A, "Investigation into co-channel interference in micro cellular mobile radio systems", IEEE transactions on vehicular technology 1992;11:Page 114-123

[27] Alouini, M.-S.; Bastami, A.; Ebbini, E.," Outage probability of cellular mobile radio systems with successive interference cancellation", *Signals, Systems, and Computers, 1999.* Conference Record of the Thirty-Third Asilomar Conference on , Volume: 1 , 1999 Page(s): 192 -196.

[28] Winters J. ,"Optimum combining in digital mobile radio with co-channel interference", *IEEE journal on selected areas in communications* 1984;pages 528-539.

[29] Winters J. ,"Smart antennas for wireless communications", *IEEE Personal Communications Magazine* 1998;pages 23-27.

[30] Ranta P, Honkasalo Z.,Tapanien,""TDMA cellular network application of an interference cancellation technique", Proceedings of IEEE Vehicular Technology Conference, Chicago. May 1995 ; Pages 296-300.

[31] Ranta P, Hottinen A, Honkasalo Z., "Co-channel interference cancellation receiver for TDMA mobile system ", *IEEE international conference on Communications*, Seattle, June 1995.

[32] Hasna M, Alouini M., "Performance evaluation of cellular mobile radio systems

with successive co-channel interference cancellation", Proceedings of 2000 IEEE Vehicular Technology Conference (Fall) ; Pages 1506-1513.

[33] Likes J.," On the distribution of certain linear functions of ordered sample from exponential population", Annals Inst. Stat. and Math. 1962; 13:225-230.

[34] Suhatme PV, " Test of significance for samples of the $x^2$ population with two degree of freedom ", *Annals of Eugenics*, 1937; 8:52-56.

[35] Arnold BC, Blakrishnan N, Nagaraja HN, " A first course in order statistics", Wiley , New York 1992.

[36] David HA," Order Statistics", Wiley, New York 1981.

[37] Annamalai A., Tellambura C, Bhargava VK, " Simple and accurate methods for outage analysis in cellular mobile radio system –a unified approach ", *IEEE Transactions on Communications* 2001;49(2)

[38] Annamalai A., " Accurate and efficient analysis of wireless digital communication system in multi-user and multipath fading environment ", PhD Dissertation, Dept of Electrical Engineering

[39] Annamalai A., Tellambura C, " Error rates for hybrid SC/MRC systems over Nakagami channels ", Proceedings of IEEE wireless communications & Networking conference. Chicago 2000.